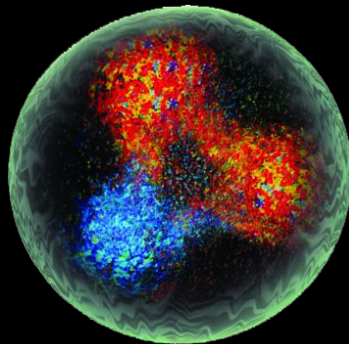
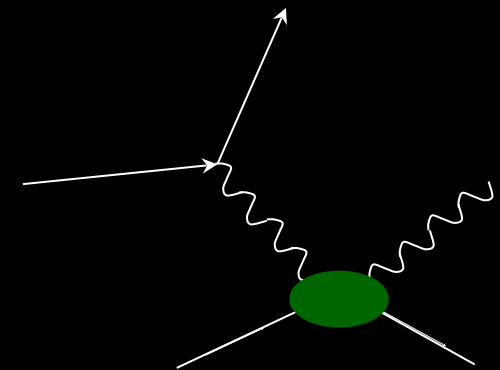


Status of DVCS experiments and open questions



Daria Sokhan

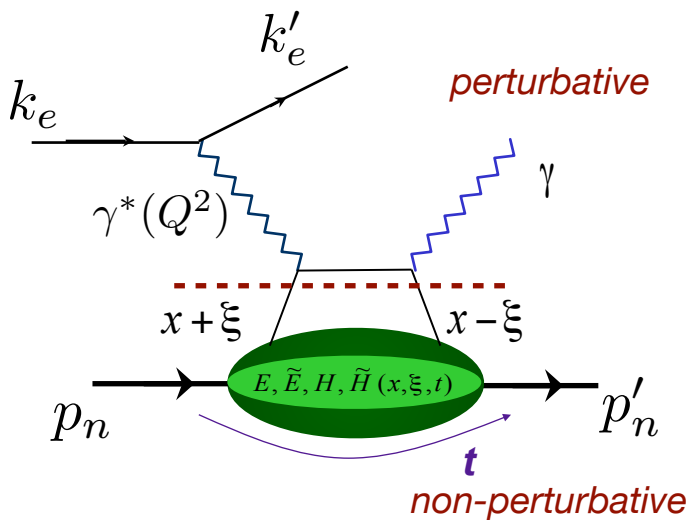
University of Glasgow, UK



Probing Nucleons and Nuclei in High Energy Collisions
Institute for Nuclear Theory, Seattle - 1st October 2018

Deeply Virtual Compton scattering

DVCS: golden channel for the extraction of GPDs.



$$Q^2 = -(\mathbf{k} - \mathbf{k}')^2 \quad t = (\mathbf{p}'_n - \mathbf{p}_n)^2$$

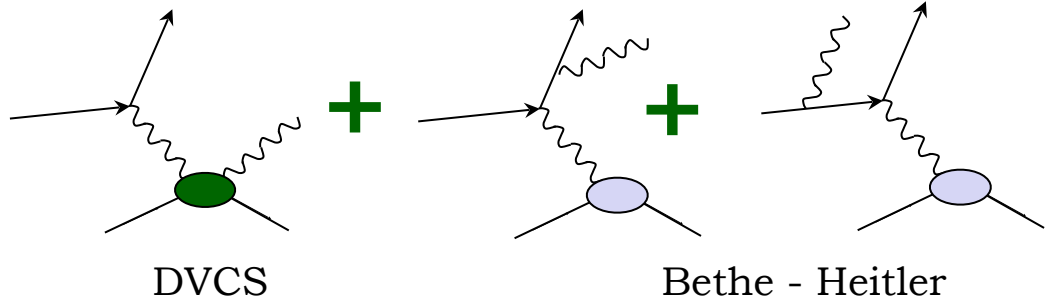
$$\text{Bjorken variable: } x_B = \frac{Q^2}{2\mathbf{p}_n \cdot \mathbf{q}}$$

$x \pm \xi$ longitudinal momentum fractions of the struck parton

$$\xi \equiv \frac{x_B}{2 - x_B}$$

* At high exchanged Q^2 and low t access to four chiral-even GPDs:

$$E^q, \tilde{E}^q, H^q, \tilde{H}^q(x, \xi, t)$$



$$d\sigma \propto |T_{DVCS}|^2 + |T_{BH}|^2 + T_{BH} T^*_{DVCS} + T_{DVCS} T^*_{BH}$$

interference term

Experimentally accessible (at leading twist, leading order):

$$T^{DVCS} \sim \int_{-1}^{+1} \frac{\text{GPDs } (x, \xi, t)}{x \pm \xi + i\varepsilon} dx + \dots \sim P \int_{-1}^{+1} \frac{\text{GPDs } (x, \xi, t)}{x \pm \xi} dx \pm i\pi \text{GPDs } (\pm \xi, \xi, t) + \dots$$

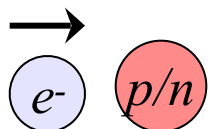
Compton Form Factors (CFF)

Which DVCS experiment?

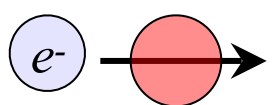
Real parts of CFFs accessible in cross-sections, beam-charge and double polarisation asymmetries,

imaginary parts of CFFs in single-spin asymmetries.

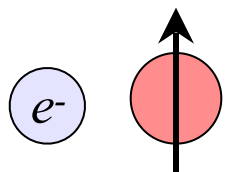
Beam, target
polarisation



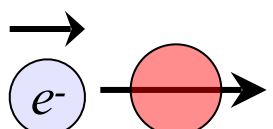
$$\Delta\sigma_{LU} \sim \sin\phi \Im(F_1 \mathbf{H} + \xi G_M \tilde{\mathbf{H}} - \frac{t}{4M^2} F_2 \mathbf{E}) d\phi \rightarrow$$



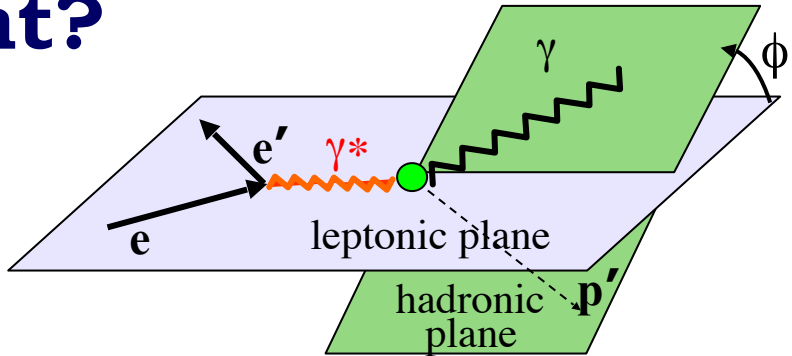
$$\Delta\sigma_{UL} \sim \sin\phi \Im(F_1 \tilde{\mathbf{H}} + \xi G_M (\mathbf{H} + \frac{x_B}{2} \mathbf{E}) - \xi \frac{t}{4M^2} F_2 \tilde{\mathbf{E}} + \dots) d\phi \rightarrow$$



$$\Delta\sigma_{UT} \sim \cos\phi \Im(\frac{t}{4M^2} (F_2 \mathbf{H} - F_1 \mathbf{E}) + \dots) d\phi \rightarrow$$



$$\Delta\sigma_{LL} \sim (A + B \cos\phi) \Re(F_1 \tilde{\mathbf{H}} + \xi G_M (\mathbf{H} + \frac{x_B}{2} \mathbf{E}) + \dots) d\phi \rightarrow$$



Proton Neutron

$$\begin{aligned} & \text{Im}\{\mathbf{H}_p, \tilde{\mathbf{H}}_p, E_p\} \\ & \text{Im}\{H_n, H_n, E_n\} \end{aligned}$$

$$\begin{aligned} & \text{Im}\{\mathbf{H}_p, \tilde{\mathbf{H}}_p\} \\ & \text{Im}\{\mathbf{H}_n, E_n, \tilde{E}_n\} \end{aligned}$$

$$\begin{aligned} & \text{Im}\{\mathbf{H}_p, E_p\} \\ & \text{Im}\{\mathbf{H}_n\} \end{aligned}$$

$$\begin{aligned} & \text{Re}\{\mathbf{H}_p, \tilde{\mathbf{H}}_p\} \\ & \text{Re}\{\mathbf{H}_n, E_n, \tilde{E}_n\} \end{aligned}$$



JLab: the experimental facility

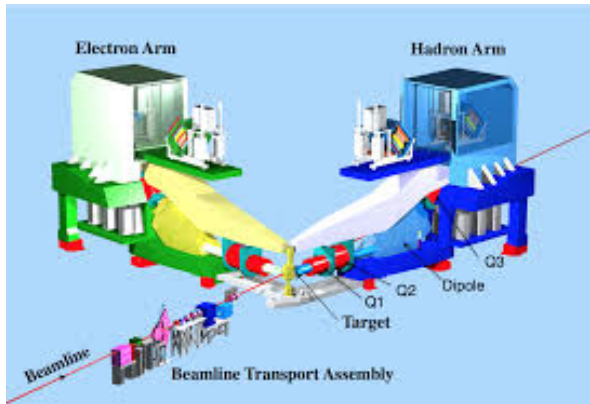
Jefferson Lab: 6 GeV era

CEBAF: Continuous Electron Beam Accelerator Facility.

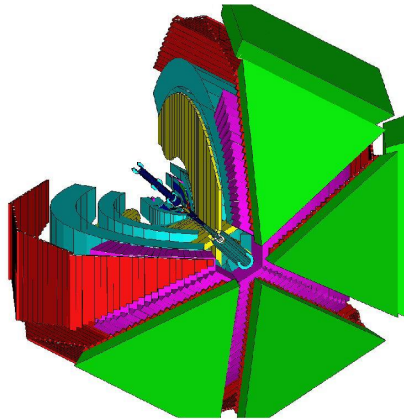
- * Energy up to ~ 6 GeV
- * Energy resolution $\delta E/E_e \sim 10^{-5}$
- * Longitudinal electron polarisation up to $\sim 85\%$



Hall A:



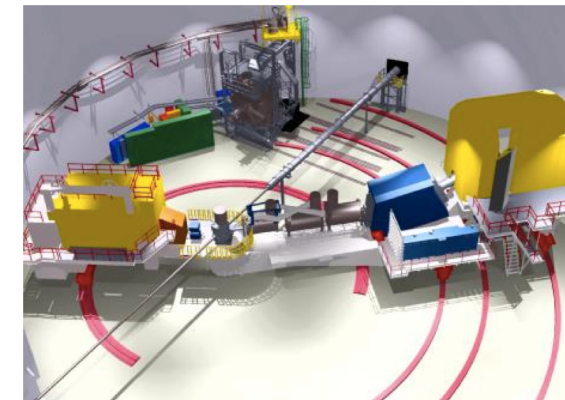
Hall B: CLAS



- * High resolution($\delta p/p = 10^{-4}$) spectrometers, very high luminosity.

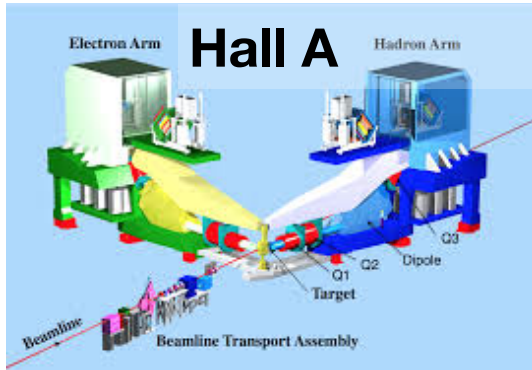
- * Very large acceptance, detector array for multi-particle final states.

Hall C:

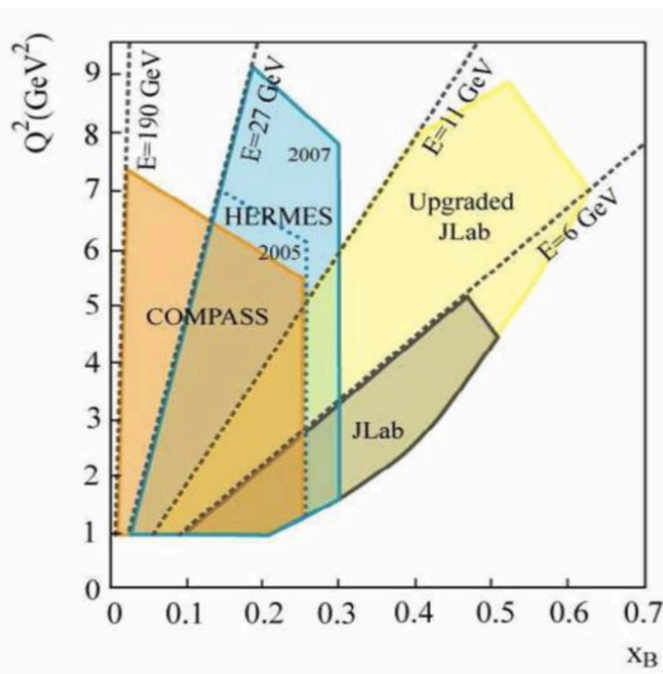


- * Two movable spectrometer arms, well-defined acceptance, high luminosity

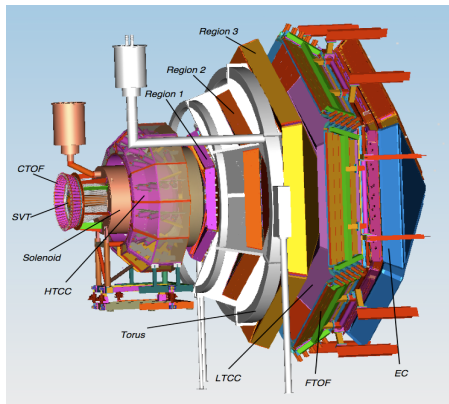
JLab @ 12 GeV



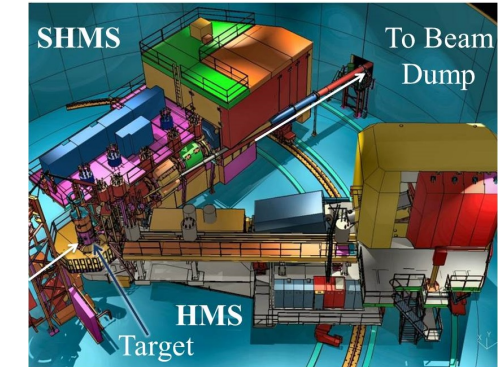
High resolution ($\delta p/p = 10^{-4}$) spectrometers, very high luminosity, large installation experiments.



Hall B: CLAS12



9 GeV tagged polarised photons, full acceptance

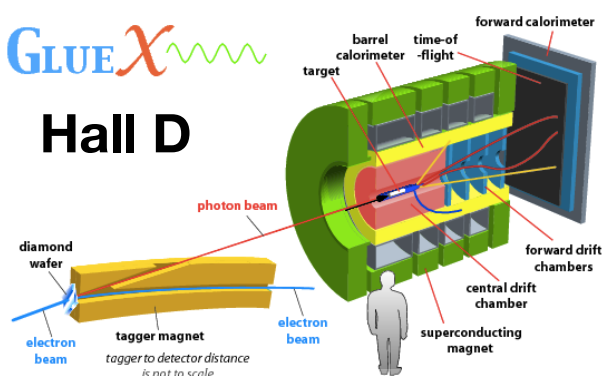


Two movable high momentum spectrometers, well-defined acceptance, very high luminosity.

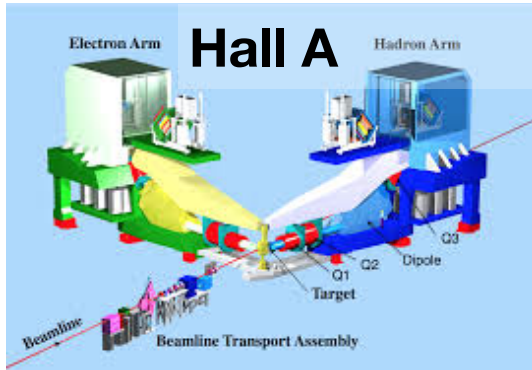
Very large acceptance, high luminosity.

GLUE

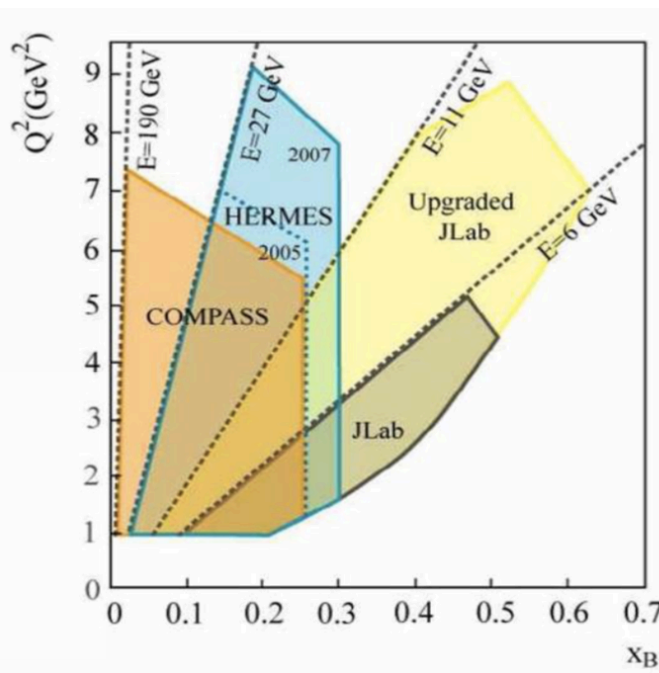
Hall D



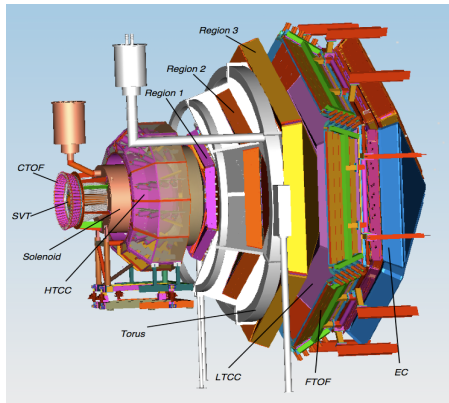
JLab @ 12 GeV



High resolution($\delta p/p = 10^{-4}$) spectrometers, very high luminosity, large installation experiments.



Hall B: CLAS12



Very large acceptance, high luminosity.

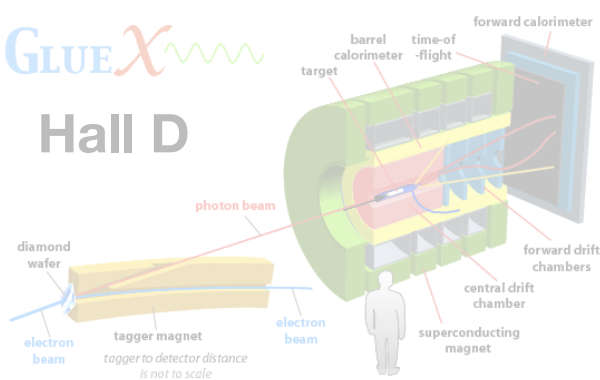


Hall C

Two movable high momentum spectrometers, well-defined acceptance, very high luminosity.

GLUE χ

Hall D



9 GeV tagged polarised photons, full acceptance

CLAS12

Design luminosity

$$L \sim 10^{35} \text{ cm}^{-2} \text{ s}^{-1}$$

High luminosity & large acceptance:

Concurrent measurement of **exclusive**, **semi-inclusive**, and **inclusive** processes

Acceptance for photons and electrons:

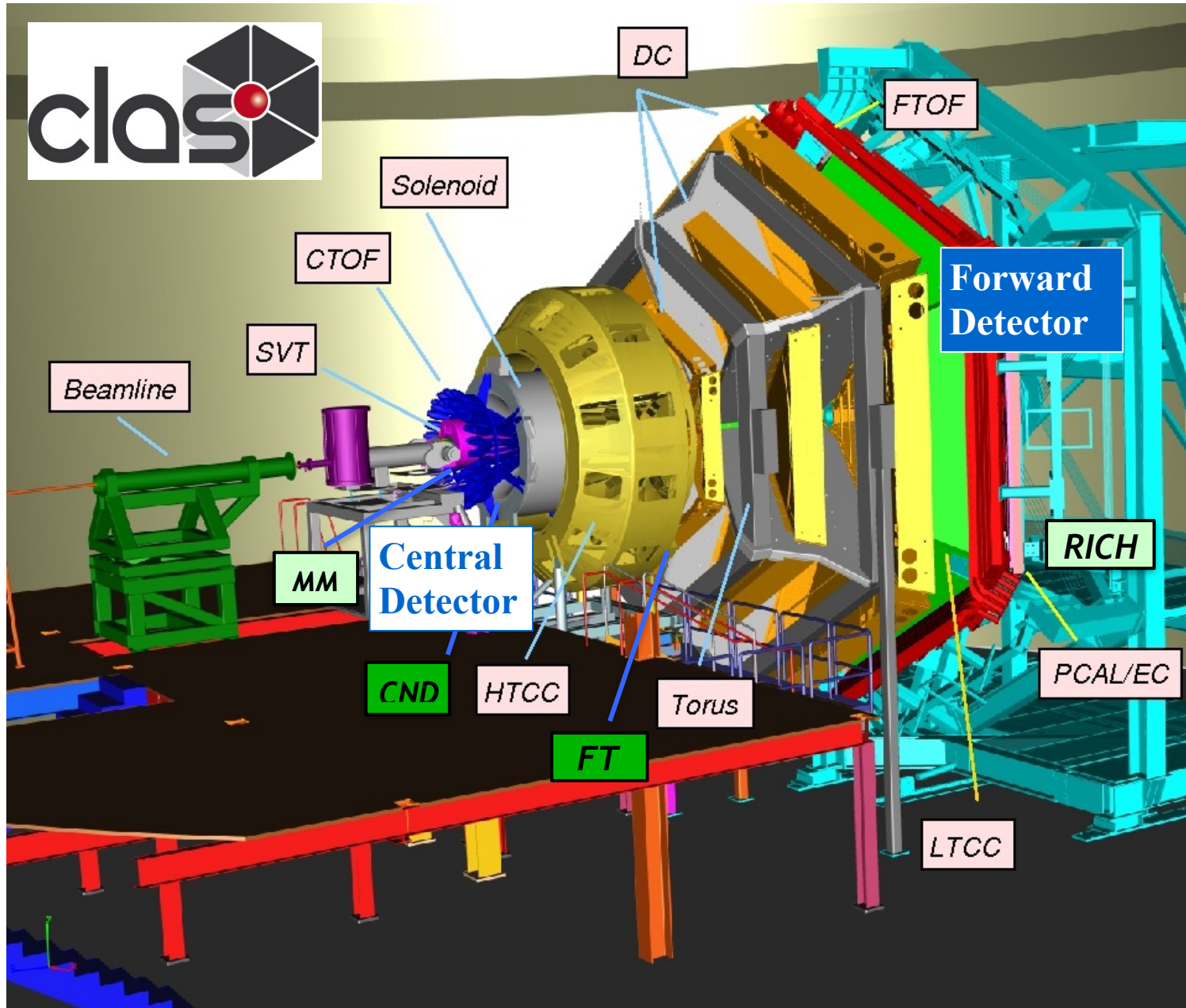
- $2.5^\circ < \theta < 125^\circ$

Acceptance for all charged particles:

- $5^\circ < \theta < 125^\circ$

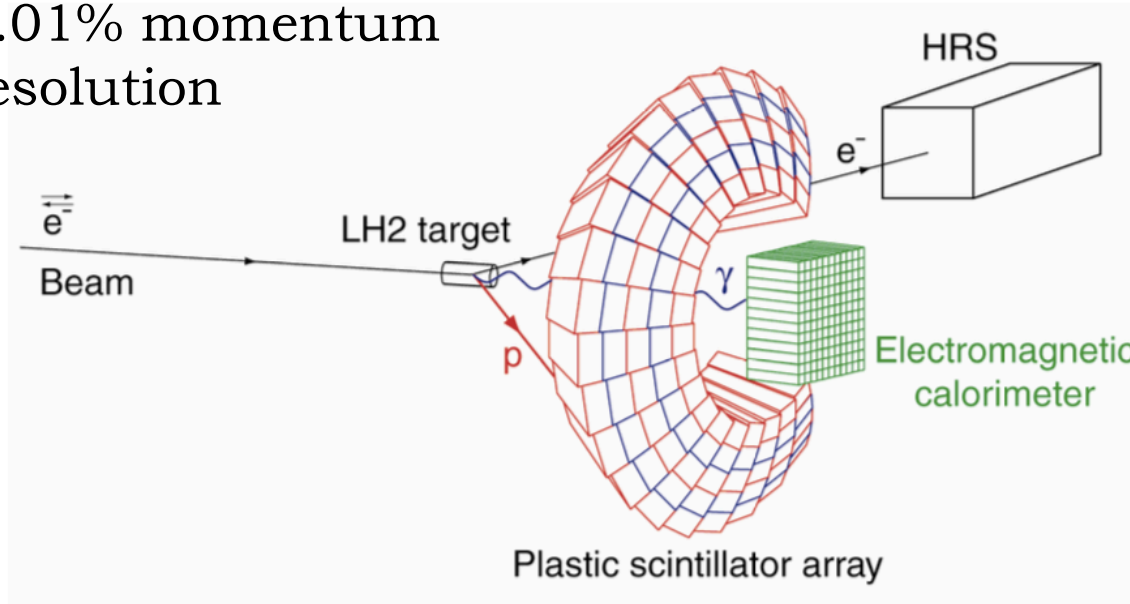
Acceptance for neutrons:

- $5^\circ < \theta < 120^\circ$



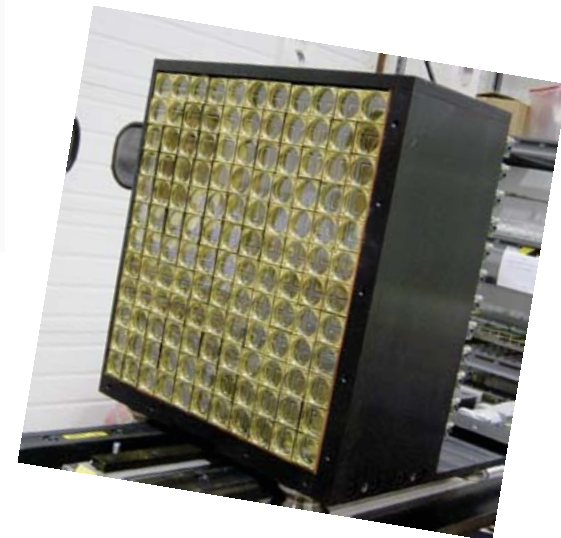
DVCS in Hall A

Detect electron in the Left
High Resolution
Spectrometer (HRS-L):
0.01% momentum
resolution



Detect recoil proton in plastic
scintillator array.

Detect photon in
PbF₂ calorimeter:
< 3% energy
resolution



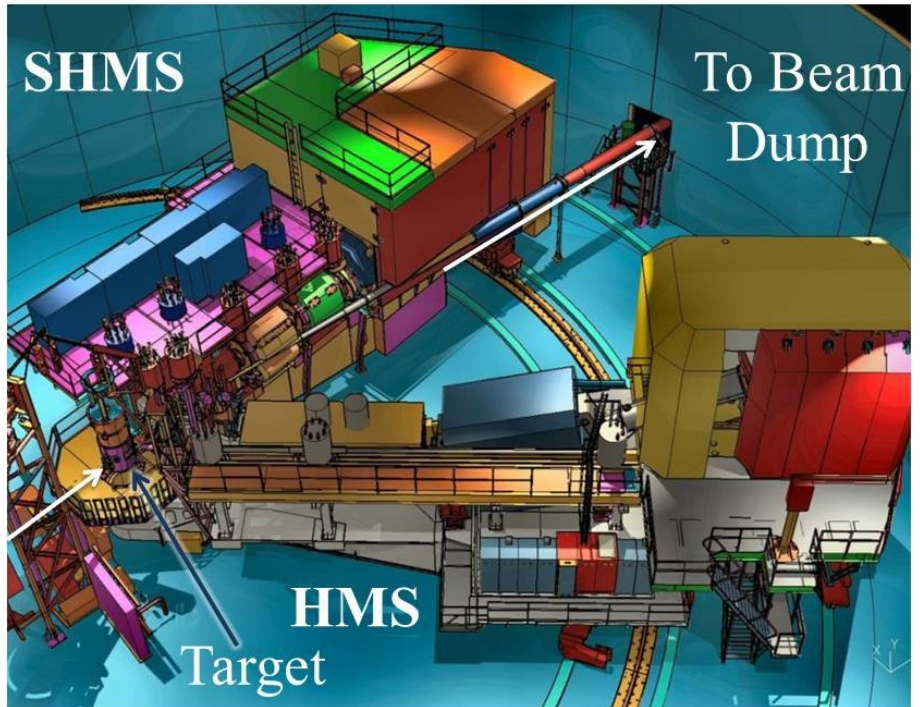
DVCS in Hall C

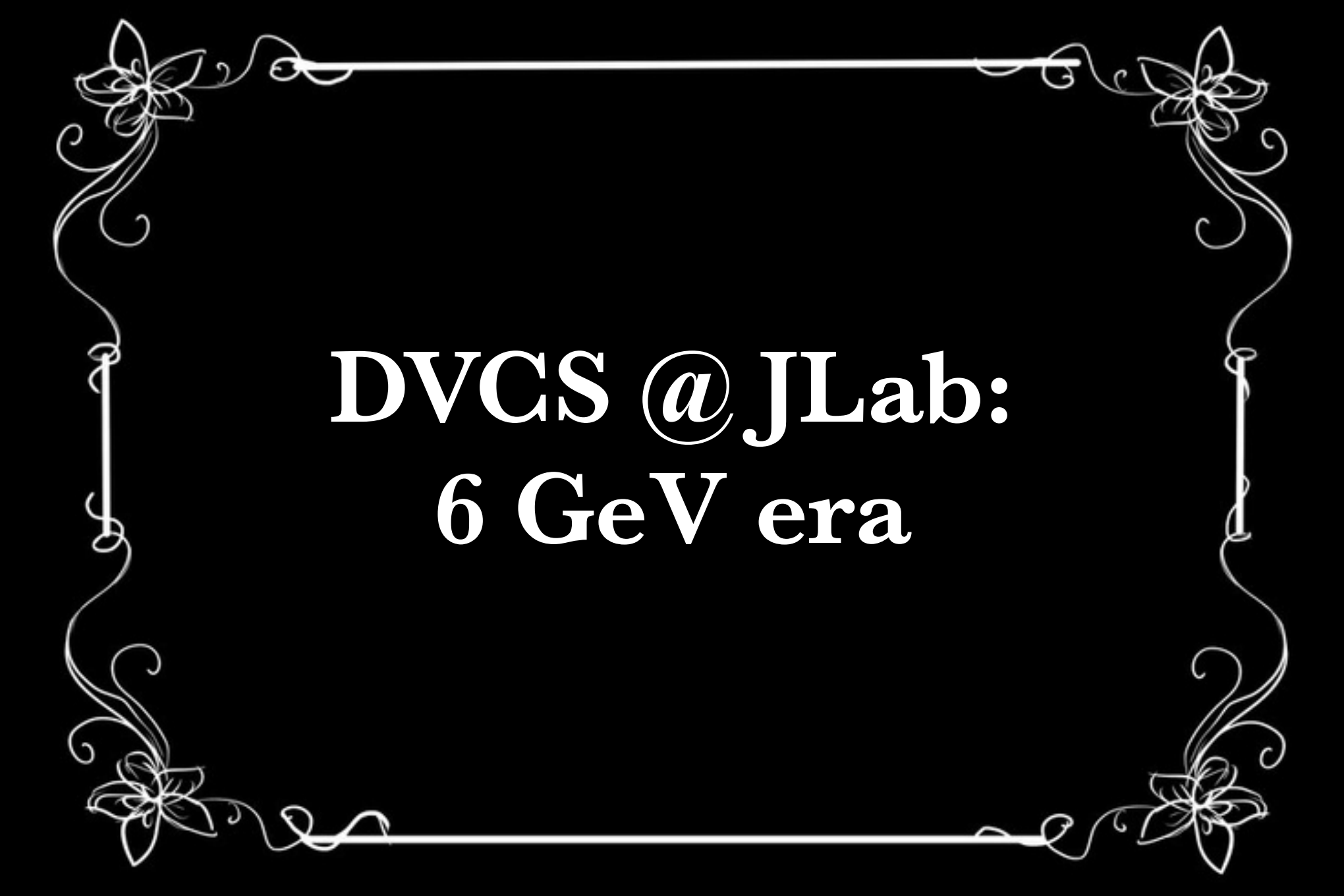
Detect electron with (Super) High Momentum Spectrometer, (S)HMS.

Detect photon in PbWO₄ calorimeter.

Sweeping magnet to reduce backgrounds in calorimeter.

Reconstruct recoiling proton through missing mass.



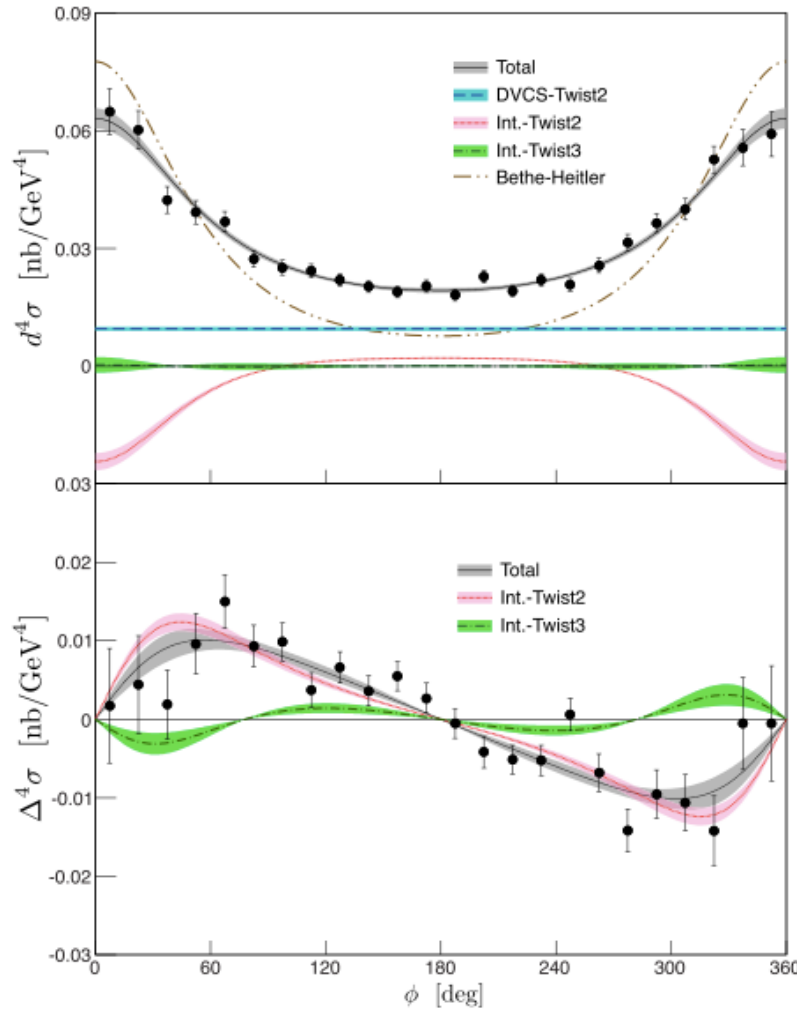


DVCS @JLab: 6 GeV era

First DVCS cross-sections in valence region

Hall A

- * E00-110: Hall A, ran in 2004, high precision, narrow kinematic range.

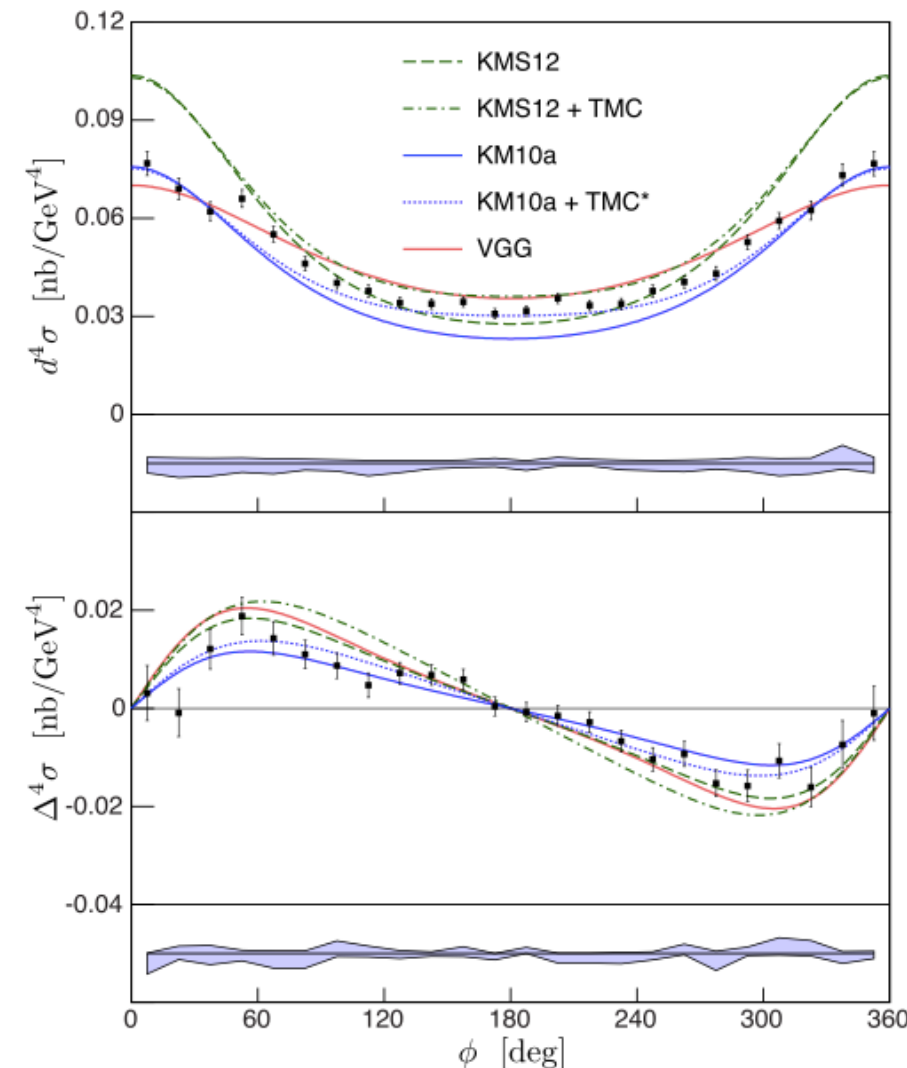


- * Luminosity = $10^{37} \text{ cm}^{-2}\text{s}^{-1}$.
- * Measure Q^2 -dependence (Q^2 : 1.5, 1.9, 2.3 GeV^2) of DVCS-BH cross-sections at fixed x_B (0.36).
- * Also x_B dependence at constant Q^2 .
- * CFFs show scaling in DVCS: leading twist (twist-2) dominance at this moderate Q^2 .
- * Strong deviation of unpolarised DVCS cross-section from BH: extraction of $|T_{DVCS}|^2$ amplitude as well as interference terms.
- * Separation of real part of the twist-2 interference term and the $|T_{DVCS}|^2$ amplitude is very sensitive to relative cross-sections at $\phi = 0^\circ$ and $\phi = 180^\circ$.

$$x_B = 0.36, Q^2 = 2.3 \text{ GeV}^2, -t = 0.32 \text{ GeV}^2$$

First DVCS cross-sections in valence region

Hall A



$$x_B = 0.36, Q^2 = 1.9 \text{ GeV}^2, -t = 0.32 \text{ GeV}^2$$

- * High precision of the data: sensitivity to subtle differences in model predictions.

VGG model: Vanderhaeghen, Guichon, Guidal

KMS model: Kroll, Moutarde, Sabatié

KM model: Kumericki, Mueller

TMC: kinematic twist-4 target-mass and finite- t corrections, calculated for proton DVCS and estimated for KMS12.

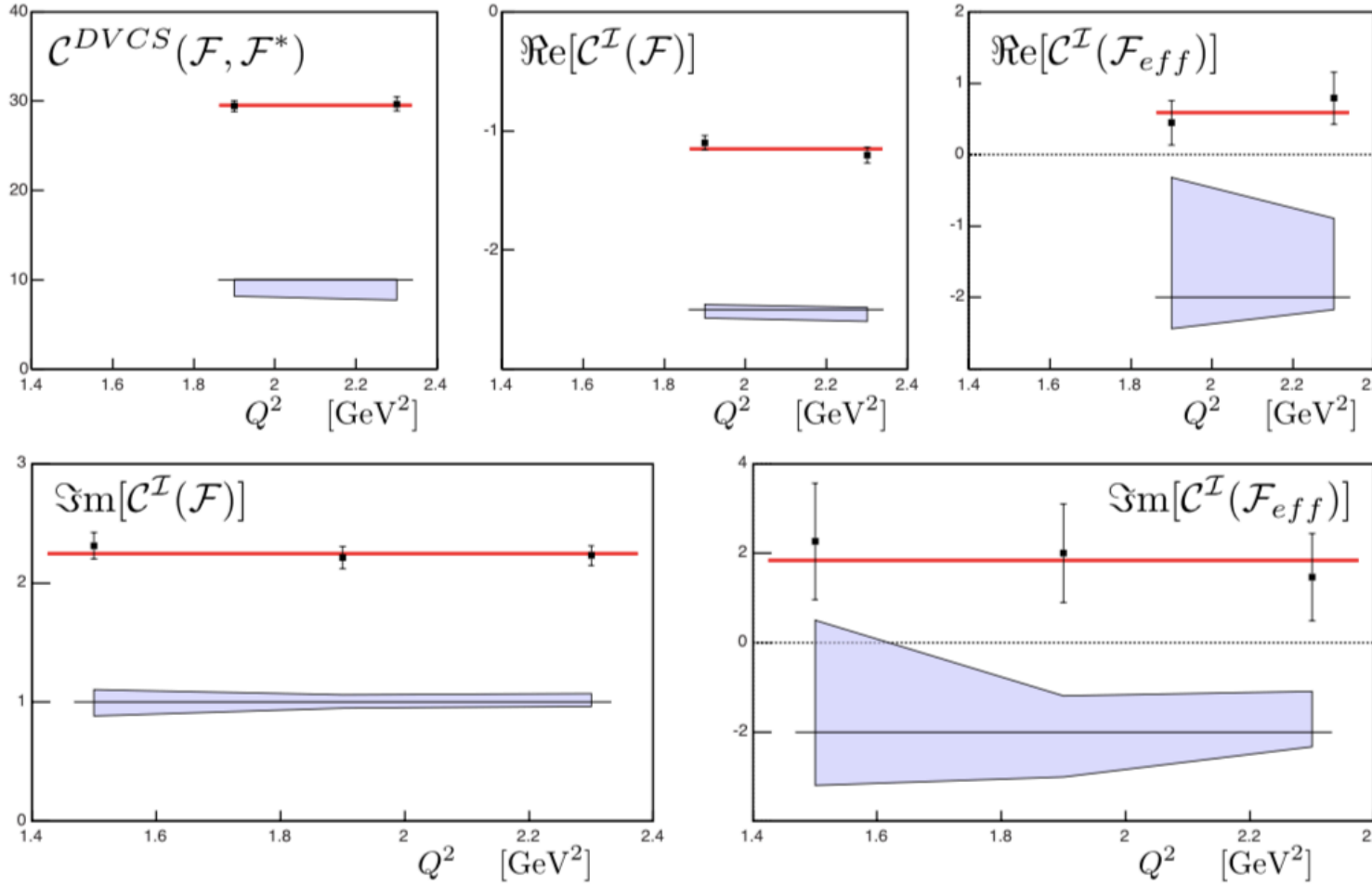
- * KMS parameters tuned on very low x_B meson-production data: not adapted to valence quarks.

→ TMC*: TMC extracted from the KMS12 model and applied to KM10a.

- * TMC improve agreement for KM10a model, especially at $\phi = 180^\circ$. Higher-twist effects?

The devil is in the detail...

CFFs from the Hall A cross-sections



No Q^2 dependence within this range: scaling.

F_{eff} : “Effective” twist-3 CFF

C terms are combinations of CFFs, eg:

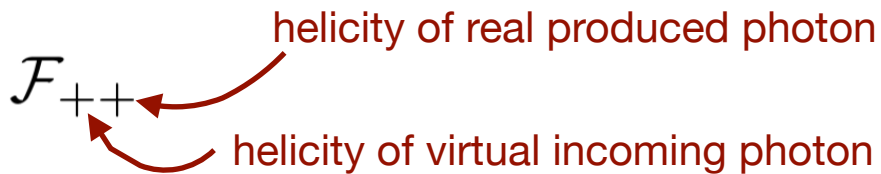
$$\mathcal{C}^{\mathcal{I}}(\mathcal{F}) = F_1 \mathcal{H} + \xi(F_1 + F_2) \tilde{\mathcal{H}} - \frac{t}{4M^2} F_2 \mathcal{E}$$

Here comes the twist...

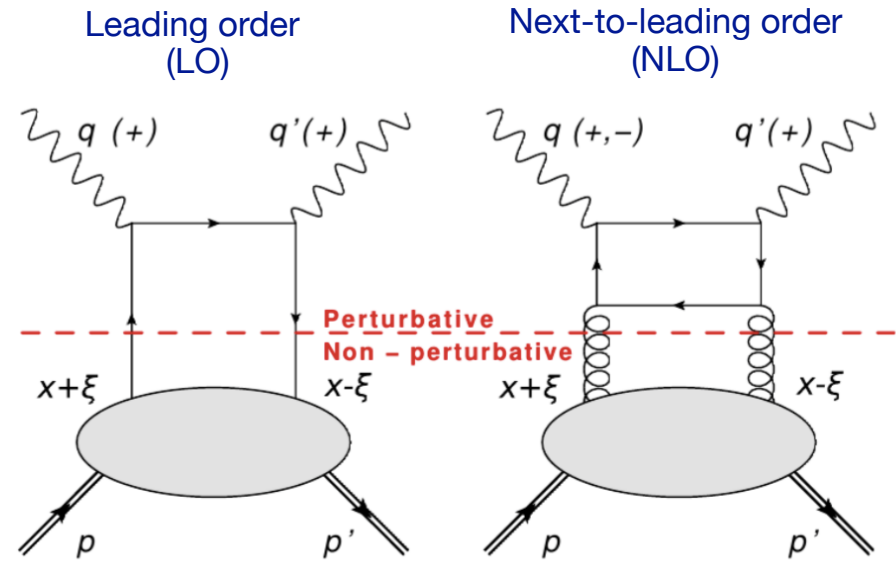
- * Twist: powers of $\frac{1}{\sqrt{Q^2}}$ in the DVCS amplitude. Leading-twist (LT) is twist-2.
- * Order: introduces powers of α_s
- * LO requires $Q^2 \gg M^2$ (M : target mass)

Bold assumption for JLab 6 GeV kinematics!

- * CFFs can be classified according to real and virtual photon helicity:



- Helicity-conserved CFFs – \mathcal{F}_{++}
- Helicity-flip (transverse) – \mathcal{F}_{-+}
- Longitudinal to transverse flip – \mathcal{F}_{0+}



- * CFFs contributing to the scattering amplitude:
 - LT in LO: only \mathcal{F}_{++}
 - LT in NLO: both \mathcal{F}_{++} and \mathcal{F}_{-+}
 - Twist-3: \mathcal{F}_{0+}

Here comes the twist...

- * At finite Q^2 and non-zero t there's ambiguity in defining the light-cone axis:

- Traditional GPD phenomenology uses the Belitsky convention, in plane of q and P :
A. Belitsky *et al*, **Nucl. Phys. B878** (2014), 214
- New, Braun definition using q and q' : more natural.
V. Braun *et al*, **Phys. Rev. D89** (2014), 074022

Reformulating CFFs in this frame absorbs most kinematic power corrections (TMC):

$$\mathcal{F}_{++} = \mathbb{F}_{++} + \frac{\chi}{2} [\mathbb{F}_{++} + \mathbb{F}_{-+}] - \chi_0 \mathbb{F}_{0+}$$

$$\mathcal{F}_{-+} = \mathbb{F}_{-+} + \frac{\chi}{2} [\mathbb{F}_{++} + \mathbb{F}_{-+}] - \chi_0 \mathbb{F}_{0+}$$

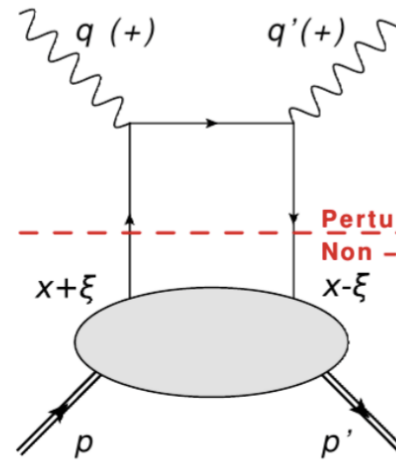
$$\mathcal{F}_{0+} = -(1 + \chi) \mathbb{F}_{0+} + \chi_0 [\mathbb{F}_{++} + \mathbb{F}_{-+}]$$



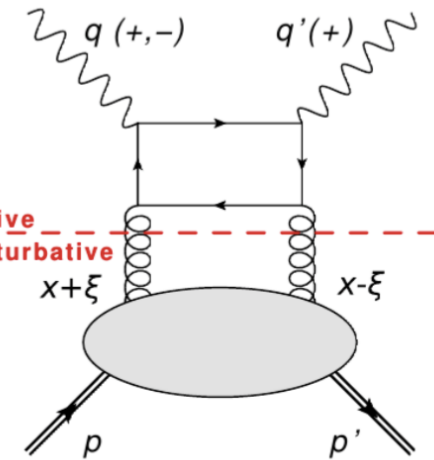
Belitsky
CFFs

Braun CFFs

Leading order
(LO)



Next-to-leading order
(NLO)



Assuming LO and LT in the Braun frame:

$$\mathcal{F}_{++} = (1 + \frac{\chi}{2}) \mathbb{F}_{++}$$

$$\mathcal{F}_{-+} = \frac{\chi}{2} \mathbb{F}_{++}$$

$$\mathcal{F}_{0+} = \chi_0 \mathbb{F}_{++}$$

HT/HO contributions in the Belitsky frame, scaled by kinematic factors χ and χ_0 .

Non-negligible at the Q^2 and x_B of the Hall A cross-section measurement:

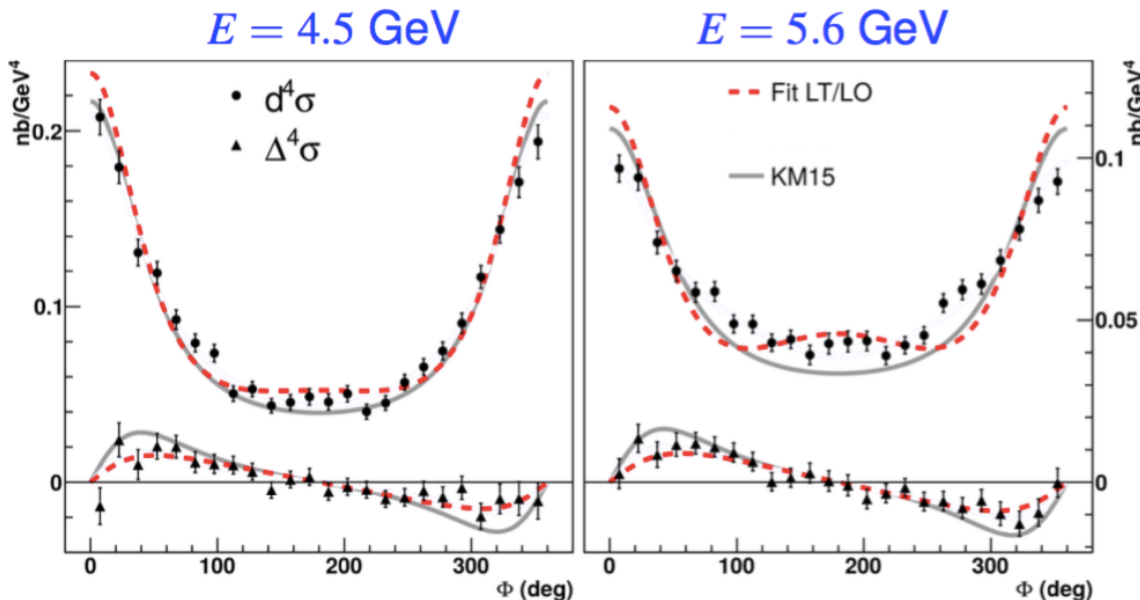
$$\chi_0 = 0.25, \chi = 0.06 \text{ for } Q^2 = 2 \text{ GeV}^2, x_B = 0.36, t = -0.24 \text{ GeV}^2$$

M. Defurne *et al*, **Nature Communications 8** (2017) 1408

Hints of higher twist or higher orders

- * Strong deviation of the measured cross-section from Bethe-Heitler: a beam-energy scan can be used to identify pure DVCS and interference terms in a Rosenbluth-like separation, and to look for higher-twist effects.

→ E07-007: Hall A experiment to measure helicity-dependent and -independent cross-sections at two beam energies and constant x_B and t .

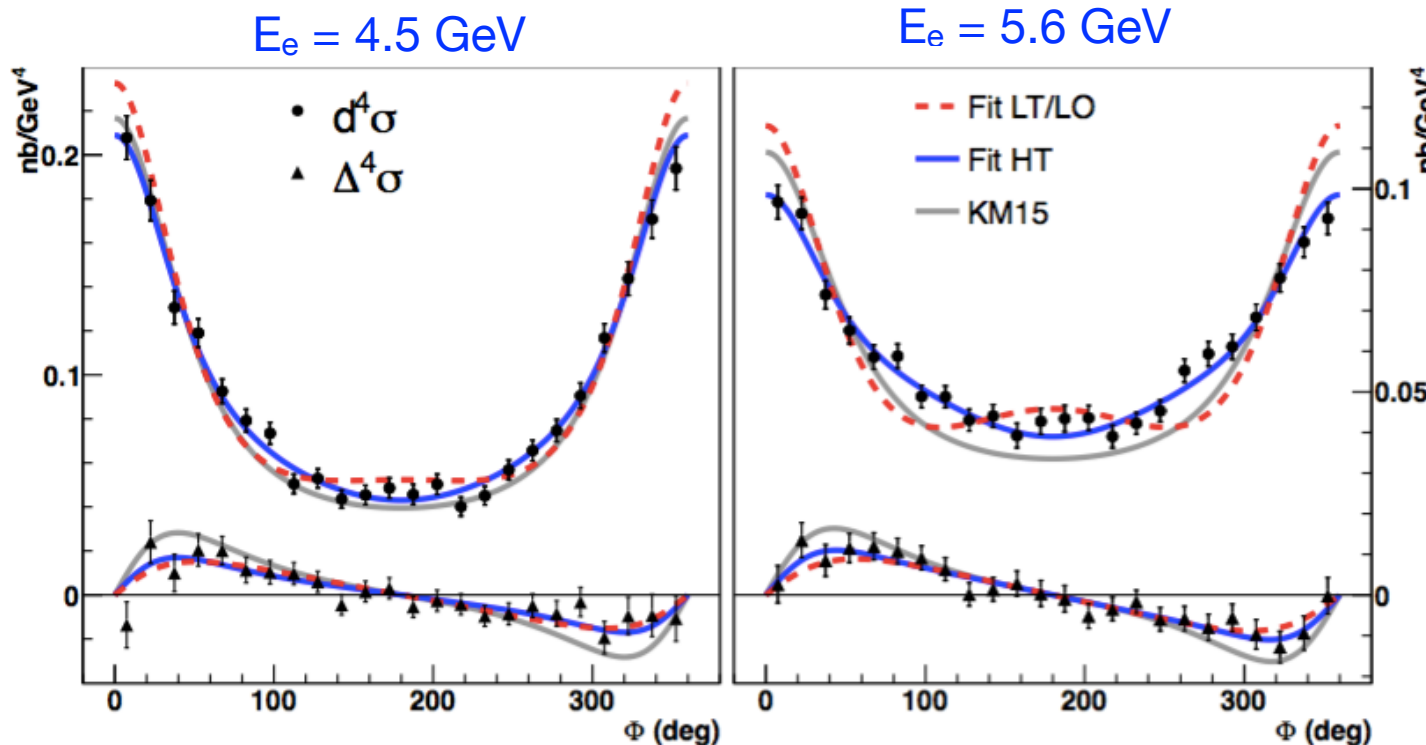


- * Simultaneous fit to cross-sections at both energies and three values of Q^2 using only leading twist and leading order (LT/LO) do not describe the cross-sections fully:
higher twist/order effects?

Using Braun's decomposition, \mathbb{H}_{-+} and \mathbb{H}_{0+} can't be neglected.

Hints of higher twist or higher orders

- * Including either higher order or higher twist effects (HT) improves the match with data:



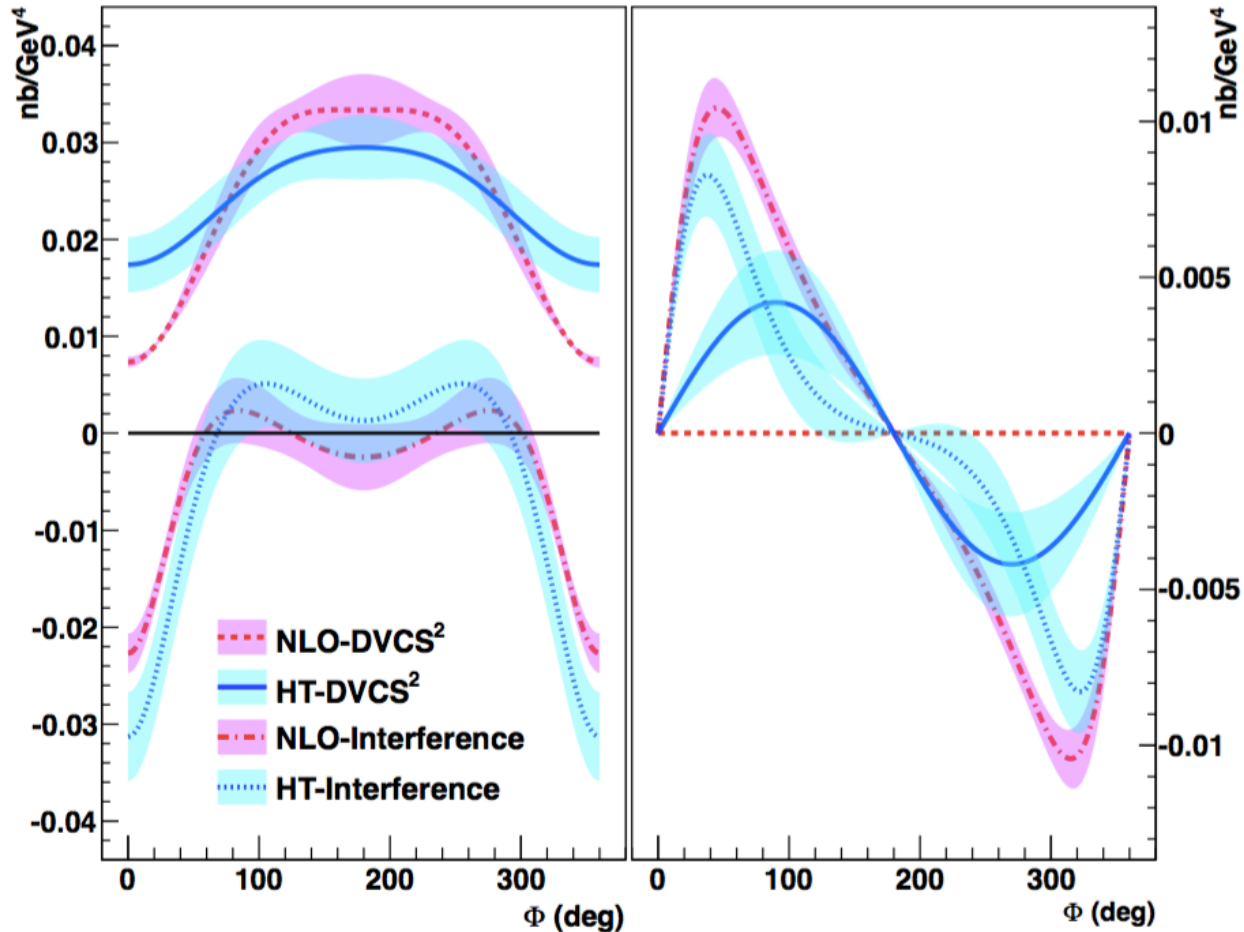
Higher-order and / or higher-twist terms are important! A glimpse of gluons.

Wider range of beam energy needed to identify the dominant effect → **JLab at 11 GeV.**

Rosenbluth separation of DVCS² and BH-DVCS terms

Hall A

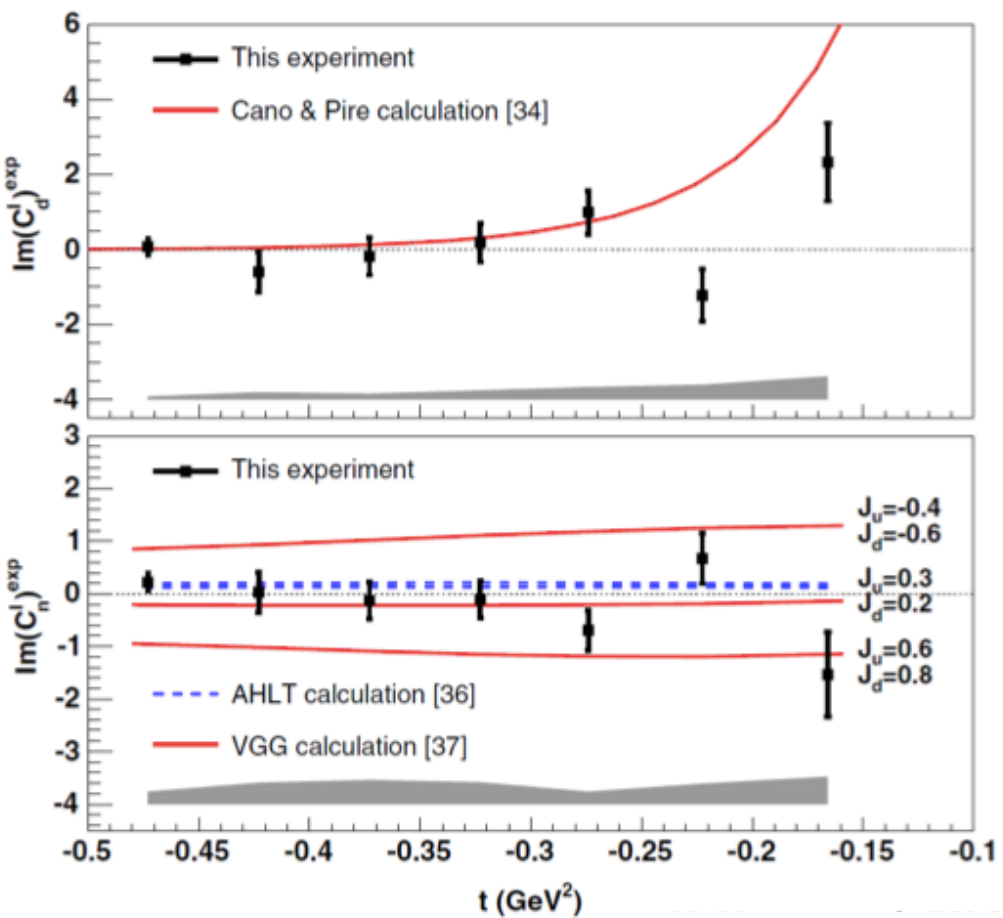
- * Generalised Rosenbluth separation of the DVCS² (scales as E_e^2) and the BH-DVCS interference (scales as E_e^3) terms in the cross-section is possible but NLO and/or higher-twist required.



- * Significant differences between pure DVCS and interference contributions.
- * Helicity-dependent cross-section has a sizeable DVCS² contribution in the higher-twist scenario.
- * Separation of HT and NLO effects requires scans across wider ranges of Q^2 and beam energy: JLab12!

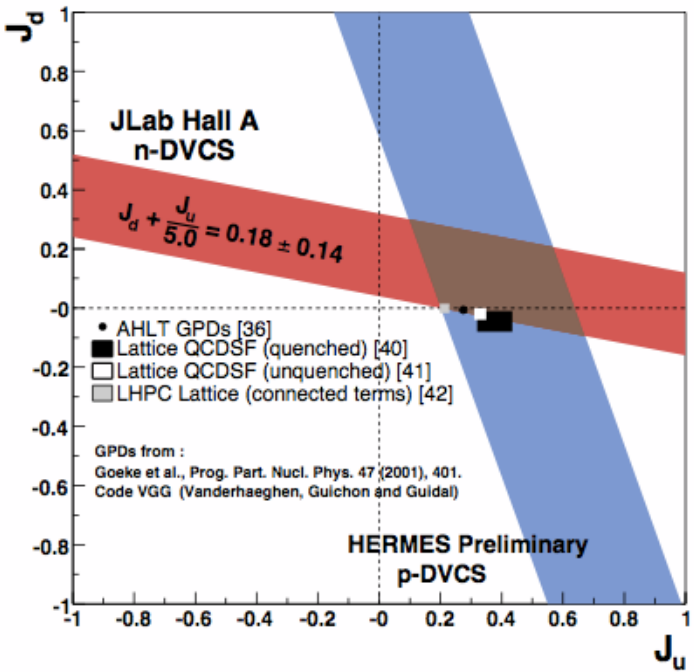
Beam-spin asymmetry in neutron DVCS

Hall A



M. Mazouz et al, PRL 99 (2007) 242501

- * First experimental constraint on E^q , through model interpretation gives constraints on orbital angular momentum of quarks.



Experiment E03-106

DVCS on neutron @ different beam energies

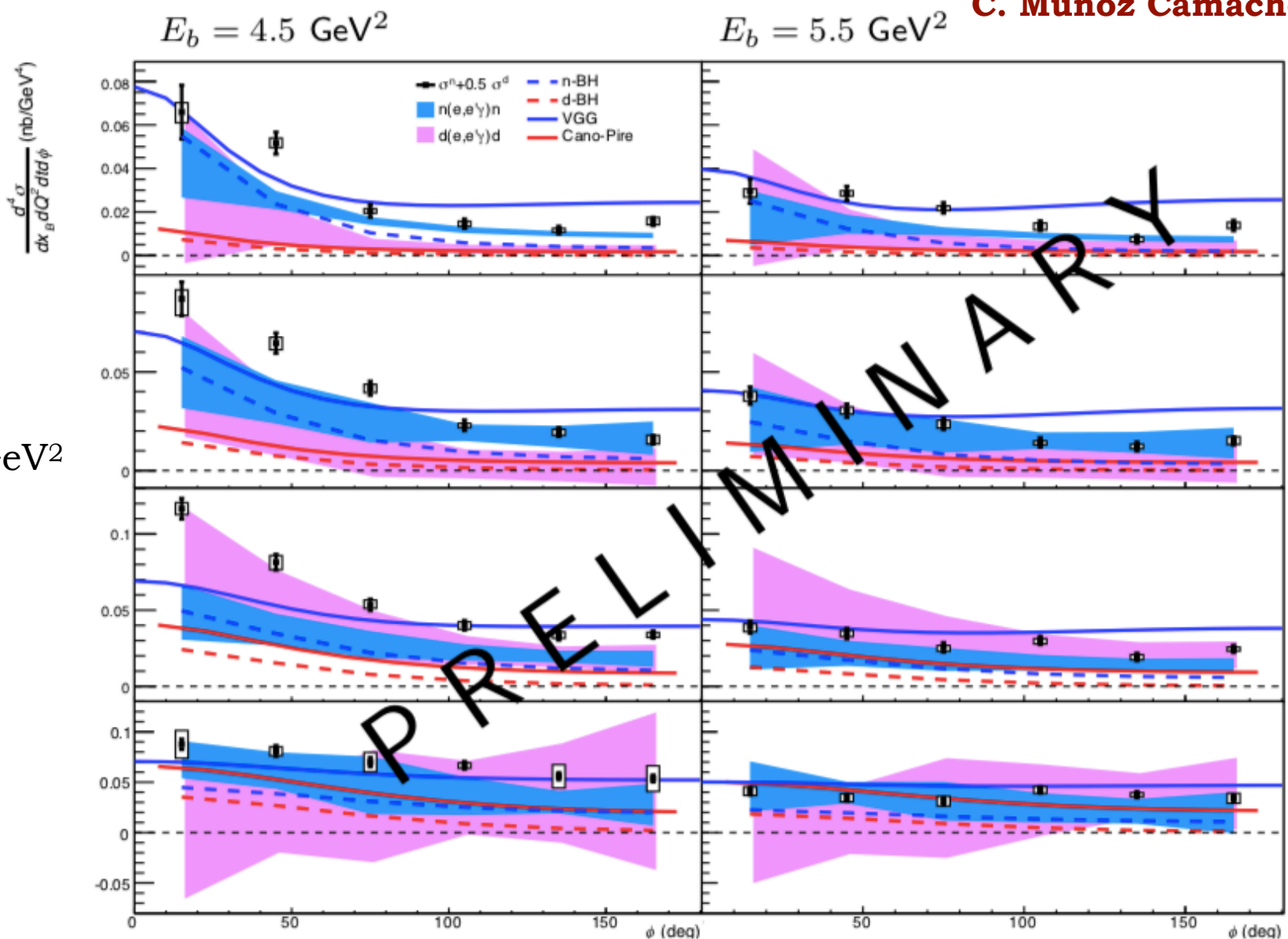
C. Muñoz Camacho

Experiment:
E08-025

LD_2 target

$\langle Q^2 \rangle = 1.75 \text{ GeV}^2$

$\langle x_B \rangle = 0.36$



DVCS on neutron @ different beam energies

C. Muñoz Camacho

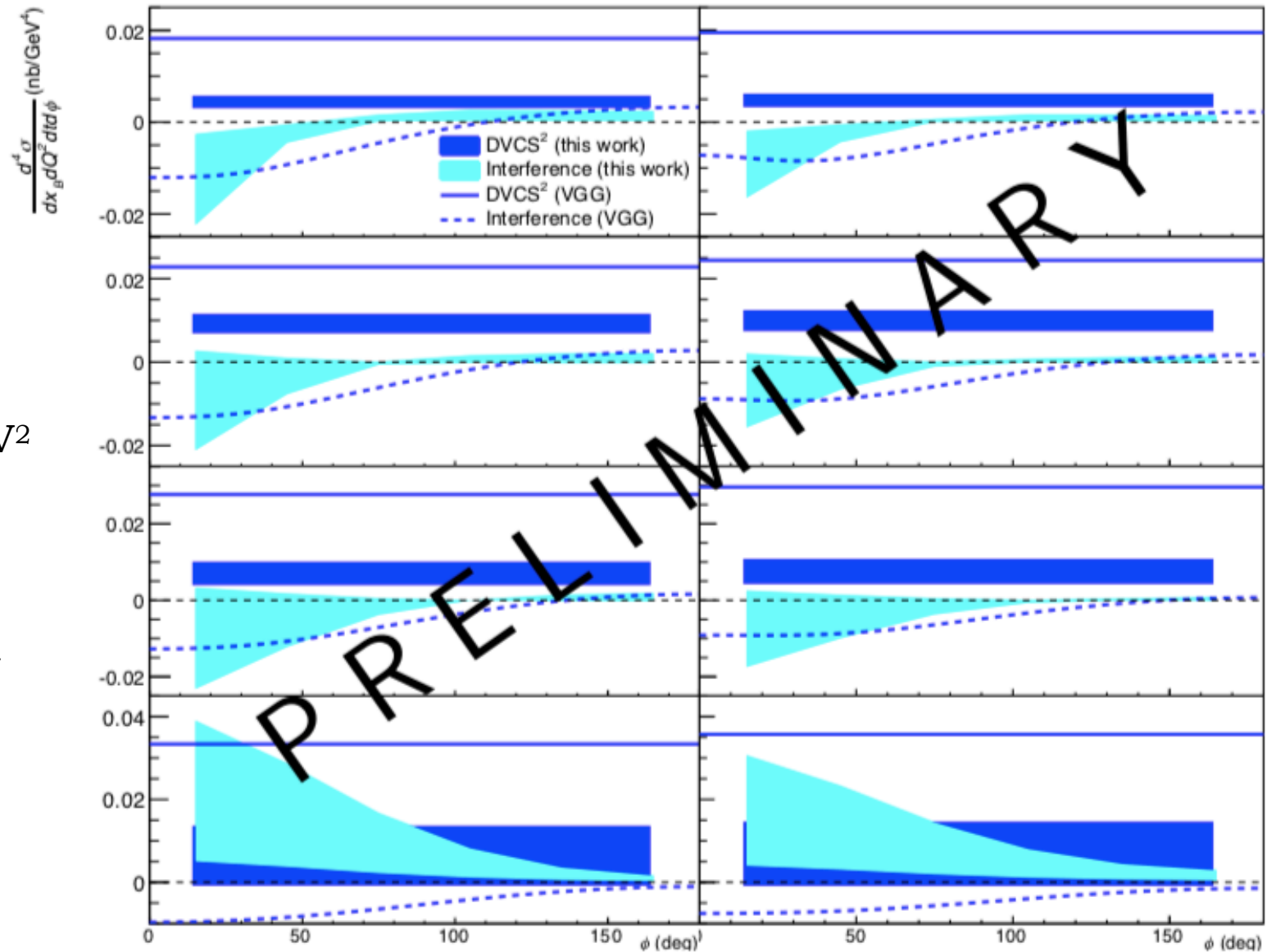
Experiment:
E08-025

LD_2 target

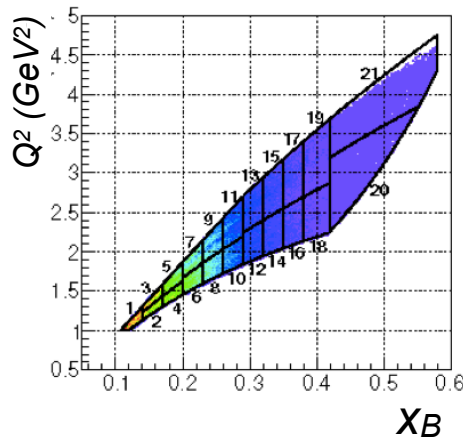
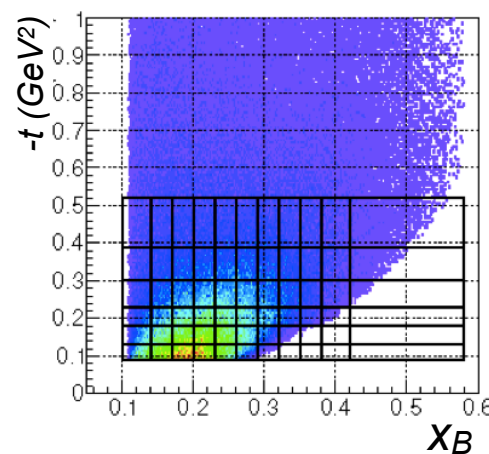
$\langle Q^2 \rangle = 1.75 \text{ GeV}^2$

$\langle x_B \rangle = 0.36$

Separation of
Interference
and DVCS
terms



CLAS unpolarised cross-sections



- BH only
- VGG (Vanderhaeghen, Guichon, Guidal) - H only
- KM10 (Kumericki, Mueller) includes strong \tilde{H}
- - KM10a (sets \tilde{H} to zero)
- - - KMS (Kroll, Moutarde, Sabatié, tuned on low x_B meson-production data)

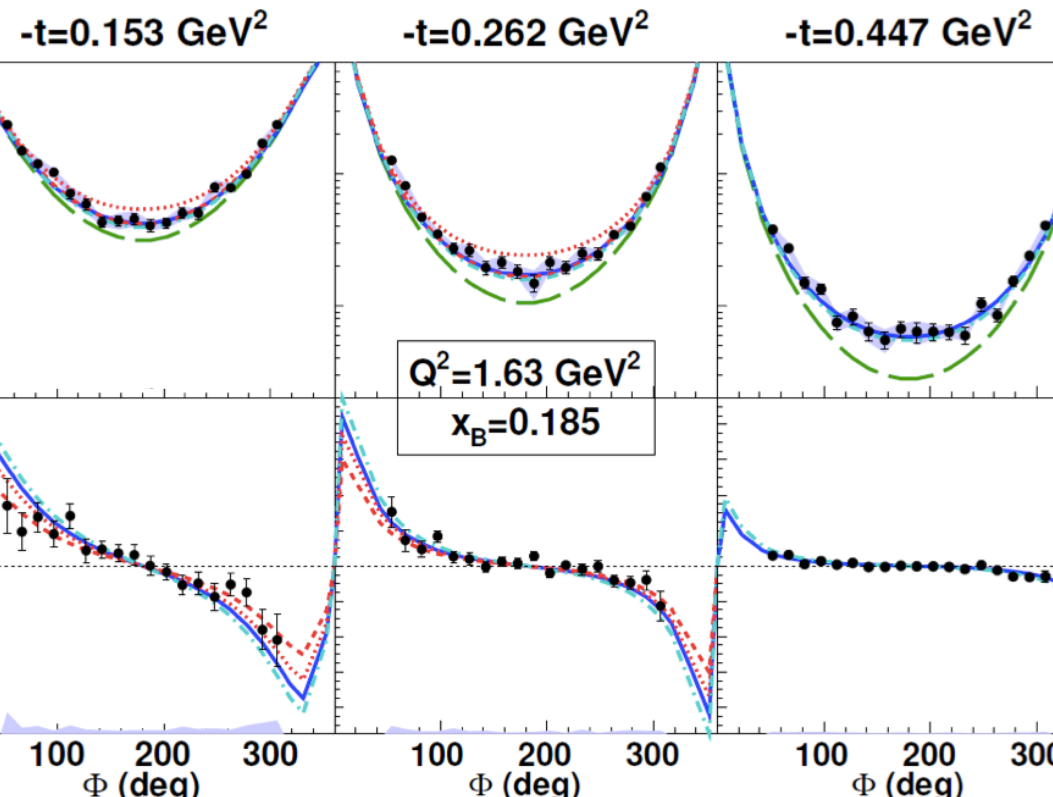
- * Widest phase space coverage in valence quark region: CFF constraints.
- * Dominance of GPD H in unpolarised cross-section.

$$\frac{d^4\sigma_{ep \rightarrow ep\gamma}}{dQ^2 dx_B dt d\Phi}$$

$$\frac{1}{2} \left(\frac{d^4\vec{\sigma}_{ep \rightarrow ep\gamma}}{dQ^2 dx_B dt d\Phi} - \frac{d^4\overleftarrow{\sigma}_{ep \rightarrow ep\gamma}}{dQ^2 dx_B dt d\Phi} \right)$$

$$d^4\sigma \text{ (nb/GeV}^4\text{)}$$

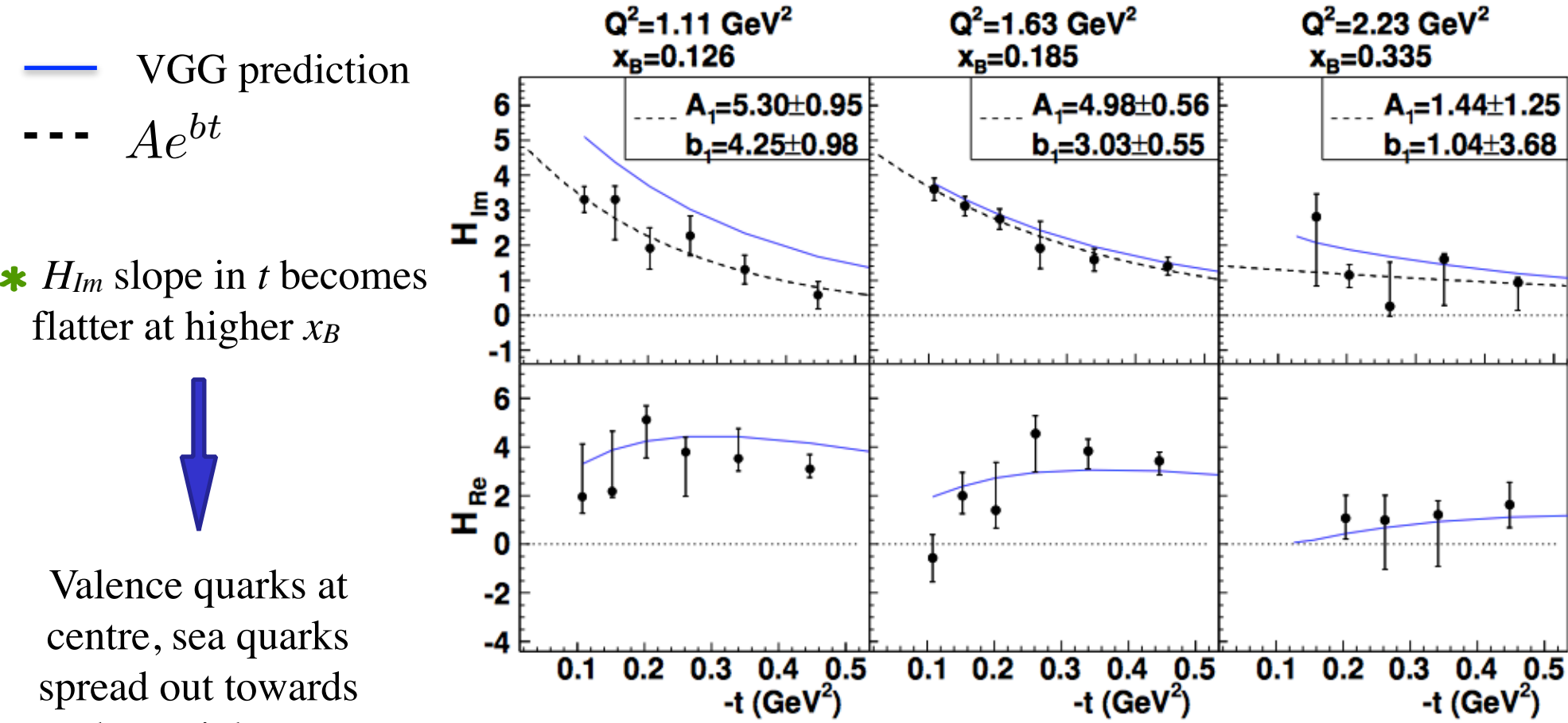
$$\Delta(d^4\sigma) \text{ (nb/GeV}^4\text{)}$$



Towards tomography of the proton

CLAS

- * CFFs extracted in a VGG fit (local fit: constraint 5 times the predicted value)
- * Imaginary part of CFF: $F_{Im}(\xi, t) = F(\xi, \xi, t) \mp F(-\xi, \xi, t)$

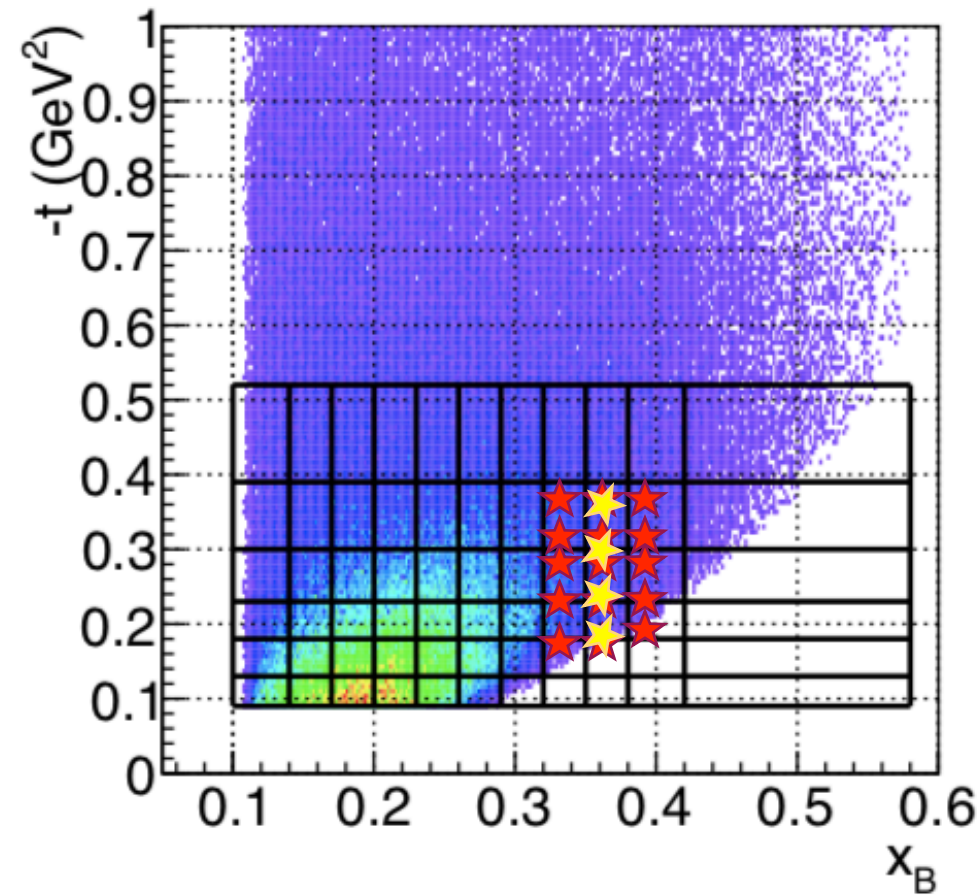
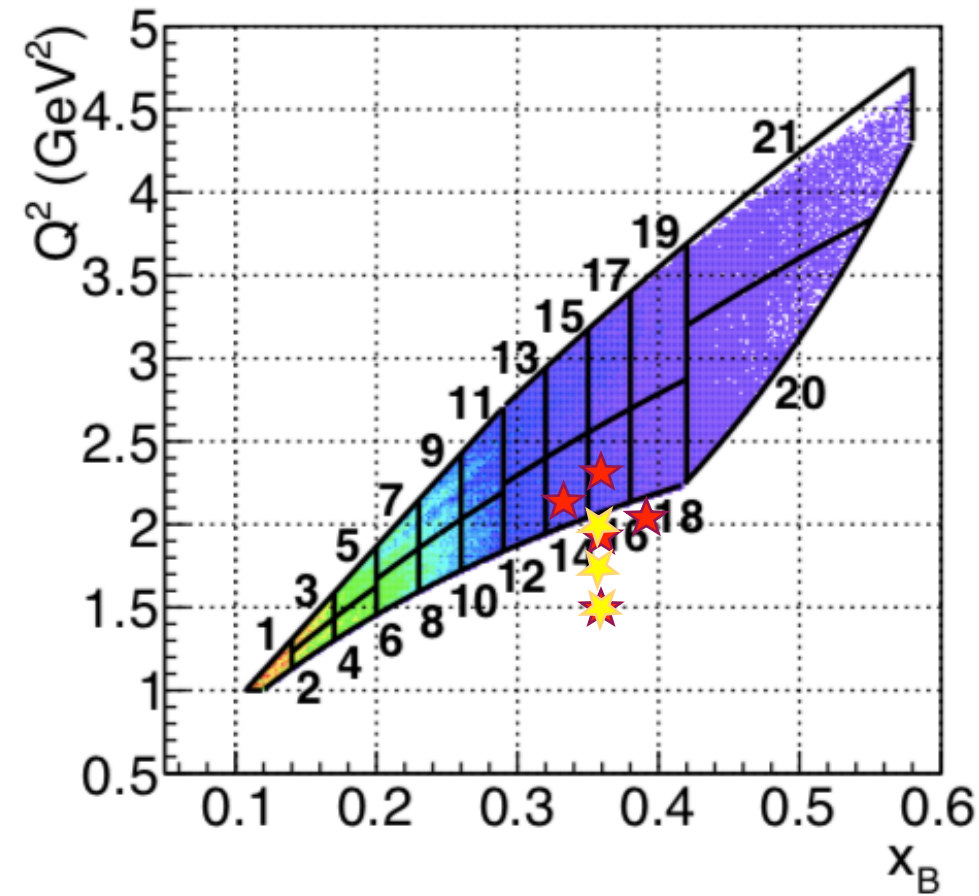


* H_{Im} slope in t becomes flatter at higher x_B



Valence quarks at centre, sea quarks spread out towards the periphery.

JLab 6 GeV era DVCS X-sections: kinematics

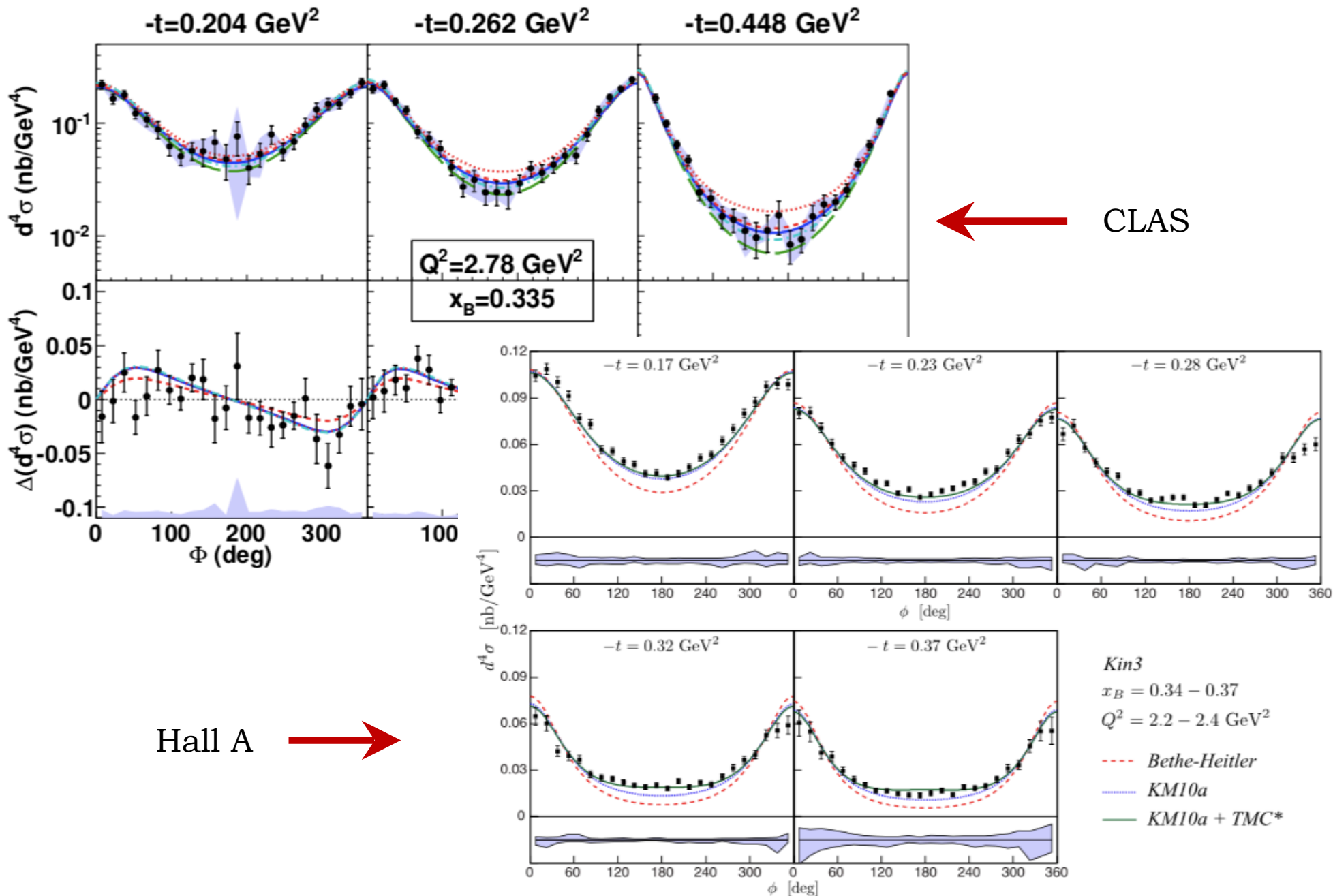


CLAS 2D distributions: H.-S. Jo *et al* (CLAS), **PRL 115** (2015) 212003

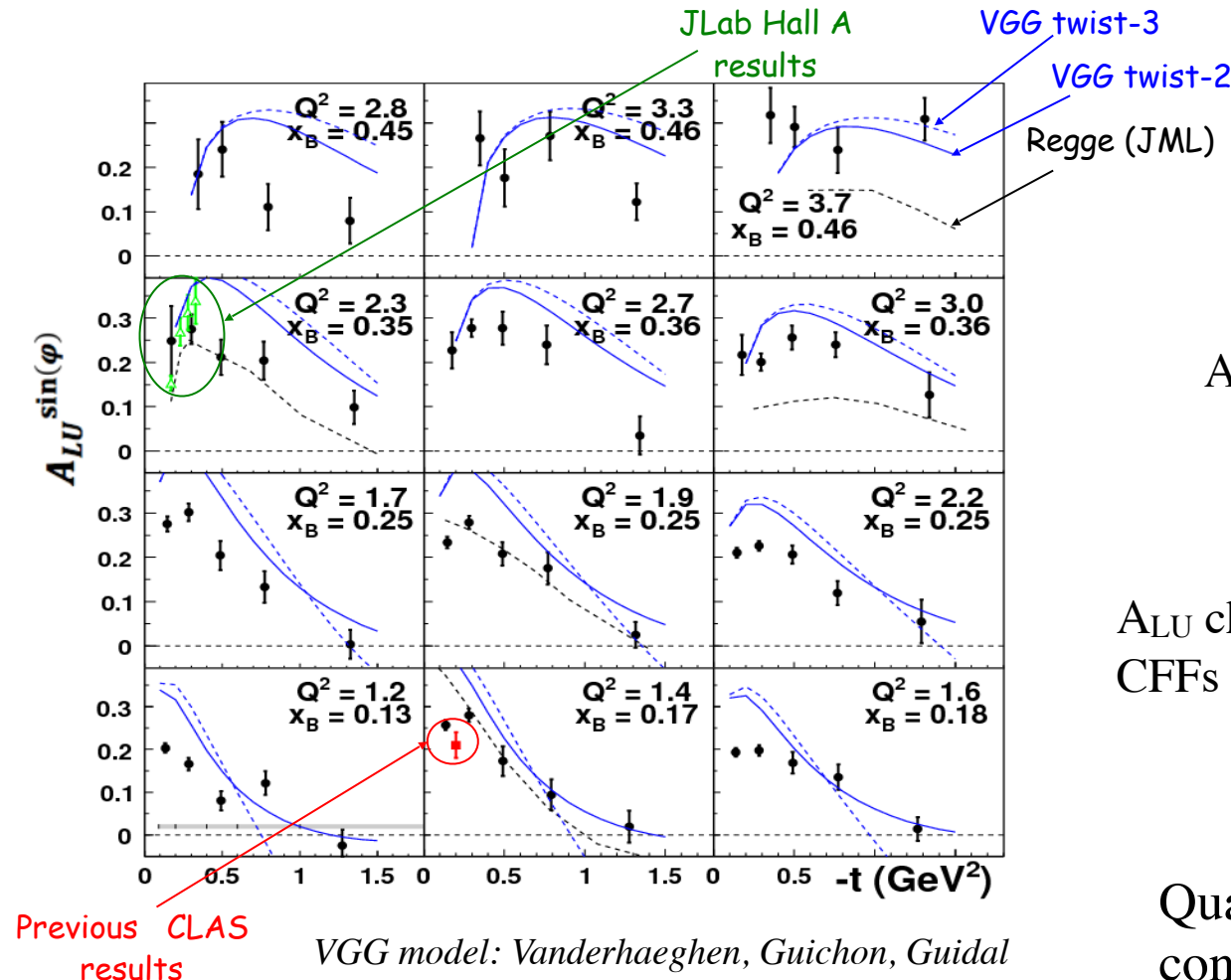
Hall A

★ M. Defurne *et al*, **PRC 92** (2015) 055202

★ M. Defurne *et al*, **Nature Communications 8** (2017) 1408



Beam-spin Asymmetry (A_{LU})



Follows first CLAS measurement:
S. Stepanyan *et al* (CLAS), **PRL 87**
(2001) 182002

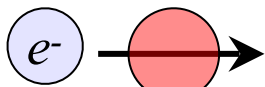
A_{LU} from fit to asymmetry:

$$A_i = \frac{\alpha_i \sin \phi}{1 + \beta_i \cos \phi}$$

A_{LU} characterised by imaginary parts of
CFFs via: $F_1 \mathbf{H} + \xi G_M \tilde{\mathbf{H}} - \frac{t}{4M^2} \mathbf{E}$

Qualitative agreement with models,
constraints on fit parameters.

Target-spin Asymmetry (A_{UL})



Follows first CLAS measurement:
 S. Chen *et al* (CLAS),
PRL 97 (2006) 072002

A_{UL} from fit to asymmetry:

$$A_i = \frac{\alpha_i \sin \phi}{1 + \beta_i \cos \phi}$$

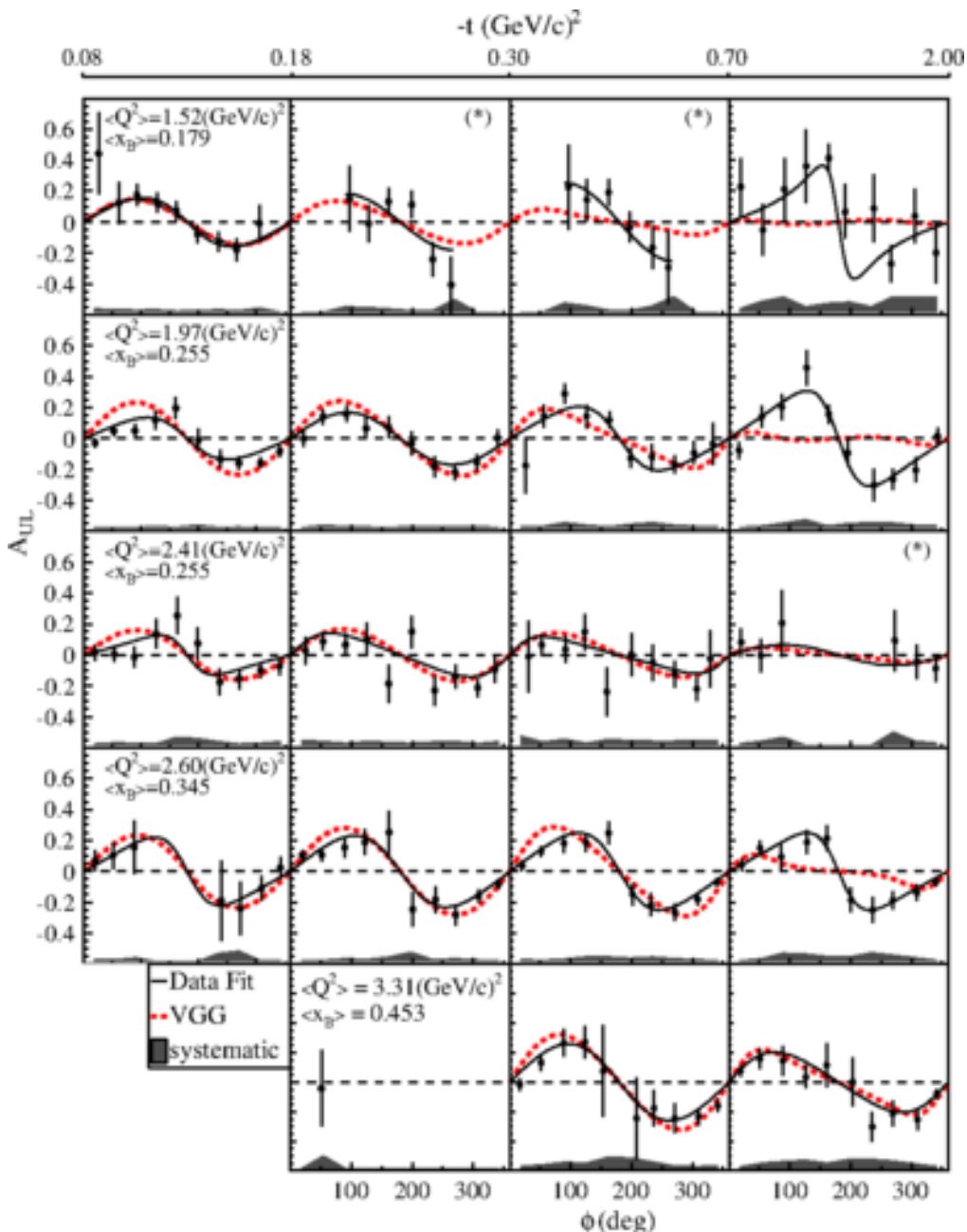
A_{UL} characterised by imaginary parts of CFFs
 via:

$$F_1 \tilde{H} + \xi G_M (\textcolor{red}{H} + \frac{x_B}{2} \textcolor{blue}{E}) - \frac{\xi t}{4M^2} F_2 \tilde{E} + \dots$$

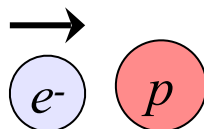
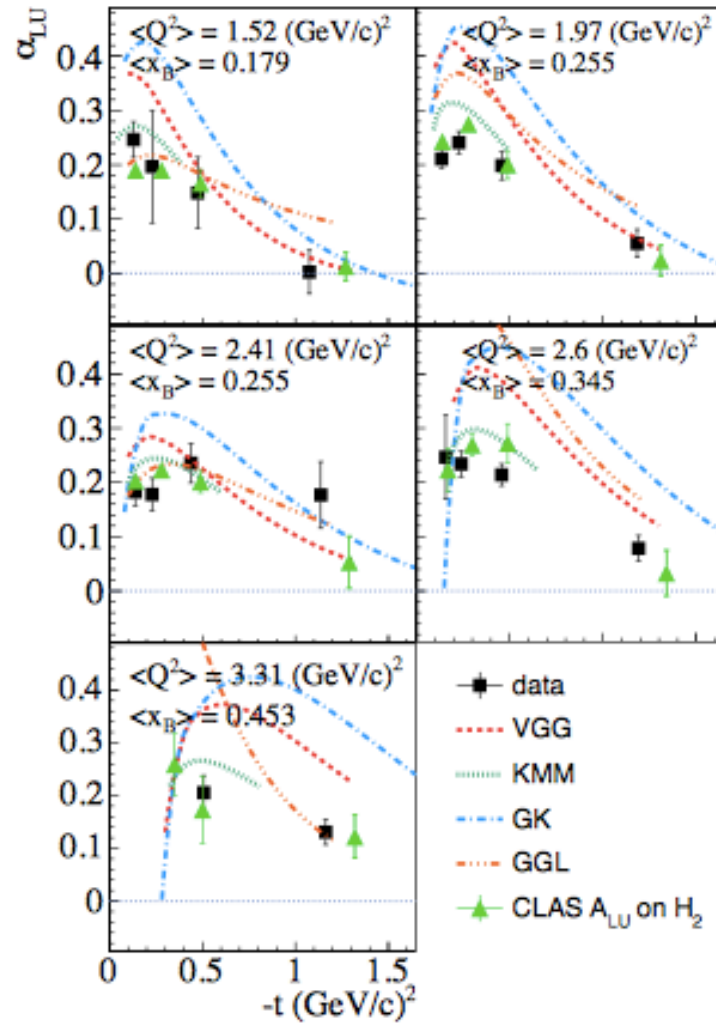
High statistics, large kinematic coverage,
 strong constraints on fits, simultaneous fit
 with BSA and DSA from the same dataset.

E. Seder *et al* (CLAS), **PRL 114** (2015) 032001

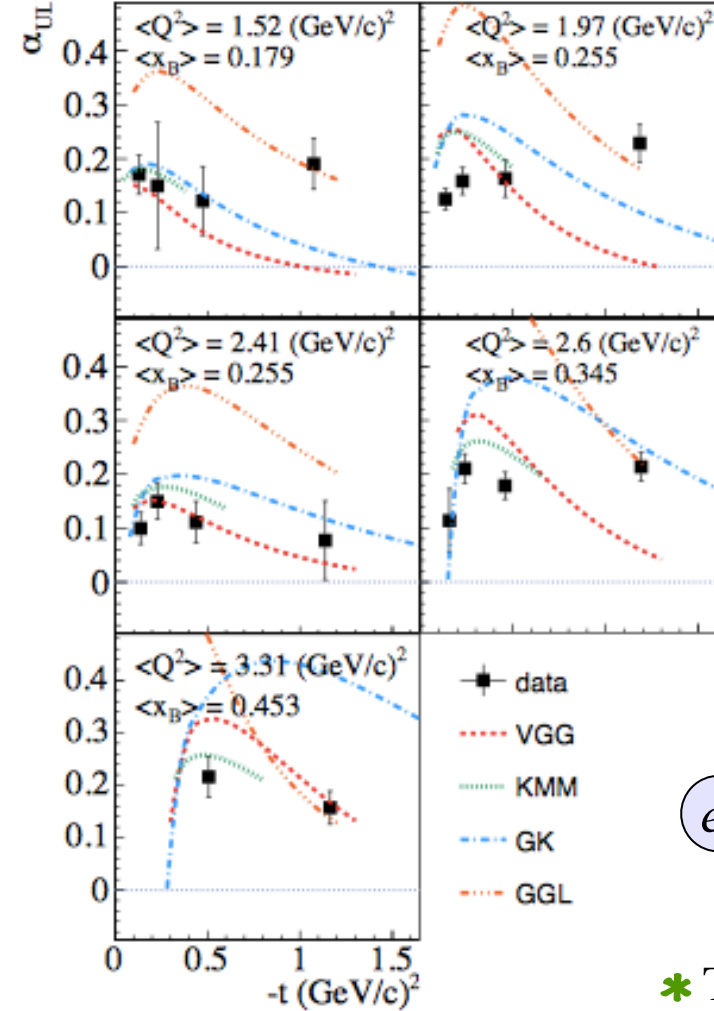
S. Pisano *et al* (CLAS), **PRD 91** (2015) 052014



Beam- and target-spin asymmetries



S. Pisano *et al* (CLAS), **PRD 91** (2015) 052014
 E. Seder *et al* (CLAS), **PRL 114** (2015) 032001



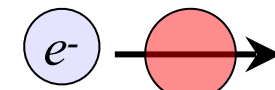
$$A = \frac{\alpha \sin \phi}{1 + \beta \cos \phi}$$

GGL: Goldstein,
Gonzalez, Liuti

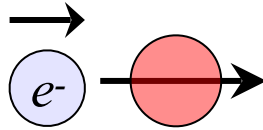
GK: Kroll, Moutarde,
Sabatié

KMM: Kumericki,
Mueller, Murray

VGG: Vanderhaeghen,
Guichon, Guidal

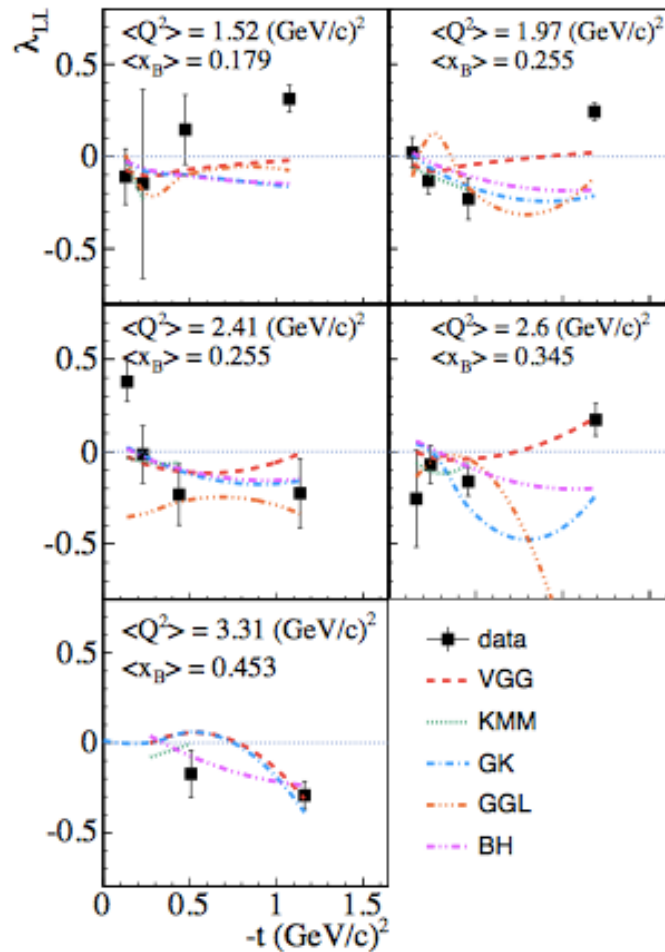
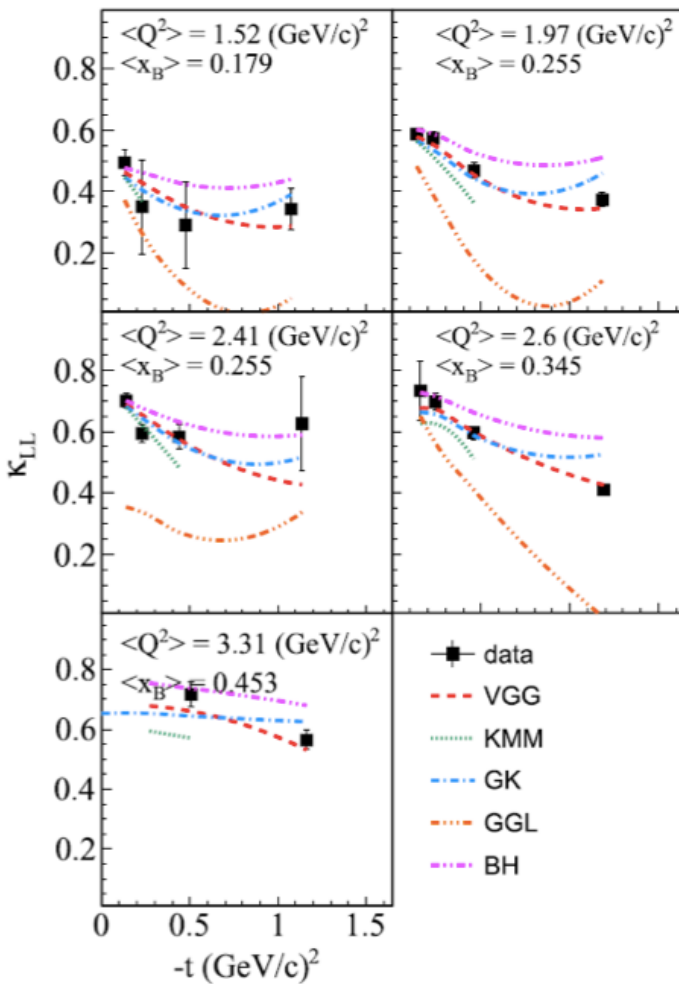


* TSA shows a flatter distribution in t than BSA.



Double-spin Asymmetry (A_{LL})

~~CLAS~~



A_{LL} from fit to asymmetry:

$$\frac{\kappa_{LL} + \lambda_{LL} \cos \phi}{1 + \beta \cos \phi}$$

ALL characterised by real parts of CFFs via:

$$F_1 \tilde{H} + \xi G_M (H + \frac{x_B}{2} E) + \dots$$

- * Fit parameters extracted from a simultaneous fit to BSA, TSA and DSA.
- * Constant term dominates and is almost entirely BH.

What can we learn from the asymmetries?

Answers hinge on a global analysis of all available data.

- * Information on relative distributions of quark momenta (PDFs) and quark helicity, $\Delta q(x)$.

$$H(x, 0, 0) = q(x) \quad \tilde{H}(x, 0, 0) = \Delta q(x)$$

- * Indications that axial charge is more concentrated than electromagnetic charge.

$$Im(H)$$

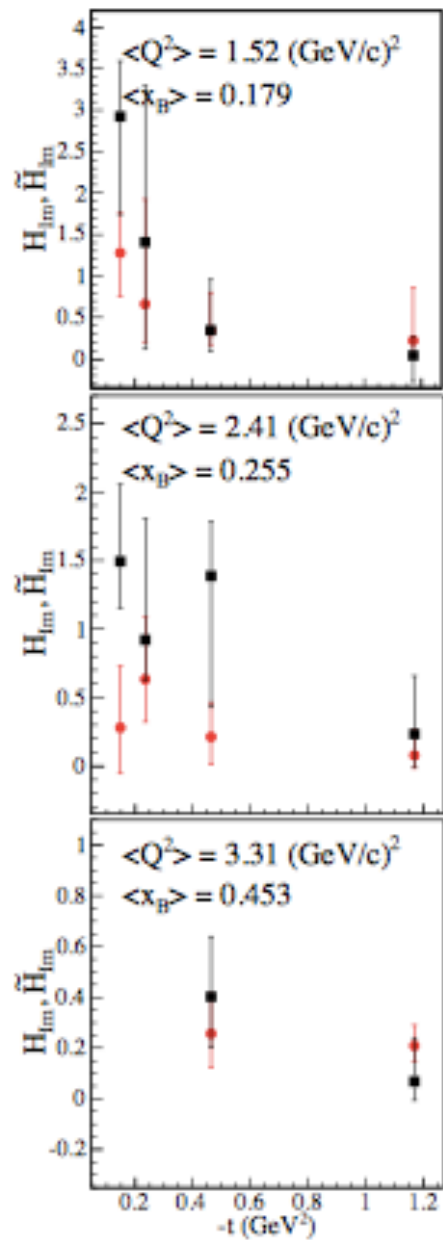
$$Im(\tilde{H})$$

VGG extraction

$$\int_{-1}^{+1} H dx = F_1$$

$$\int_{-1}^{+1} \tilde{H} dx = G_A$$

E. Seder *et al* (CLAS), **PRL 114** (2015) 032001
 S. Pisano *et al* (CLAS), **PRD 91** (2015) 052014



Towards nucleon tomography

Quasi model-independent extraction of CFFs based on a local fit:

- * Set 8 CFFs as free parameters to fit, at each (x_B, t) point, the available observables.
- * Limits imposed within $+/- 5$ times the VGG model predictions (Vanderhaeghen-Guichon-Guidal).
- * Leading-twist DVCS amplitude parametrisation based on Double Distributions.

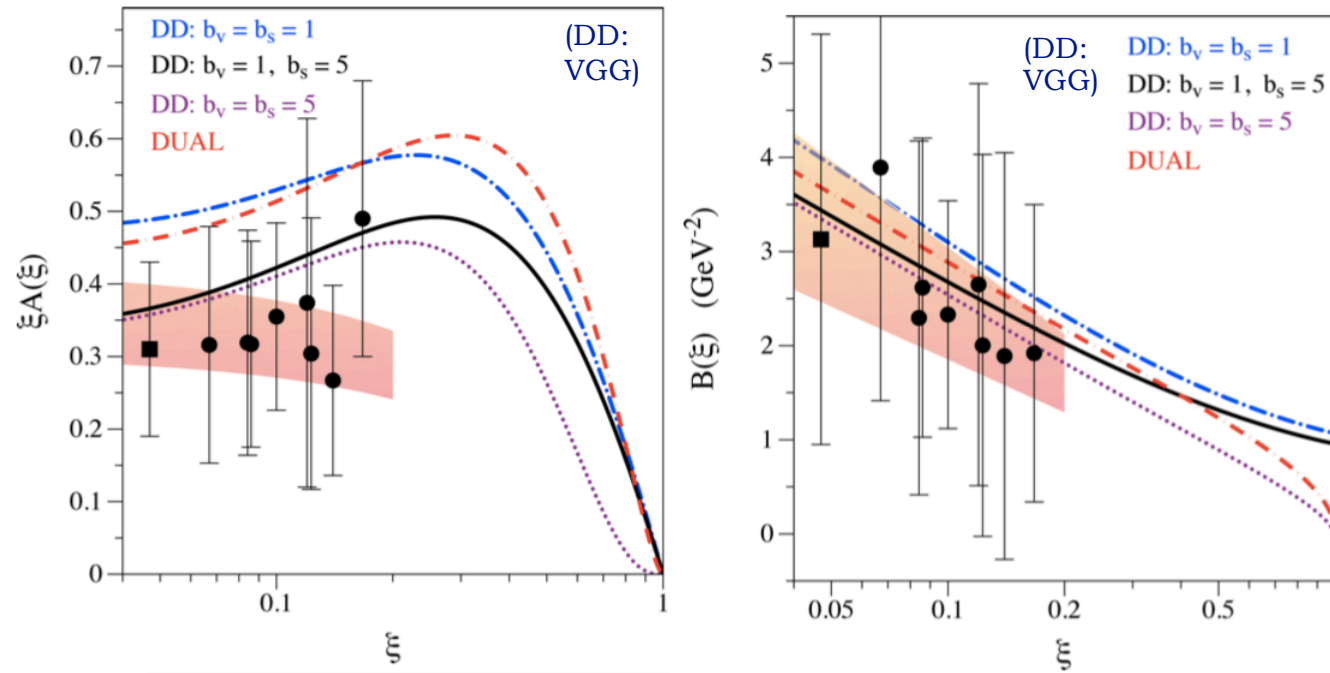
The best constraints in fits to CLAS data were obtained on H_{Im} .

Parametrise its dependence on t :

$$H_{Im}(\xi, t) = A(\xi)e^{B(\xi)t}$$

Relates to quark density

Inverse relation to spatial distribution



Towards nucleon tomography

Relating the impact parameter to helicity-averaged transverse distribution:

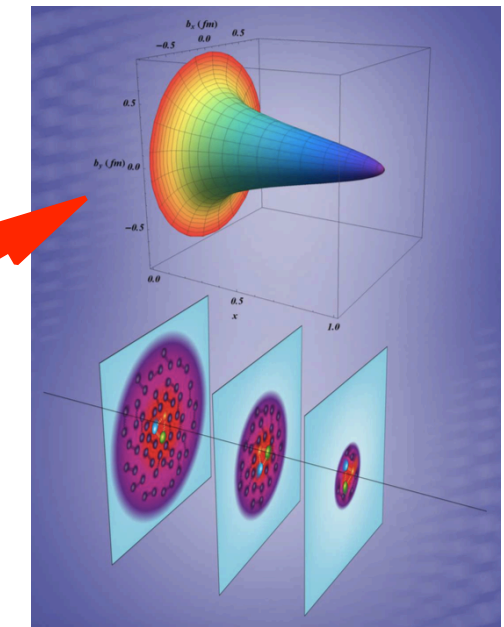
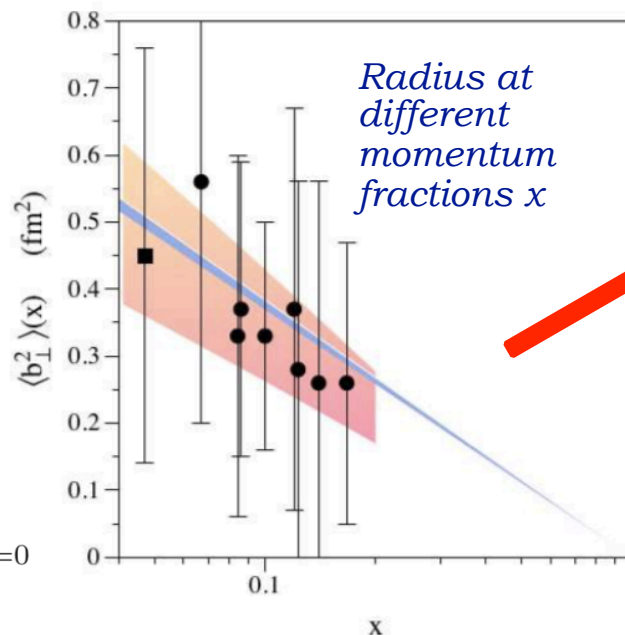
$$\rho^q(x, \mathbf{b}_\perp) = \int \frac{d^2 \Delta_\perp}{(2\pi)^2} e^{-i \mathbf{b}_\perp \cdot \Delta_\perp} H_-^q(x, 0, -\Delta_\perp^2)$$

$$H_-^q(x, 0, t) \equiv H^q(x, 0, t) + H^q(-x, 0, t)$$

Transverse four-momentum transfer to nucleon

Assuming leading-twist and exponential dependence of GPD on t , using models to extrapolate to the zero skewness point $\xi = 0$ and assuming similar behaviour for u and d quarks there:

$$\langle b_\perp^2 \rangle^q(x) = -4 \frac{\partial}{\partial \Delta_\perp^2} \ln H_-^q(x, 0, -\Delta_\perp^2) \Big|_{\Delta_\perp=0}$$



Tentative hints of 3D distributions are emerging.

Imaging pressure within the nucleon

* GPDs provide indirect access to mechanical properties of the nucleon (encoded in the gravitational form factors, GFFs, of the energy-momentum tensor).

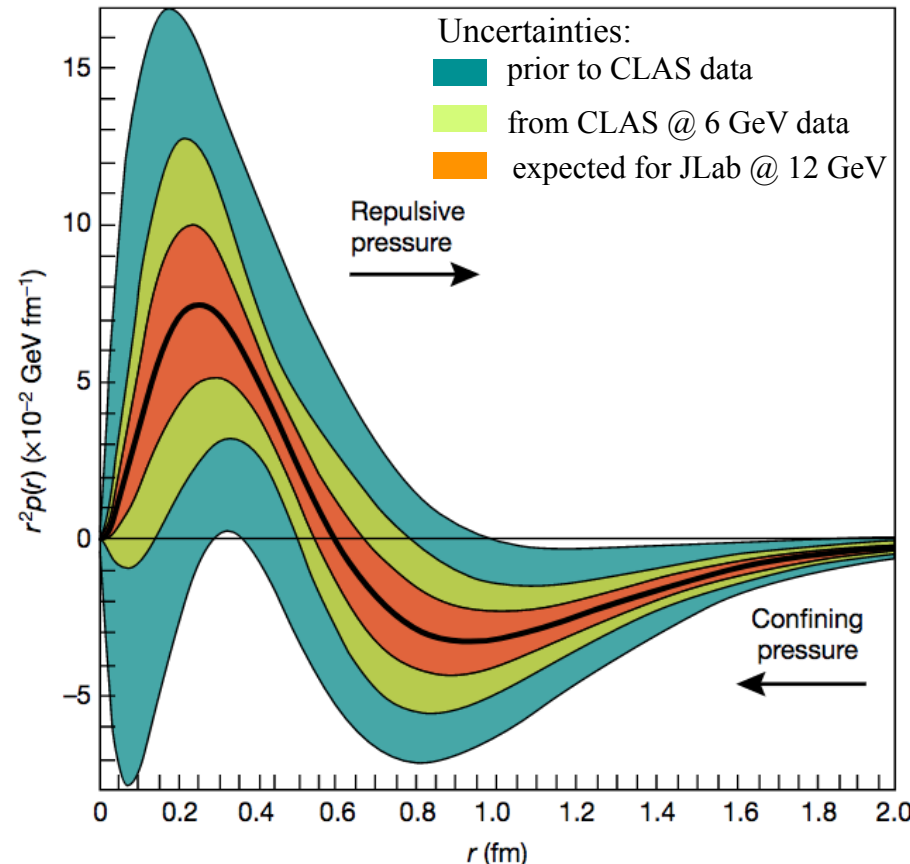
* Three scalar GFFs, functions of t : encode pressure and shear forces ($d_1(t)$), mass ($M_2(t)$) and angular momentum distributions ($J(t)$).

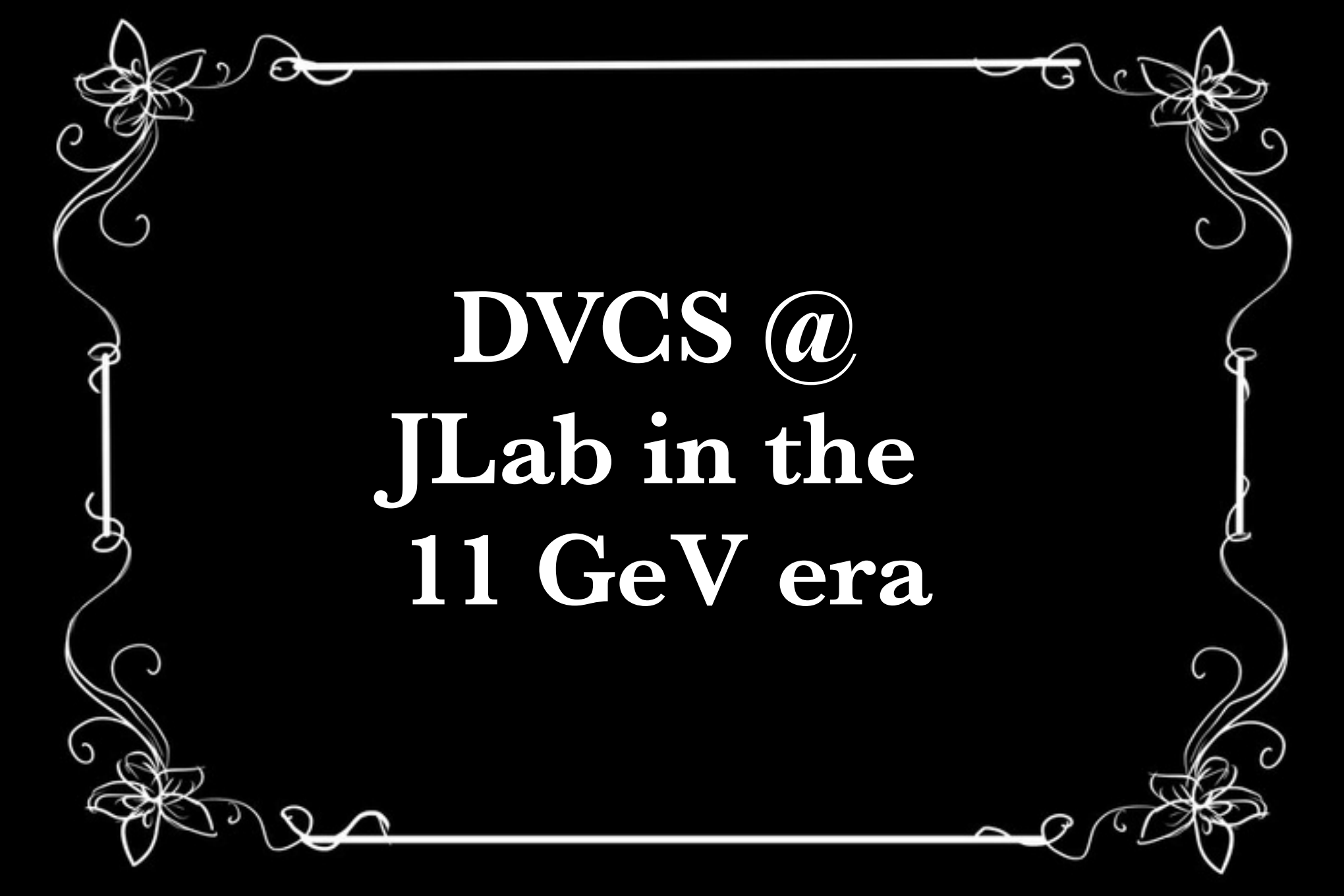
* Can be related to GPDs via sum rules:

$$\int x [H(x, \xi, t) + E(x, \xi, t)] dx = 2J(t)$$

$$\int x H(x, \xi, t) dx = M_2(t) + \frac{4}{5} \xi^2 d_1(t)$$

* Possibility of extracting pressure distributions! More data needed.





DVCS @
JLab in the
11 GeV era

DVCS Cross-sections: Halls A and C

Experiments:

E12-06-114 (Hall A, 100 days),

E12-13-010 (Hall C, 53 days)

C. Muñoz Camacho et al.,

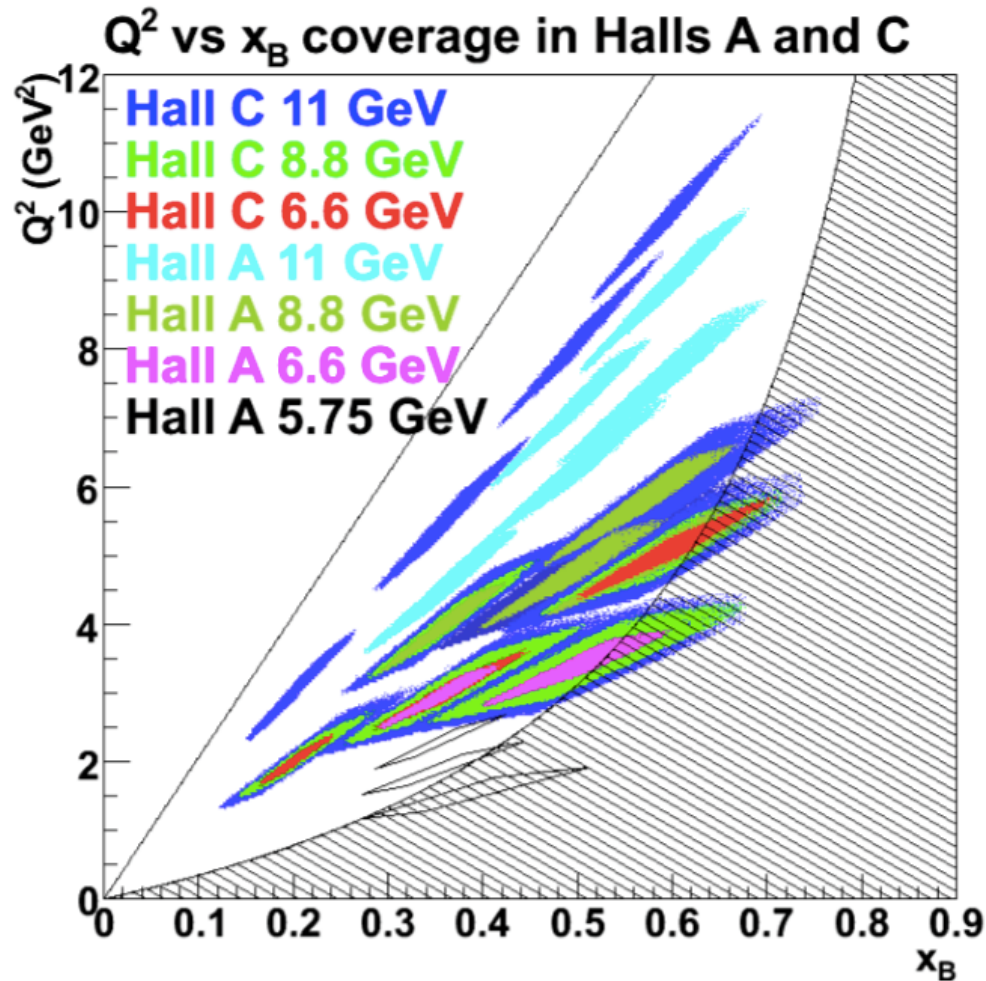
C. Hyde et al.

Unpolarised liquid H₂ target:

- Beam energies: 6.6, 8.8, 11 GeV
- Scans of Q^2 at fixed x_B .
- Hall A: aim for absolute cross-sections with 4% relative precision.

* Azimuthal, energy and helicity dependencies of cross-section to separate $|T_{DVCS}|^2$ and interference contributions in a wide kinematic coverage.

* Separate *Re* and *Im* parts of the DVCS amplitude.



Hall A started taking data last spring!

Proton DVCS @ 11 GeV



Experiment E12-06-119

F. Sabatié et al.

$P_{\text{beam}} = 85\%$

$L = 10^{35} \text{ cm}^{-2}\text{s}^{-1}$

$1 < Q^2 < 10 \text{ GeV}^2$

$0.1 < x_B < 0.65$

$-t_{\min} < -t < 2.5 \text{ GeV}^2$

*Kinematics similar for all proton DVCS
@ 11 GeV with CLAS12 experiments*

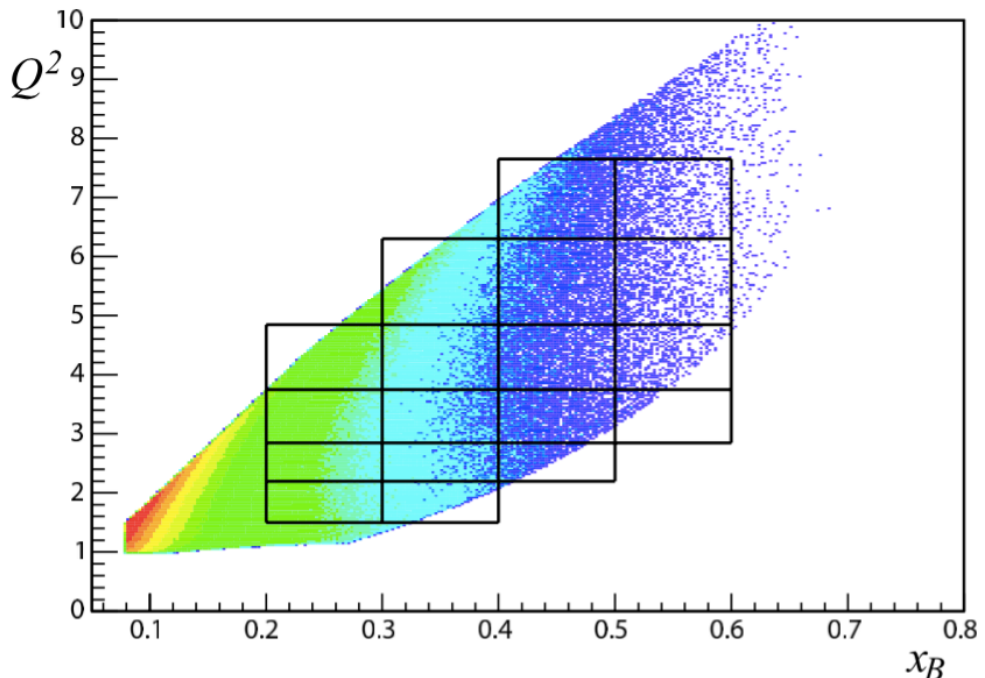
Unpolarised liquid H₂ target:

- Statistical error: 1% - 10% on $\sin\varphi$ moments
- Systematic uncertainties: ~ 6 - 8%

ALU characterised by imaginary parts of

CFFs via:

$$F_1 \mathbf{H} + \xi G_M \tilde{\mathbf{H}} - \frac{t}{4M^2} \mathbf{E} \longrightarrow \mathbf{Im}(\mathbf{H}_p)$$



First experiment with CLAS12

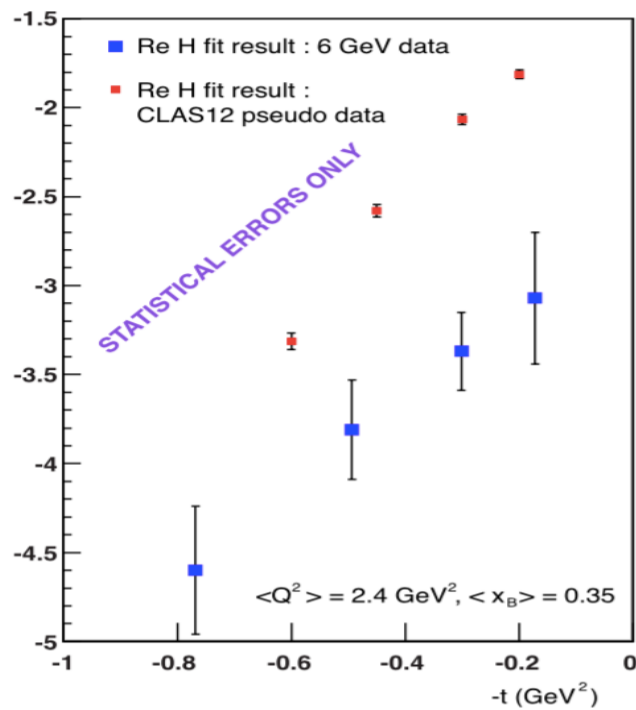
Started this February!

Proton DVCS @ 11 GeV

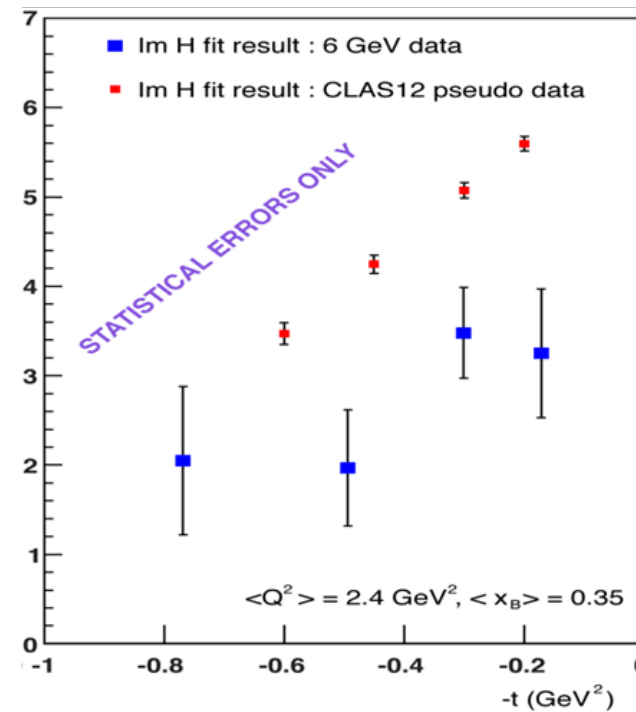


Impact of CLAS12 unpolarised target proton-DVCS data on the extraction of $\text{Re}(H)$ and $\text{Im}(H)$.

$\text{Re}(H)$



$\text{Im}(H)$



(CLAS 6 GeV extraction H. Moutarde)

DVCS at lower energies with CLAS12

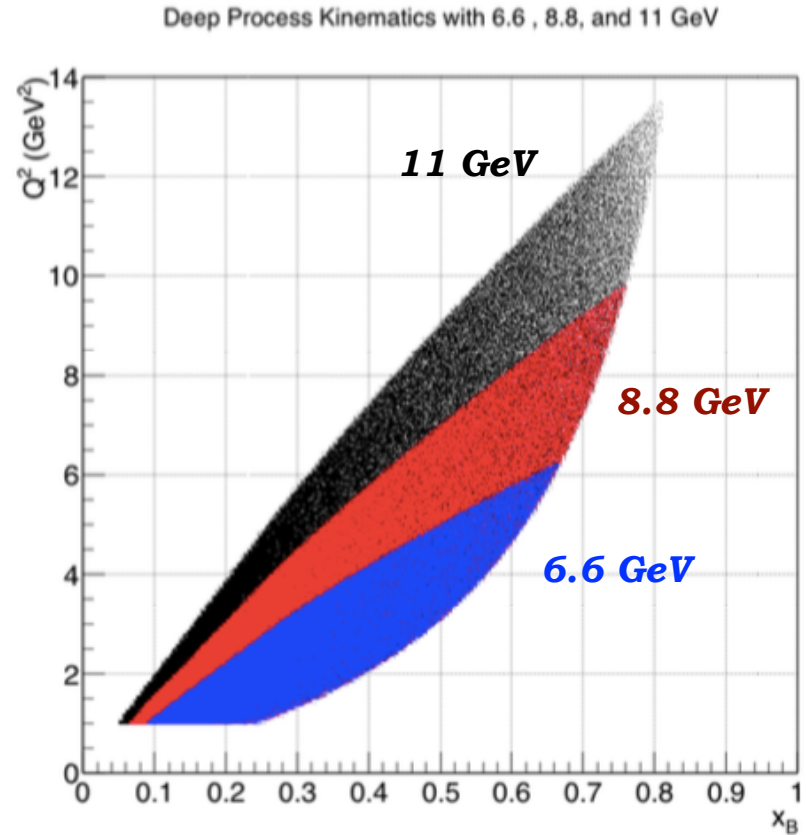


Experiment E12-16-010B

F.-X. Girod et al.

Unpolarised liquid H₂ target:

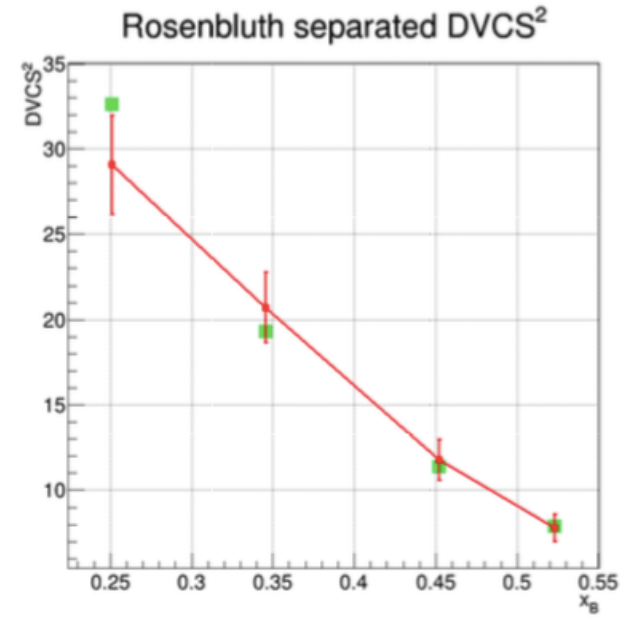
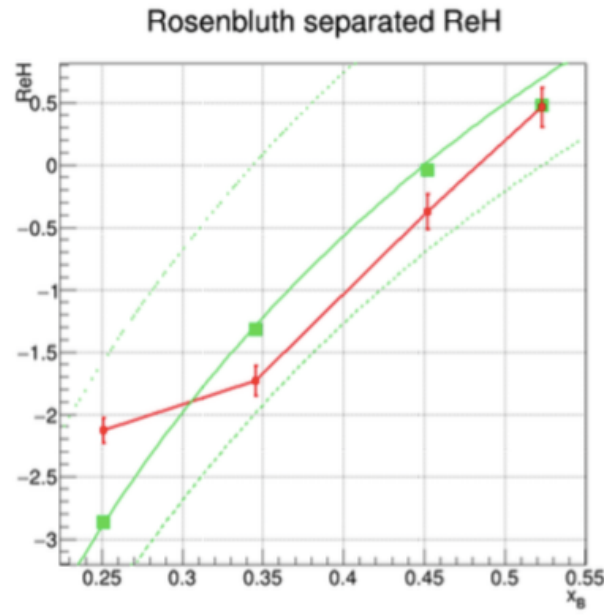
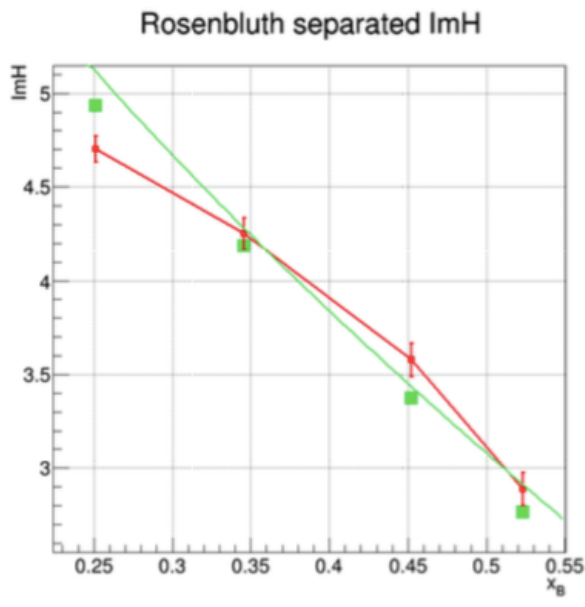
- Beam energies: 6.6, 8.8 GeV
 - Simultaneous fit to beam-spin and total cross-sections.
- * Rosenbluth separation of interference and $|T_{DVCS}|^2$ terms in the cross-section
- * Scaling tests of the extracted CFFs
- * Model-dependent determination of the D-term in the Dispersion Relation between *Re* and *Im* parts of CFFs: sensitivity to Gravitational Form Factors.



Compare with measurements from Halls A and C: cross-check model and systematic uncertainties.

DVCS at lower energies with CLAS12

Projected extraction of CFFs (red) compared to generated values (green). Three curves on the $Re(H)$ show three different scenarios for the D-term.

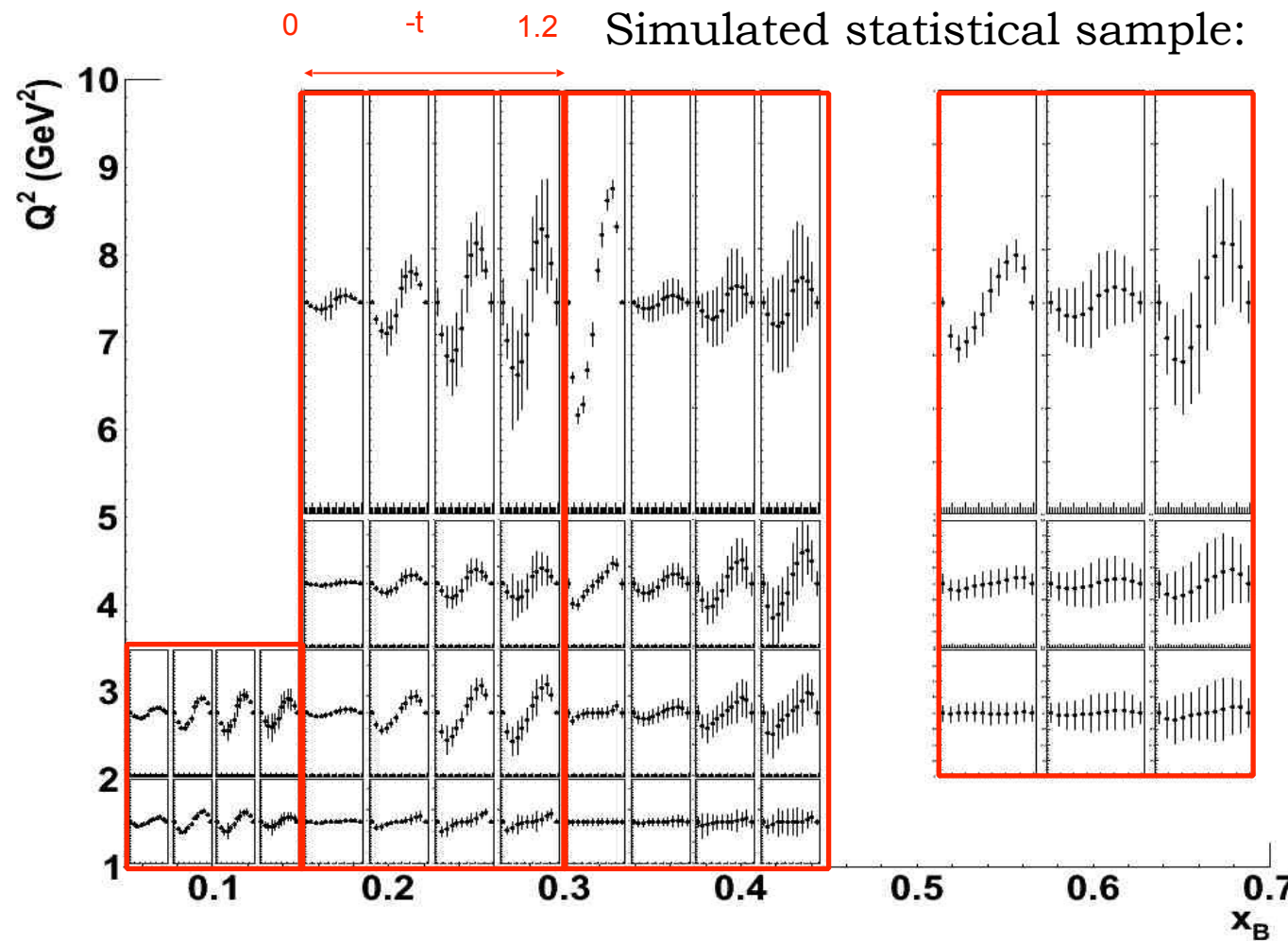




Neutron DVCS @ 11 GeV

Experiment E12-11-003
S. Niccolai, D. Sokhan et al.

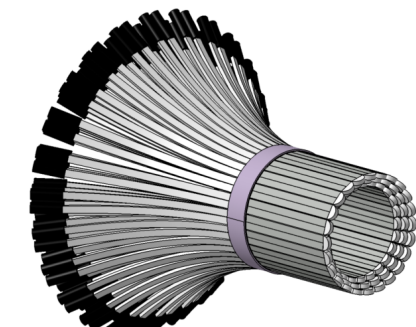
$$\Delta\sigma_{LU} \sim \sin\phi \operatorname{Im}\{F_1 H + \xi(F_1 + F_2) \tilde{H} - k F_2 E\} d\phi$$



$\operatorname{Im}(E_n)$ dominates.

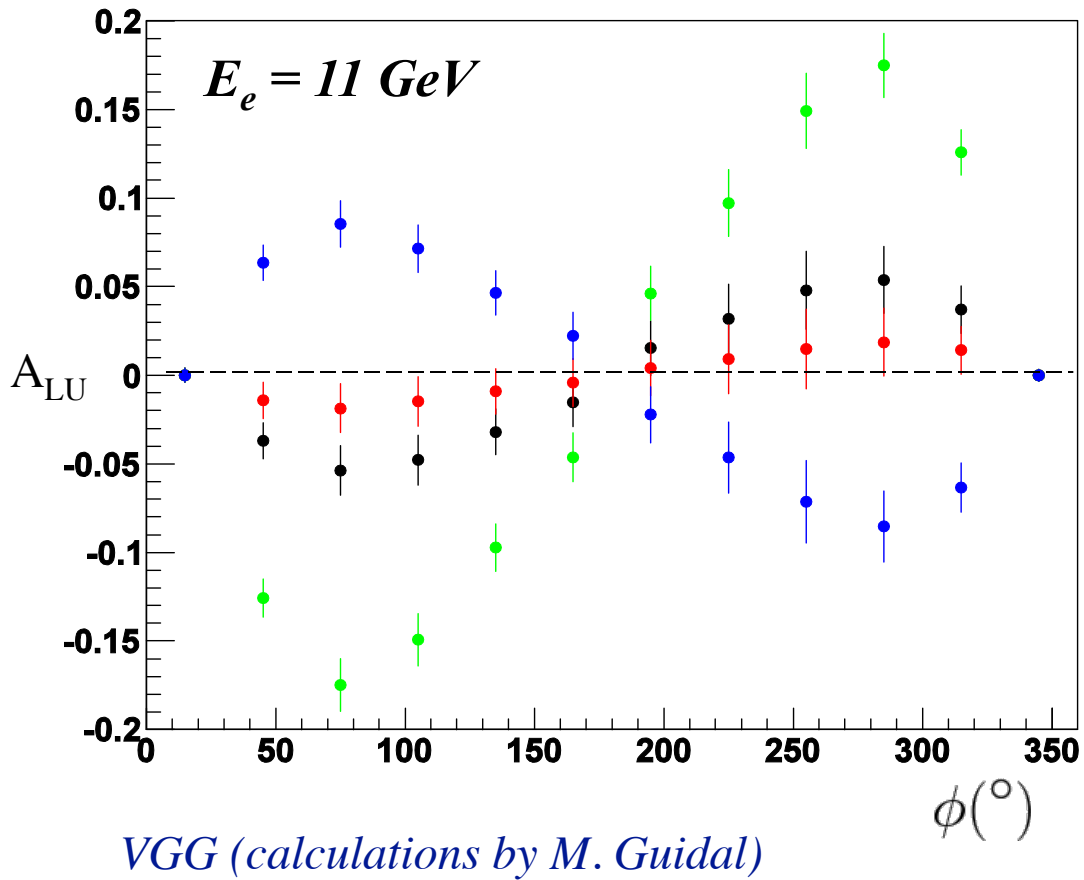
$L = 10^{35} \text{ cm}^{-2}\text{s}^{-1}/\text{nucleon}$
 $e + d \rightarrow e' + \gamma + n + (p_s)$

CLAS12 +
Forward Tagger +
Neutron Detector



Scheduled: 2019

Beam-spin asymmetry in neutron DVCS @ 11 GeV



$J_u = 0.3, J_d = -0.1$	$J_u = 0.3, J_d = 0.1$
$J_u = 0.1, J_d = 0.1$	$J_u = 0.3, J_d = 0.3$

* At 11 GeV, beam spin asymmetry (A_{LU}) in neutron DVCS *is very* sensitive to J_u, J_d

* Wide coverage needed!

Fixed kinematics: $x_B = 0.17$ $Q^2 = 2 \text{ GeV}^2$ $t = -0.4 \text{ GeV}^2$



Proton DVCS with a longitudinally polarised target

Experiment E12-06-119

F. Sabatié et al.

AUL characterised by imaginary parts of CFFs
via:

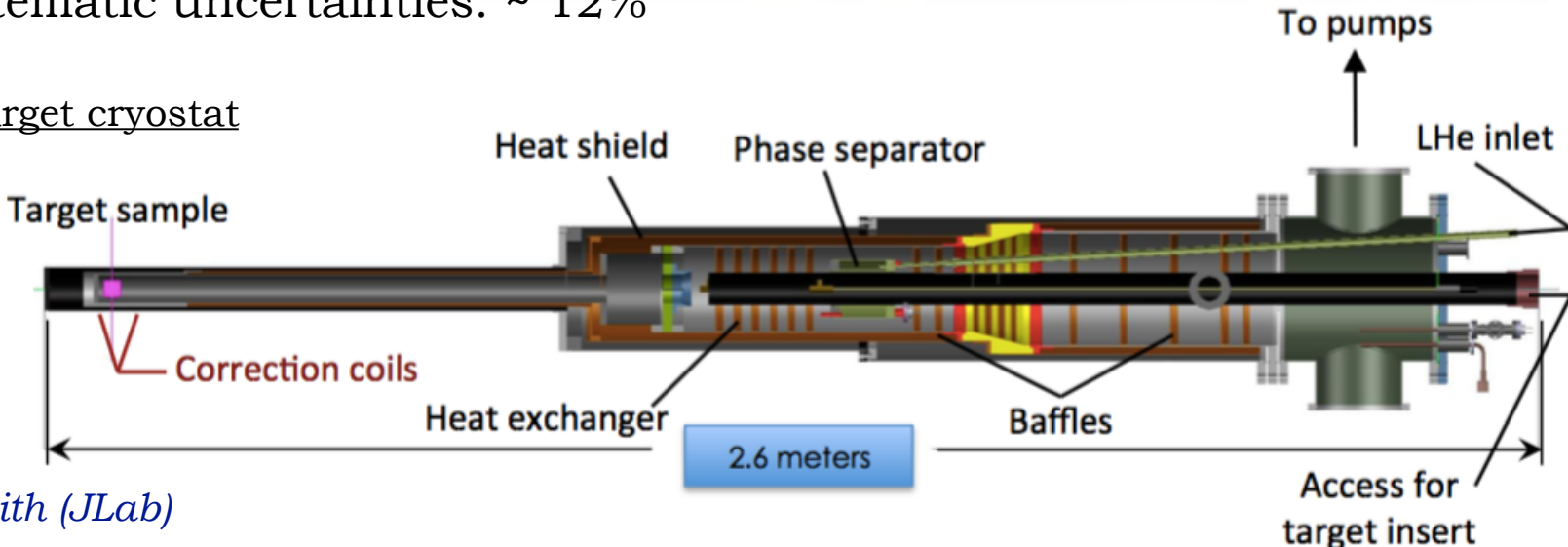
$$F_1 \tilde{H} + \xi G_M (\textcolor{red}{H} + \frac{x_B}{2} \textcolor{blue}{E}) - \frac{\xi t}{4M^2} F_2 \tilde{E} + \dots$$

Longitudinally polarised NH₃ target:

- Dynamic Nuclear Polarisation (DNP) of target material, cooled to 1K in a *He* evaporation cryostat.
- $P_{\text{proton}} > 80\%$
- Statistical error: 2% - 15% on $\sin\varphi$ moments
- Systematic uncertainties: $\sim 12\%$

$$\rightarrow \text{Im}(\tilde{H}_p)$$

Tentative schedule: 2020



C. Keith (JLab)



Neutron DVCS with a longitudinally polarised target

Experiment E12-06-109A.

S. Niccolai, D. Sokhan et al.

Longitudinally polarised ND₃ target:

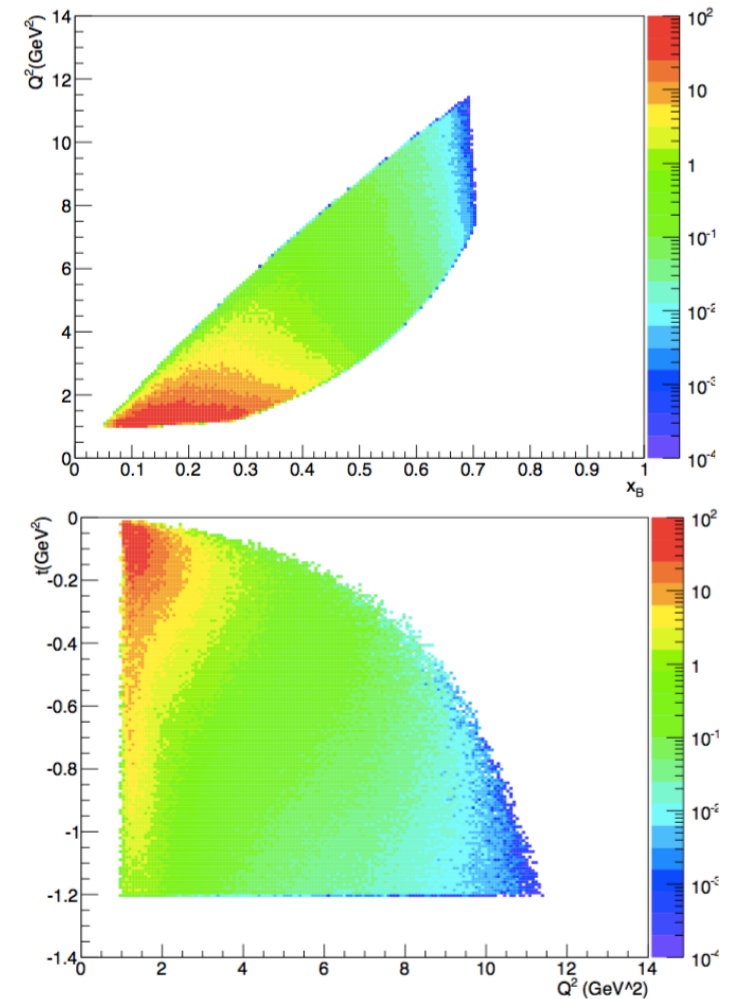
- Dynamic Nuclear Polarisation (DNP) of target material in a cryostat shared with the NH₃ target.
- P_{deuteron} up to 50%
- Systematic uncertainties: ~ 12%

AUL characterised by imaginary parts of CFFs via:

$$F_1 \tilde{H} + \xi G_M (\textcolor{red}{H} + \frac{x_B}{2} \textcolor{blue}{E}) - \frac{\xi t}{4M^2} F_2 \tilde{E} + \dots$$

$$\rightarrow \textcolor{red}{Im}(\mathbf{H}_n)$$

In combination with pDVCS, will allow flavour-separation of the H_q CFFs.



Tentative schedule: 2020



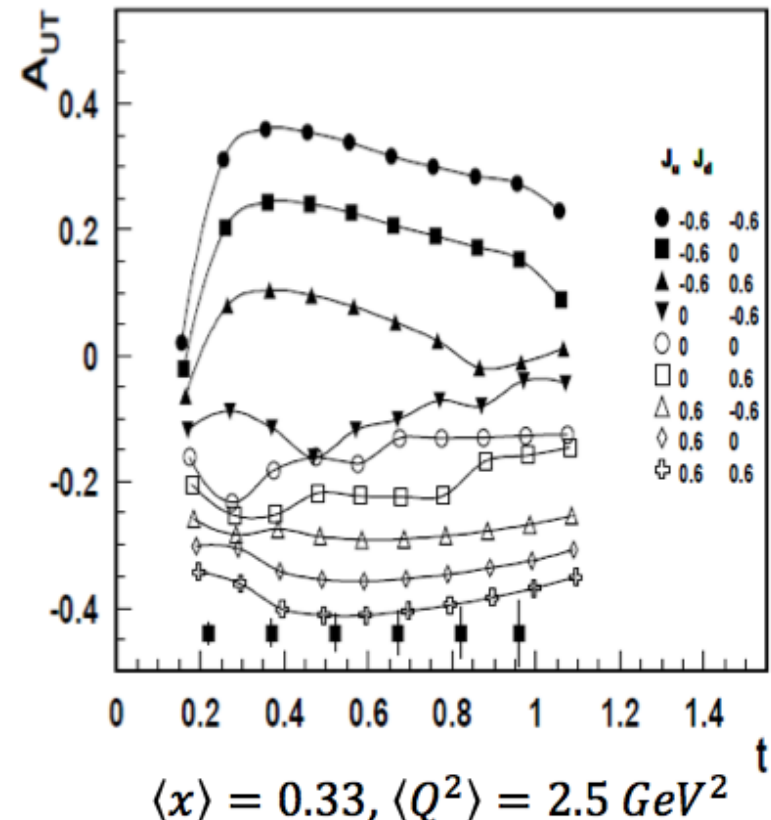
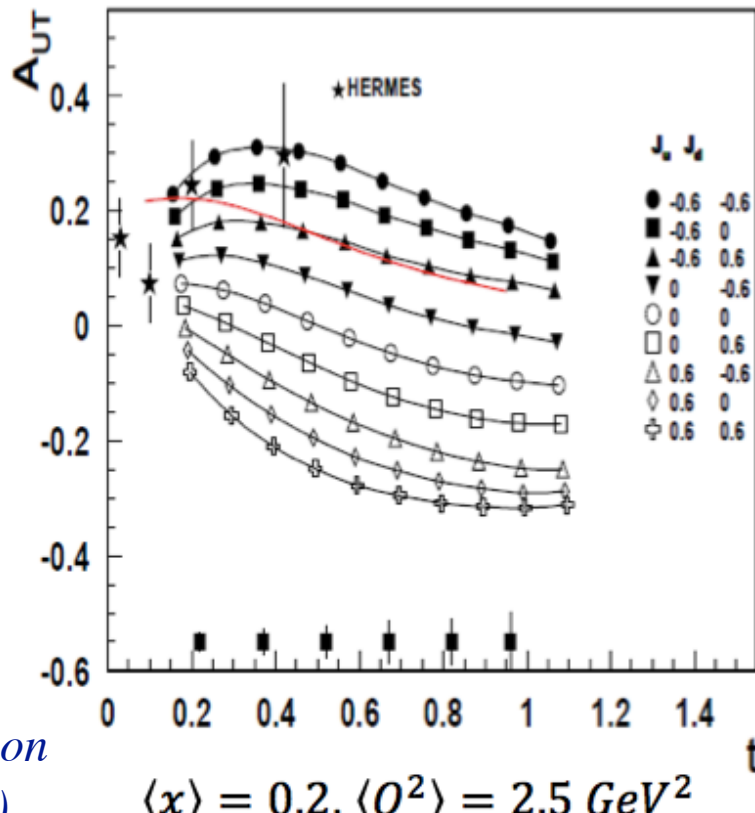
Proton DVCS with transversely polarised target at CLAS12

C12-12-010: with transversely polarised HD target (conditionally approved).

L. Elouardhiri et al.

$$\Delta\sigma_{UT} \sim \cos\phi \operatorname{Im}\{k(F_2H - F_1E) + \dots\} d\phi$$

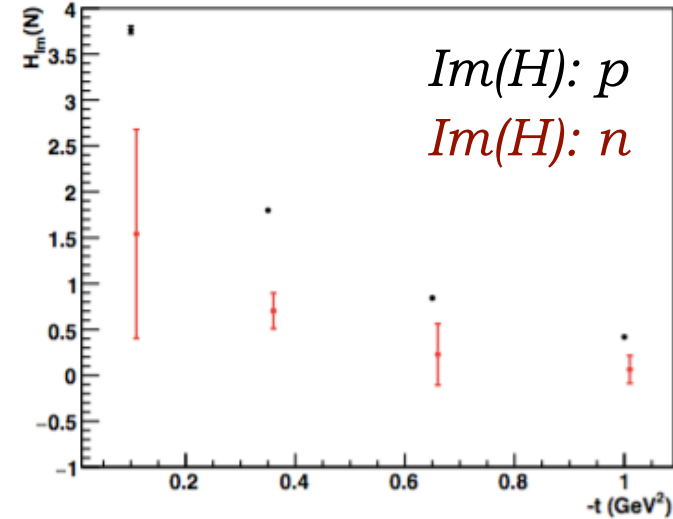
Sensitivity to **Im(E)** for the proton.



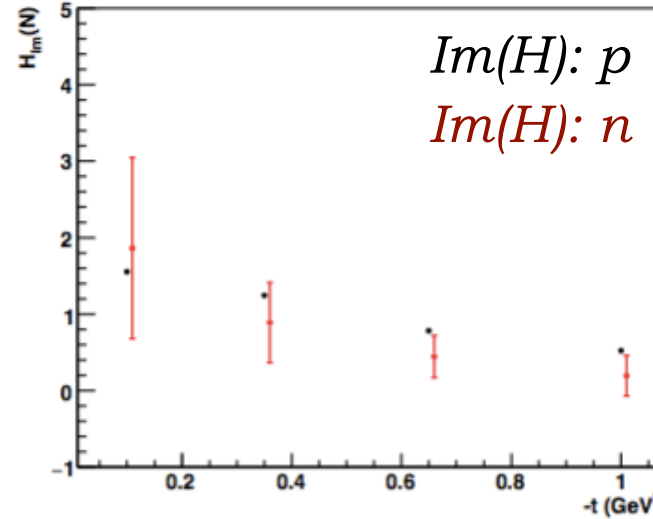
Projected sensitivities to $Im(H)$ CFF



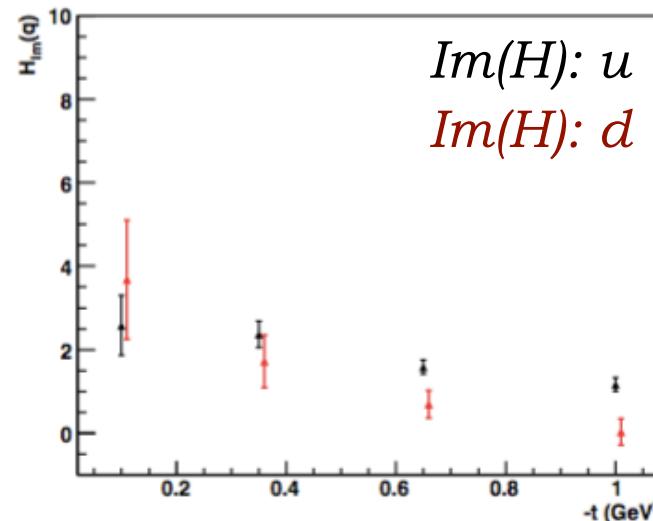
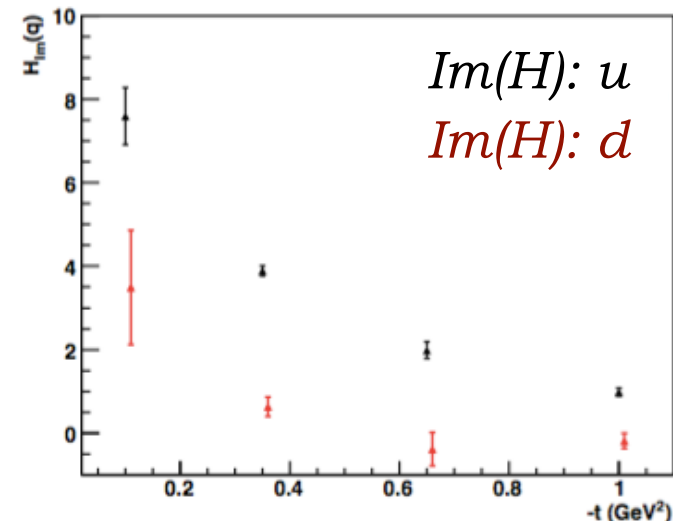
$Q^2 = 2.6 \text{ GeV}^2, x_B = 0.23$



$Q^2 = 5.9 \text{ GeV}^2, x_B = 0.35$



Projections for $Im(H)$ neutron and proton and up and down CFFs extracted from approved CLAS12 experiments.

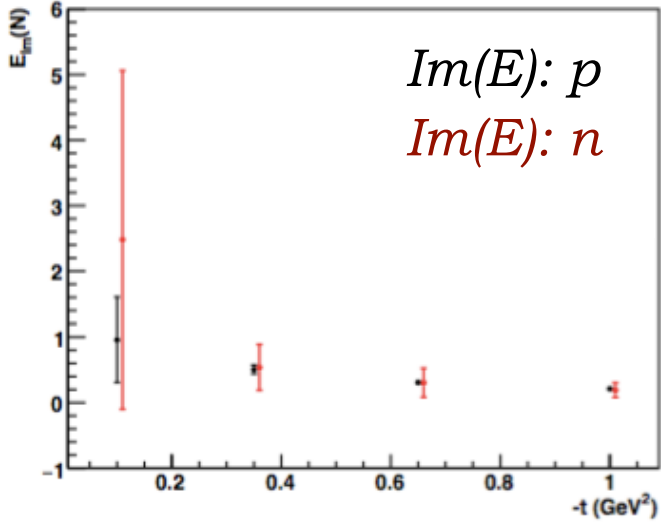


VGG fit (M. Guidal)

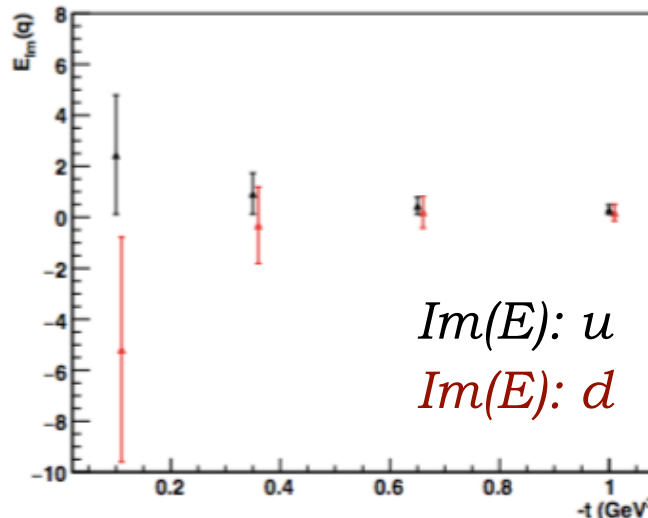
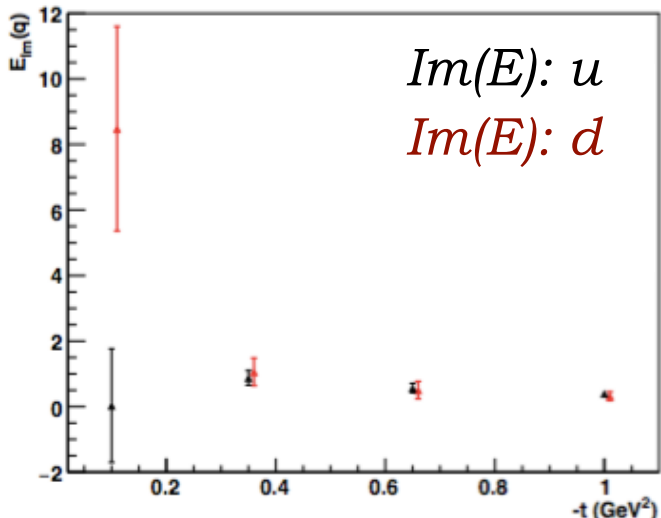
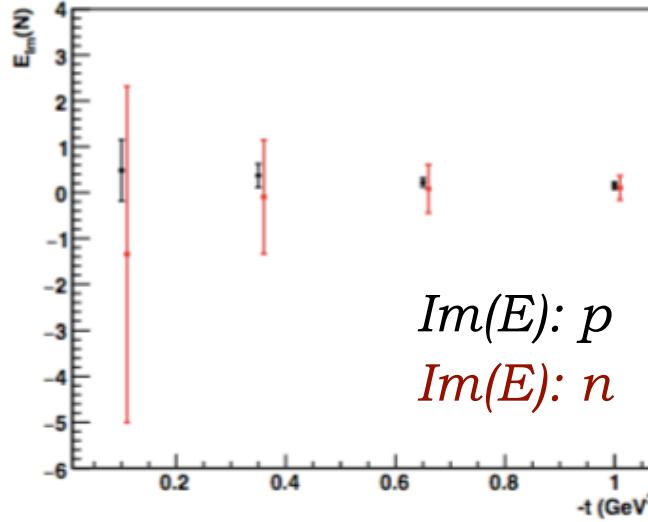
Projected sensitivities to $Im(E)$ CFF



$Q^2 = 2.6 \text{ GeV}^2, x_B = 0.23$



$Q^2 = 5.9 \text{ GeV}^2, x_B = 0.35$



Projections for $Im(E)$ neutron and proton and up and down CFFs extracted from approved and conditionally-approved CLAS12 experiments.

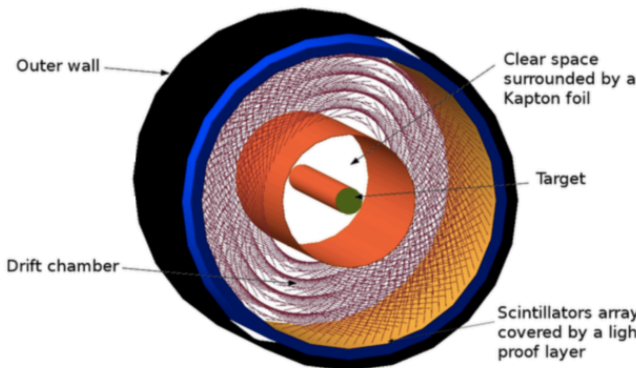
VGG fit (M. Guidal)

DVCS on ${}^4\text{He}$: CLAS12 with ALERT

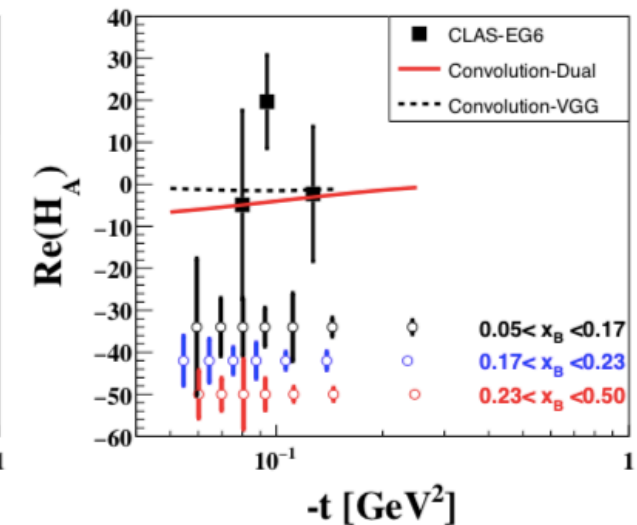
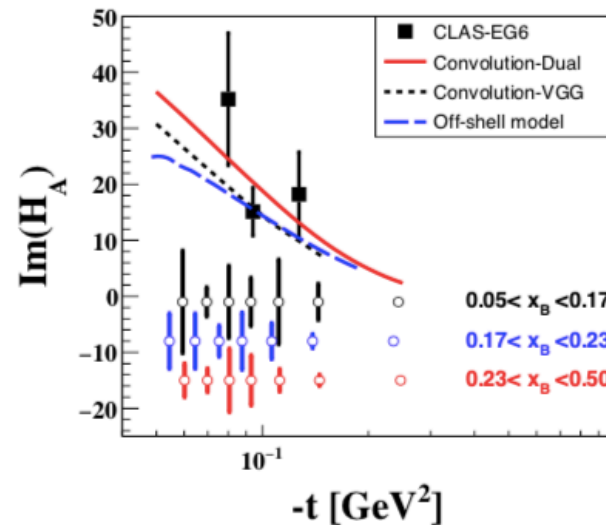
Experiment E12-17-012: Measurement of BSA in coherent DVCS from a
Z.-E. Meziani et al. ${}^4\text{He}$ target: partonic structure of nuclei.

* Spin 0 target, so at leading twist only one chiral-even GPD: \mathbf{H}_A .

11 GeV beam, 80% polarised.
Gas target straw @ 3 atm
 $L = 6 \times 10^{34}$ nucleon $\text{cm}^{-2}\text{s}^{-1}$
with 1000 nA beam.



CLAS12 + ALERT: central
recoil detector



Experiment E12-17-012B
W. Armstrong et al.

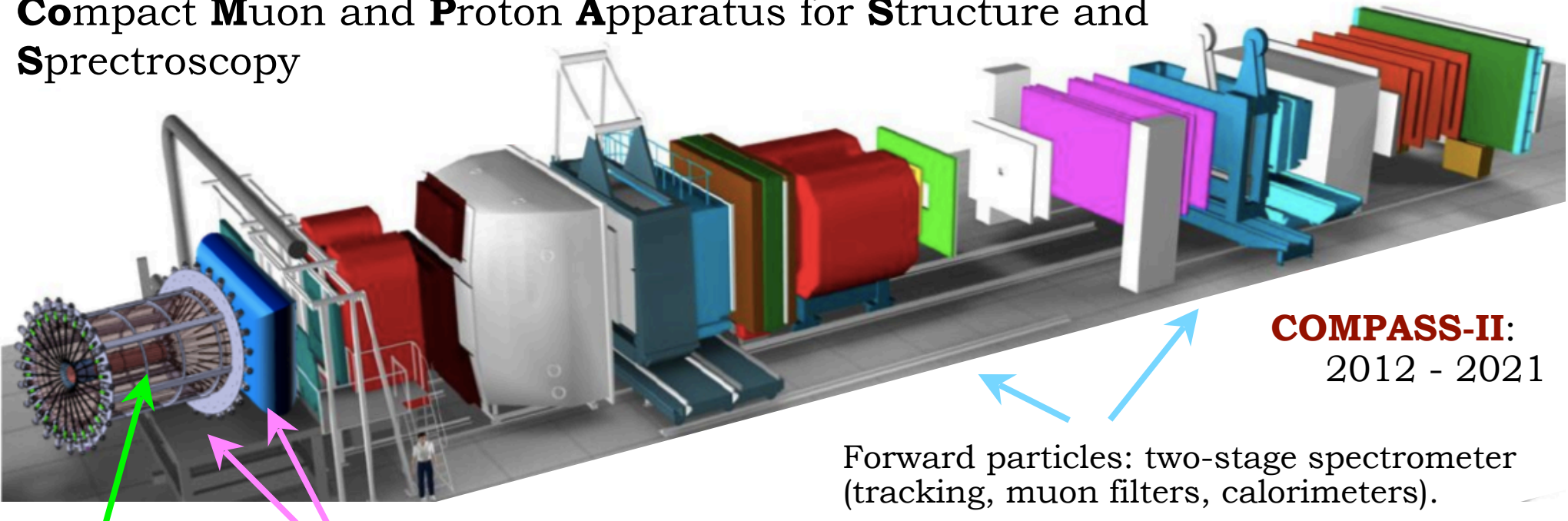
Incoherent, spectator-tagged DVCS
on ${}^4\text{He}$ and d .



DVCS at COMPASS: sea quarks

COMPASS @ Cern (SPS)

Compact Muon and Proton Apparatus for Structure and Spectroscopy



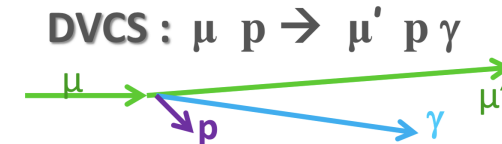
2.5m liquid H₂ target

Upgrades: new scintillator ToF for recoil proton detection & new EM calorimeter.

- * 160 GeV 80% polarised μ^+/μ^-
- * $\sim 4 \times 10^8 \mu/\text{spill}$, 9.6s/40s duty cycle

Forward particles: two-stage spectrometer (tracking, muon filters, calorimeters).

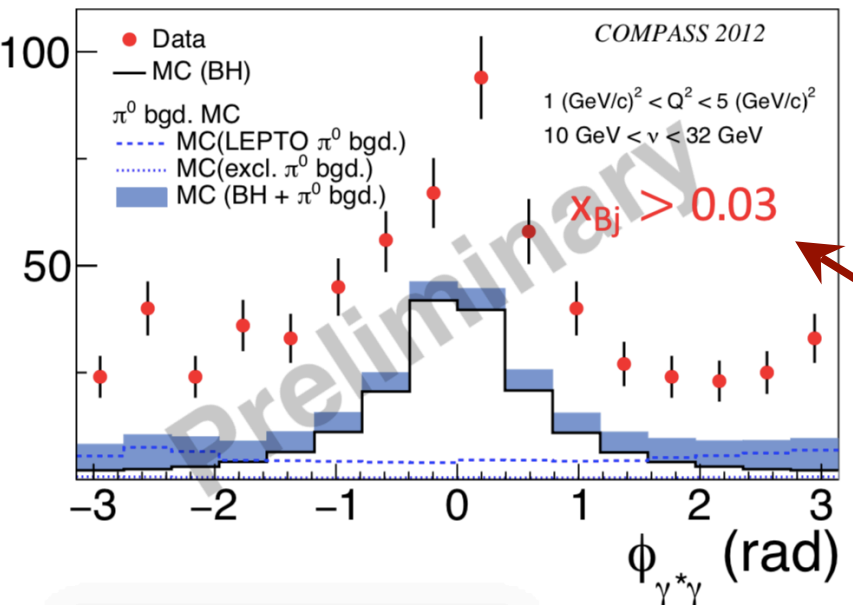
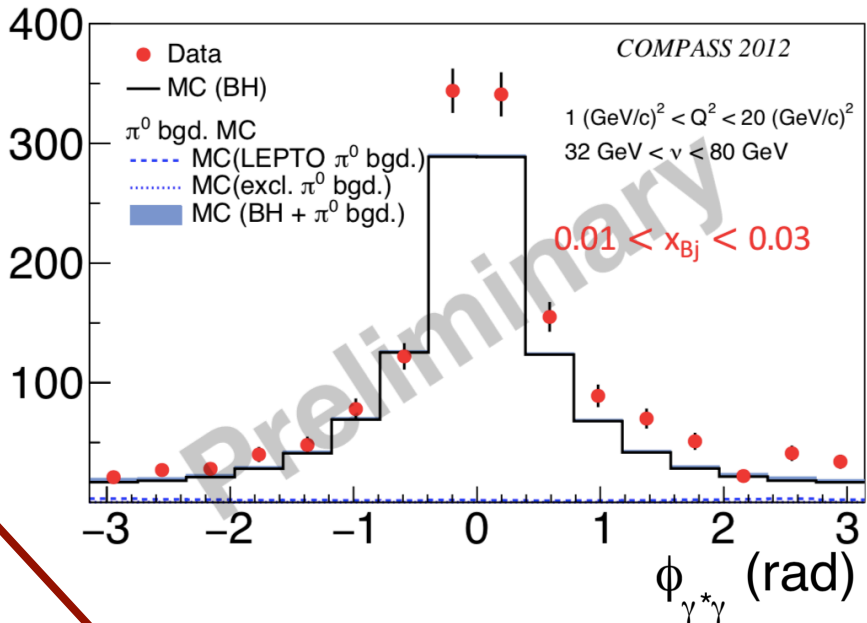
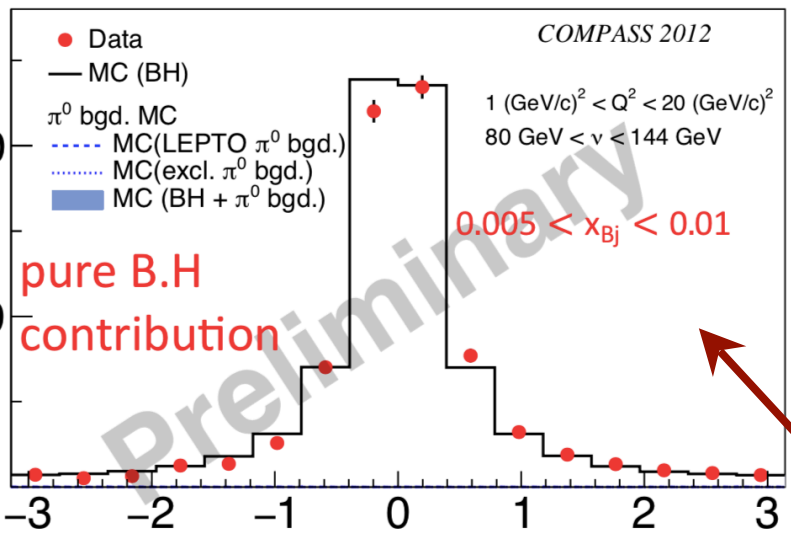
COMPASS-II:
2012 - 2021



Full exclusive reconstruction

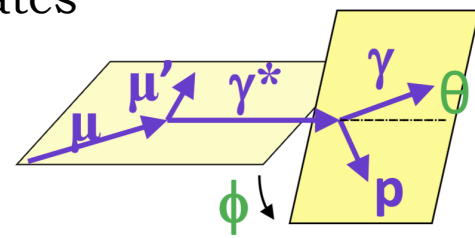
- Data:**
- * 2008 & 2009: two v. short test runs, 40 cm LH_2 target.
 - * COMPASS-II: 1 month in 2012, 6 months in 2016 & 2017 each (GPD **H**).
 - * 2022+: transversely pol. NH_3 target (GPD **E**). LOI stage...

DVCS @ COMPASS (2012 run)



Bethe-Heitler dominates
at very low x_B

DVCS dominates at these kinematics



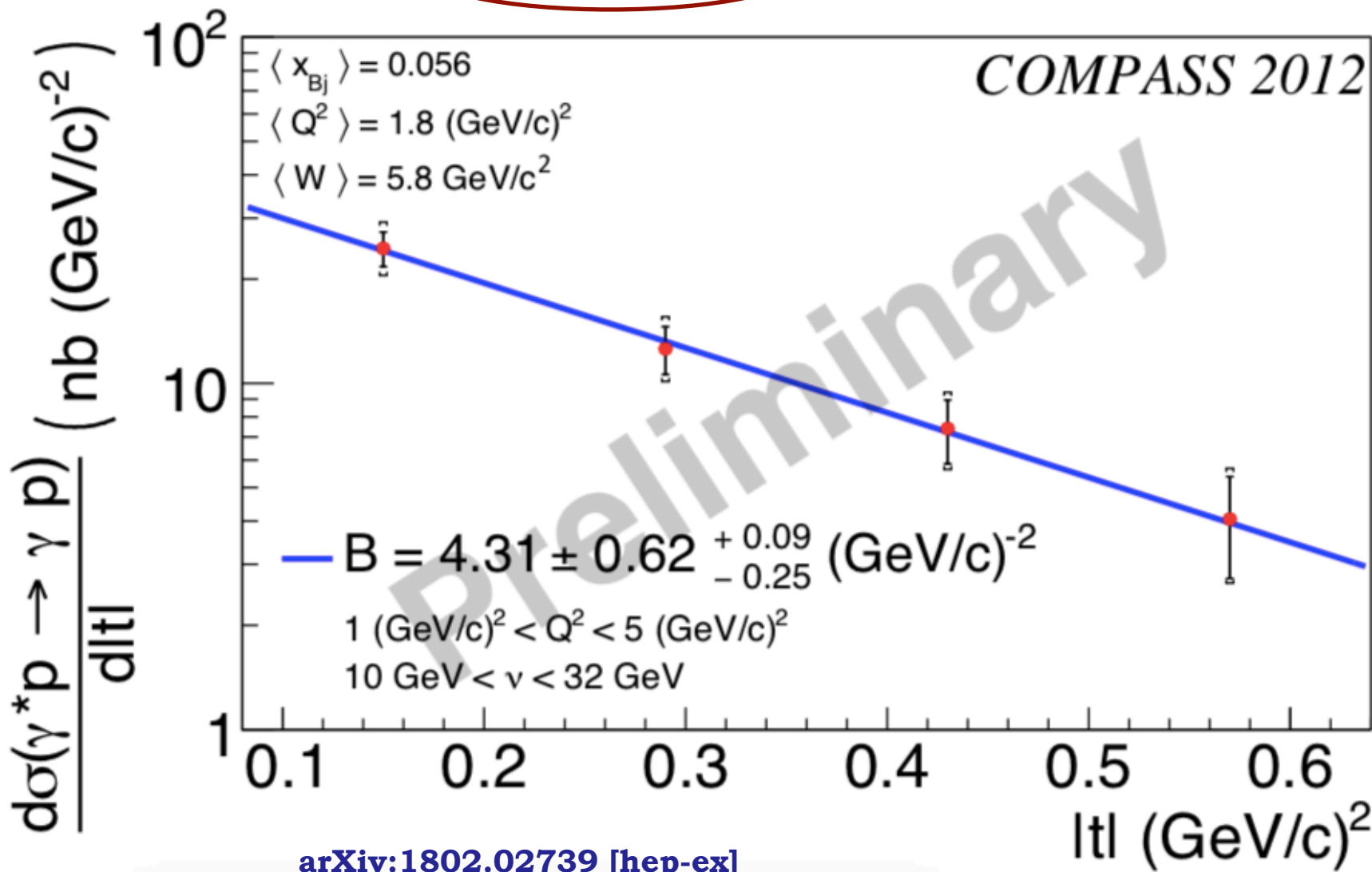
Slide mash-up from N. d'Hose and A. Ferrero

DVCS x-section and t-slope extraction

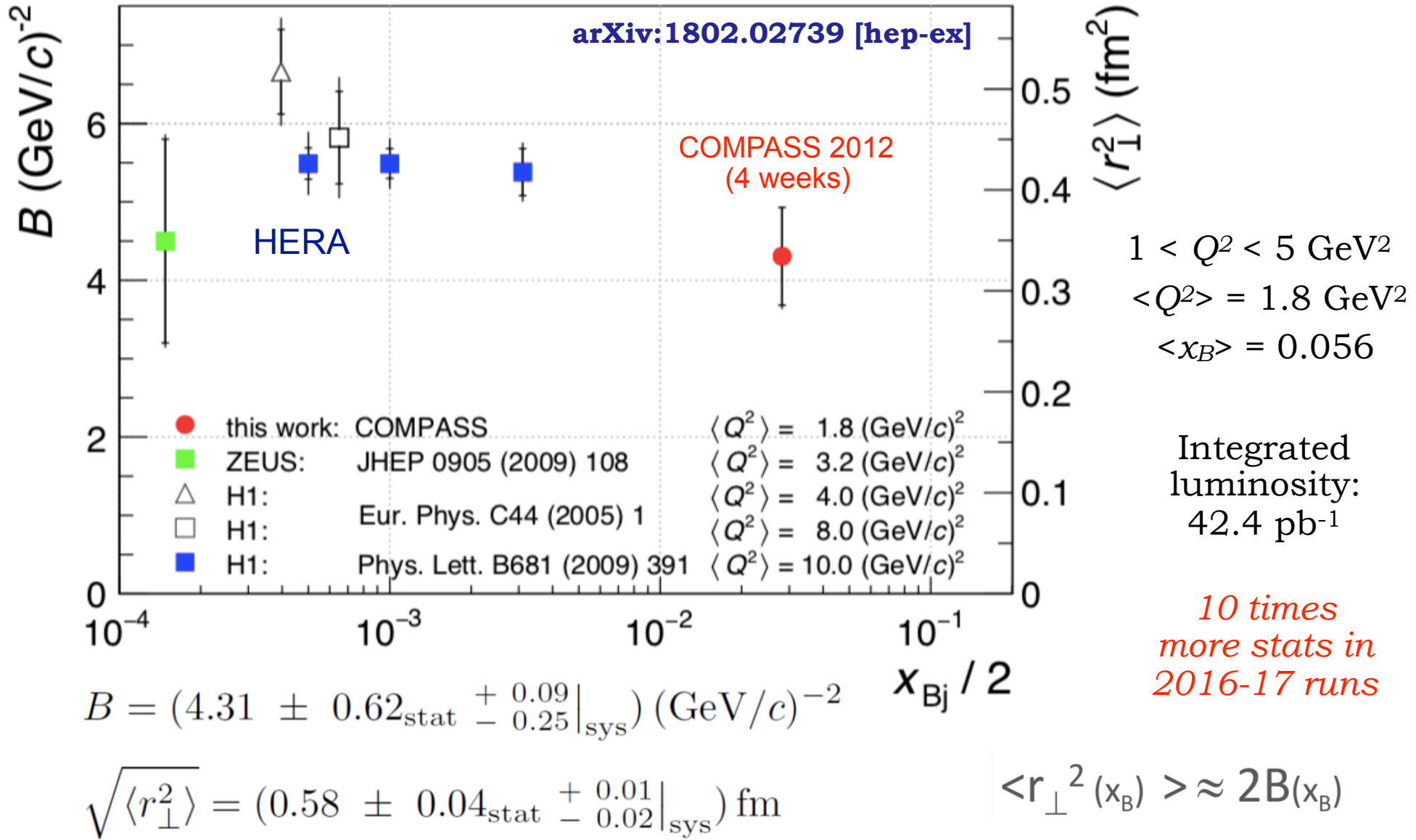
Kinematically constrained
vertex fit applied

Slide from: A. Ferrero @ SPIN 2018

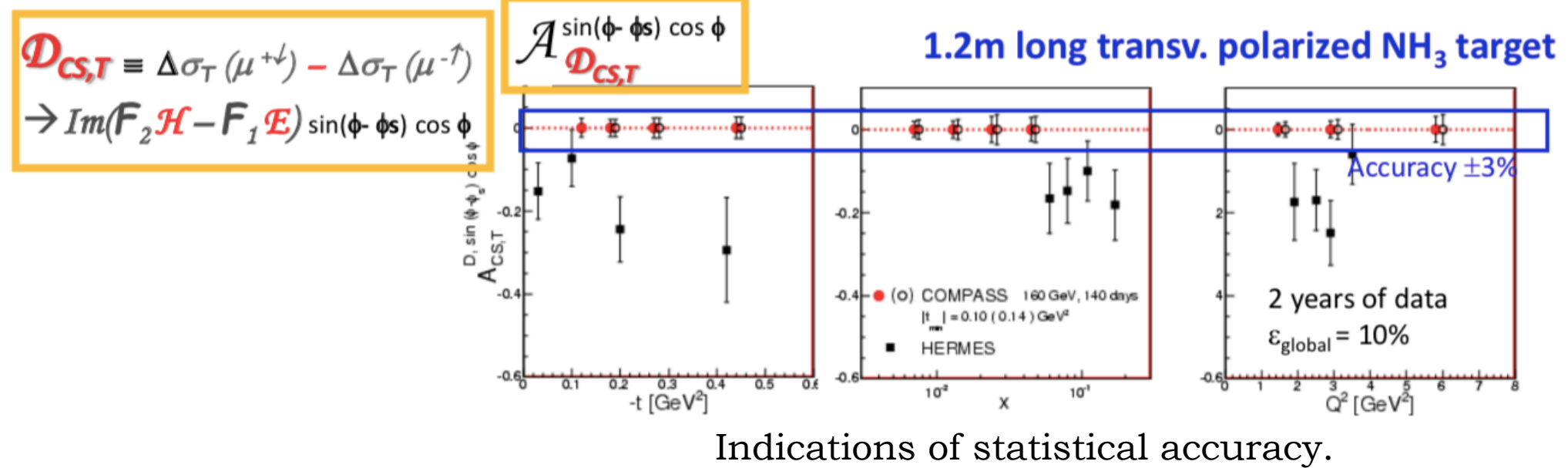
$$d\sigma^{\text{DVCS}}/dt = e^{-B|t|}$$



Tomography of sea quarks



DVCS with transversely polarised target @ COMPASS



Summary

JLab 6 GeV programme:

- * Experimental support for factorisation & the handbag diagram, evidence of scaling
- * Indications of higher-twist or higher-orders at play: hint of gluons?
- * Constraints for GPD models
- * Most information on Re and Im parts of \mathbf{H}_p CFF, a little on $\tilde{\mathbf{H}}_p, \mathbf{E}_n$
- * First attempt at tomography with the limited data

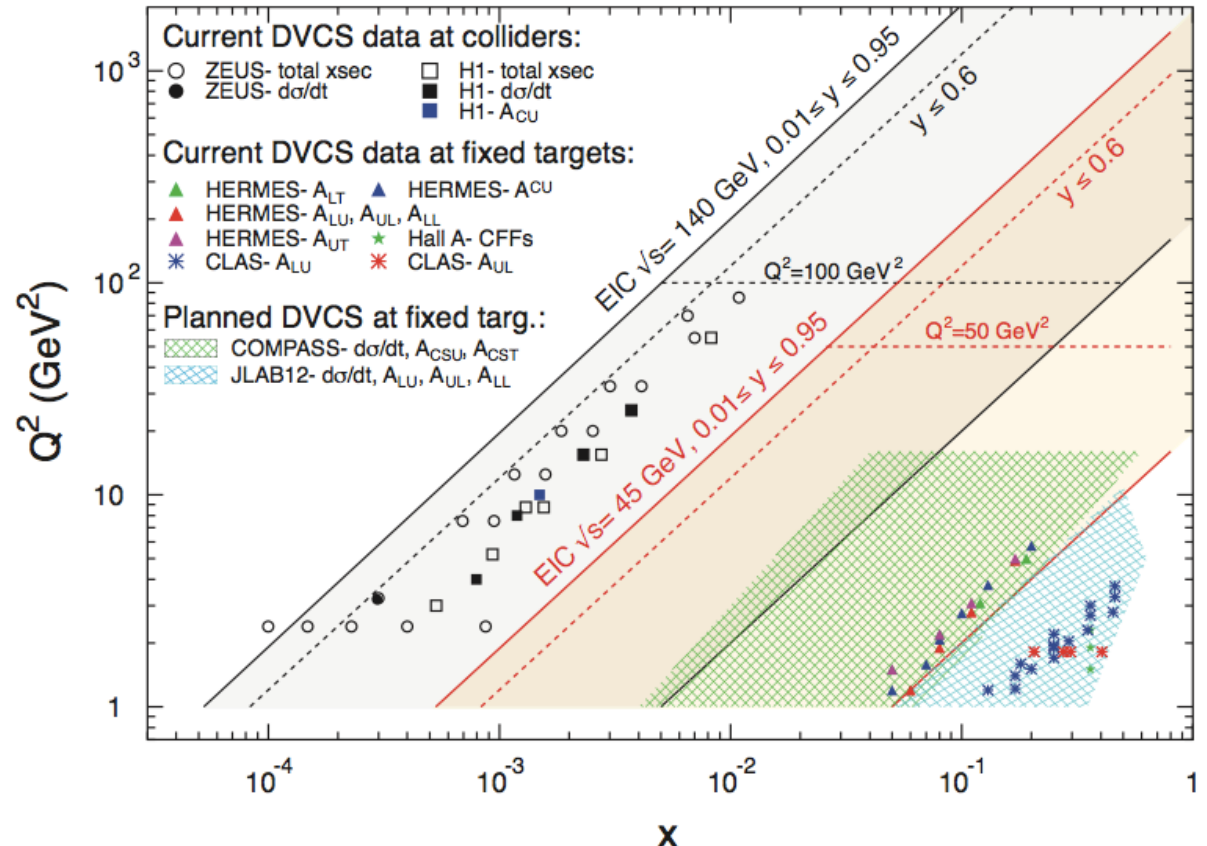
JLab 12 GeV programme:

- * High precision — separation of DVCS and interference terms: sensitivity to higher twist and higher orders, gluons.
- * Extensive mapping of a wider kinematic region — tomography.
- * Extraction of Re and Im parts of \mathbf{H} CFF, $\tilde{\mathbf{H}}$, \mathbf{E} , flavour-separation: u/d.
- * OAM contribution to spin, tomography within the valence region, constraints on GPD models.

COMPASS:

- * \mathbf{H} and \mathbf{E} CFFs - tomography, OAM of the sea quarks, model constraints.

Some questions for the EIC...



EIC White Paper, Eur. Phys. J. A 52, 9 (2016)

- * Tomography of sea quarks: wide kinematic reach.
- * Higher-twist / higher-order: what sensitivity to this will we have? Luminosity factor of 10 3 -10 4 lower than Hall A, *but* can run more or less continuously.
- * Access to gluons easier through DVMP...
- * H, \tilde{H}, E — what about \tilde{E} ?
- * Energy scans - separation of DVCS / Interference.
- * Q^2 scans - scaling.
- * Overlap of kinematics valuable: check of systematics by comparison to JLab, COMPASS results.
- * ... ?

Thank you!



Back-up and sundry

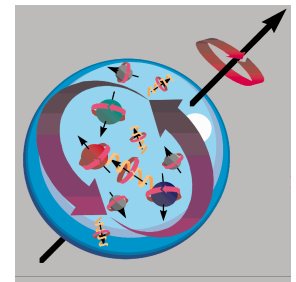
GPDs and nucleon spin

$$J_N = \frac{1}{2} = \frac{1}{2} \Sigma_q + L_q + J_g$$

* Ji's relation: $J^q = \frac{1}{2} - J^g = \frac{1}{2} \int_{-1}^1 x dx \left\{ H^q(x, \xi, 0) + E^q(x, \xi, 0) \right\}$

H accessible in DVCS off the proton, first experimental constraint on E , through neutron-DVCS:

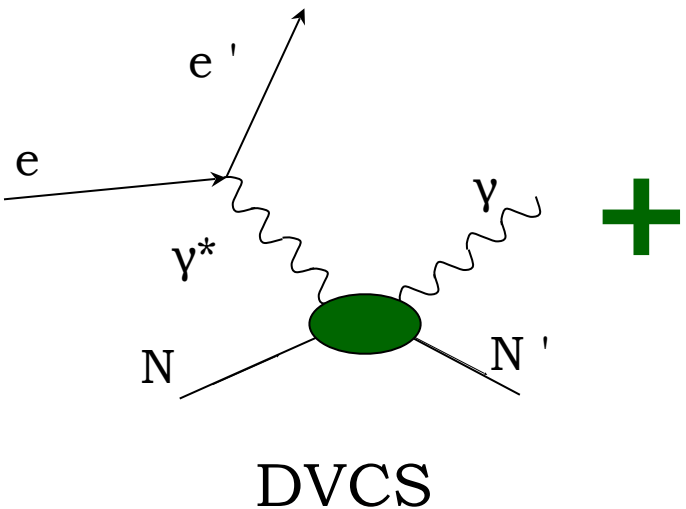
M. Mazouz et al, PRL 99 (2007) 242501



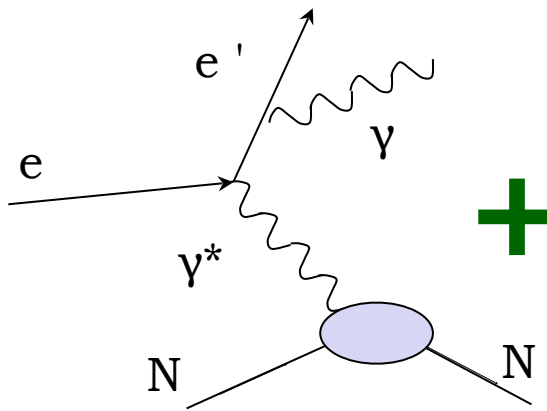
* GPDs can provide insight into the orbital angular momentum contribution to nucleon spin: **the spin puzzle**.

DVCS in experiment

* Process measured in experiment:



DVCS



Bethe - Heitler

$$d\sigma \propto |T_{DVCS}|^2 + |T_{BH}|^2 + \underbrace{T_{BH} T^{*}_{DVCS} + T_{DVCS} T^{*}_{BH}}$$

Amplitude parameterised in terms of Compton Form Factors

Amplitude calculable from elastic Form Factors and QED

Interference term

$$|T_{DVCS}|^2 \ll |T_{BH}|^2$$

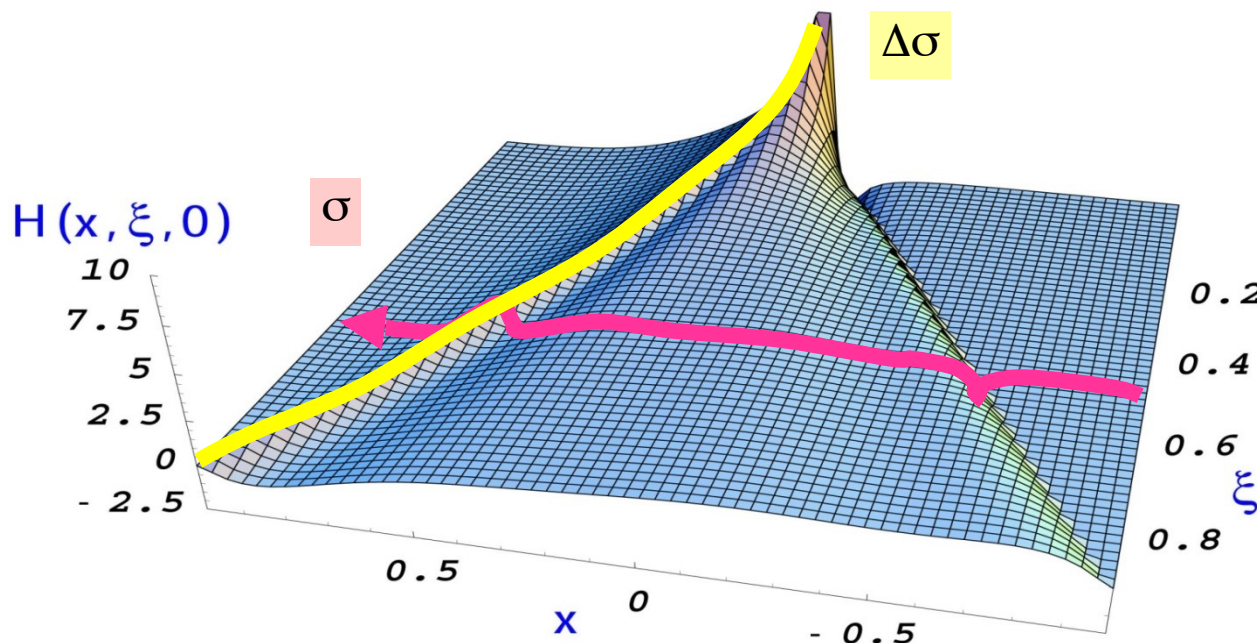
Compton Form Factors in DVCS

Experimentally accessible in DVCS cross-sections and spin asymmetries, eg:

$$A_{LU} = \frac{d\vec{\sigma} - d\bar{\sigma}}{d\vec{\sigma} + d\bar{\sigma}} = \frac{\Delta\sigma_{LU}}{d\vec{\sigma} + d\bar{\sigma}}$$

At leading twist, leading order:

$$T^{DVCS} \sim \int_{-1}^{+1} \frac{GPDs(x, \xi, t)}{x \pm \xi + i\varepsilon} dx + \dots \sim P \int_{-1}^{+1} \frac{GPDs(x, \xi, t)}{x \pm \xi} dx \pm i\pi GPDs(\pm\xi, \xi, t) + \dots$$



Only ξ and t are accessible experimentally!

To get information on x need extensive measurements in Q^2 .

Need measurements off proton and neutron to get flavour separation of CFFs in DVCS.

The DVCS/BH amplitude

$$\mathcal{T}^2 = |\mathcal{T}_{\text{BH}}|^2 + |\mathcal{T}_{\text{DVCS}}|^2 + \mathcal{I} \quad \xleftarrow{\text{Interference term for DVCS/BH}}$$

$$|\mathcal{T}_{\text{BH}}|^2 = \frac{e^6}{x_B^2 y^2 (1 + \epsilon^2)^2 t \mathcal{P}_1(\phi) \mathcal{P}_2(\phi)} [c_0^{\text{BH}} + \sum_{n=1}^2 c_n^{\text{BH}} \cos n\phi + s_1^{\text{BH}} \sin \phi]$$

$$|\mathcal{T}_{\text{DVCS}}|^2 = \frac{e^6}{y^2 Q^2} \{c_0^{\text{DVCS}} + \sum_{n=1}^2 [c_n^{\text{DVCS}} \cos n\phi + s_n^{\text{DVCS}} \sin n\phi]\}$$

$$\mathcal{I} = \frac{e^6}{x_B y^3 t \mathcal{P}_1(\phi) \mathcal{P}_2(\phi)} \{c_0^{\mathcal{I}} + \sum_{n=1}^3 [c_n^{\mathcal{I}} \cos n\phi + s_n^{\mathcal{I}} \sin n\phi]\}$$

Intermediate lepton propagators

*Coefficients depending on
Compton Form Factors*

From asymmetries to CFFs

At leading twist, beam-spin asymmetry (BSA) can be expressed as:

$$A_{\text{LU}}(\phi) \sim \frac{s_{1,\text{unp}}^{\mathcal{I}} \sin \phi}{c_{0,\text{unp}}^{\text{BH}} + (c_{1,\text{unp}}^{\text{BH}} + c_{1,\text{unp}}^{\mathcal{I}} + \dots) \cos \phi \dots} \quad \text{higher-twist terms...}$$

The leading coefficient is related to the imaginary part of the Compton Form Factors:

$$s_{1,\text{unp}}^{\mathcal{I}} \propto \Im[\bar{F}_1 \mathcal{H} + \xi(F_1 + F_2)\tilde{\mathcal{H}} - \frac{t}{4M^2} F_2 \mathcal{E}]$$

At CLAS kinematics, this dominates

*F₁, F₂: Dirac,
Pauli form factors*

Likewise, for the target-spin asymmetry (TSA):

$$A_{\text{UL}}(\phi) \sim \frac{s_{1,\text{LP}}^{\mathcal{I}} \sin \phi}{c_{0,\text{unp}}^{\text{BH}} + (c_{1,\text{unp}}^{\text{BH}} + c_{1,\text{unp}}^{\mathcal{I}} + \dots) \cos \phi + \dots}$$

$$s_{1,\text{LP}}^{\mathcal{I}} \propto \Im[\bar{F}_1 \tilde{\mathcal{H}} + \xi(F_1 + F_2)(\mathcal{H} + \frac{x_B}{2} \mathcal{E}) - \xi(\frac{x_B}{2} F_1 + \frac{t}{4M^2} F_2) \tilde{\mathcal{E}}]$$

At CLAS kinematics, these CFFs dominate

- * Obtain coefficients from fitting the phi-dependence of the asymmetry:

$$A_i = \frac{\alpha_i \sin \phi}{1 + \beta_i \cos \phi}$$

Double-spin asymmetry

At leading twist, double-spin asymmetry (DSA) can be expressed as:

$$A_{LL}(\phi) \sim \frac{c_{0,Lp}^{BH} + c_{0,Lp}^{\mathcal{I}} + (c_{1,Lp}^{BH} + c_{1,Lp}^{\mathcal{I}}) \cos \phi}{c_{0,unp}^{BH} + (c_{1,unp}^{BH} + c_{1,unp}^{\mathcal{I}} + \dots) \cos \phi \dots}$$

$$c_{0,Lp}^{\mathcal{I}}, c_{1,Lp}^{\mathcal{I}} \propto \Re e[F_1 \hat{\mathcal{H}} + \xi(F_1 + F_2)(\mathcal{H} + \frac{x_B}{2}\mathcal{E}) - \xi(\frac{x_B}{2}F_1 + \frac{t}{4M^2}F_2)\tilde{\mathcal{E}}]$$

At CLAS kinematics, leading-twist dominance of these CFFs

- * Fit function for the phi-dependence of the asymmetry:

$$\frac{\kappa_{LL} + \lambda_{LL} \cos \phi}{1 + \beta \cos \phi}$$

Shares denominator with BSA and TSA!

If measurements at same kinematics, can do a simultaneous fit.

Transverse extension of partons in the proton

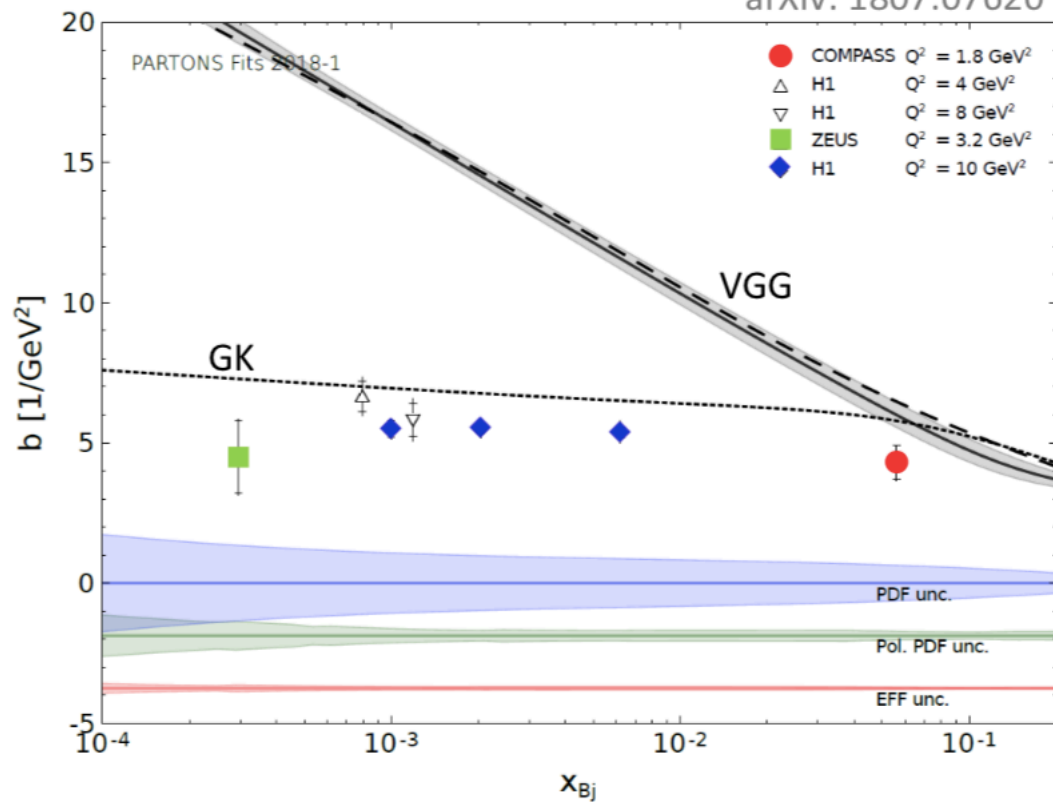
Comparison to GPD models

Figure from Moutarde, Sznajder, Wagner
arXiv: 1807.07620

The grey band is a global fit of CFF
in the PARTON framework
at LO and LT using a GPD parametrization
(only valence and sea quarks)

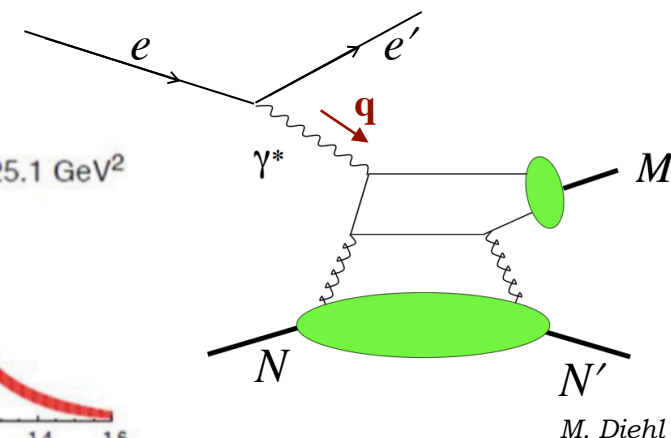
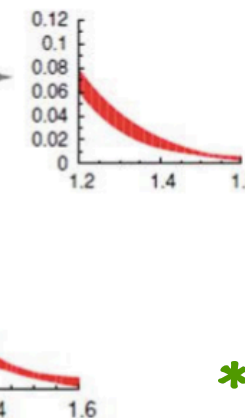
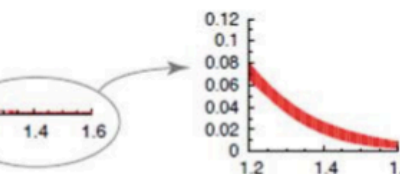
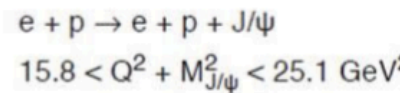
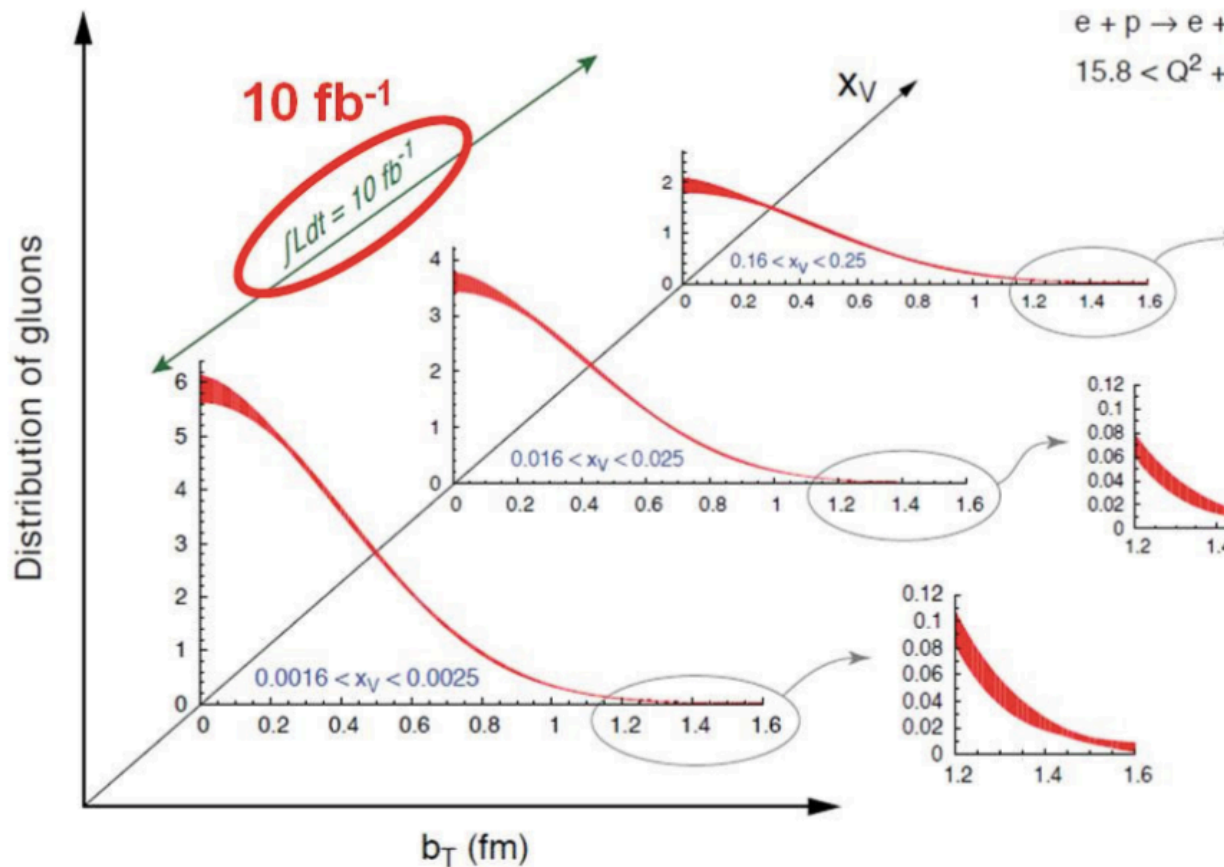
GK includes gluons (at next order in α_s)

Manifestation of gluons or NLO



Nucleon tomography: imaging glue

- * Gluon GPDs can be accessed through deeply virtual meson production (DVMP), eg: J/Ψ
- * Access to spatial distributions of gluons at different longitudinal momentum fractions:



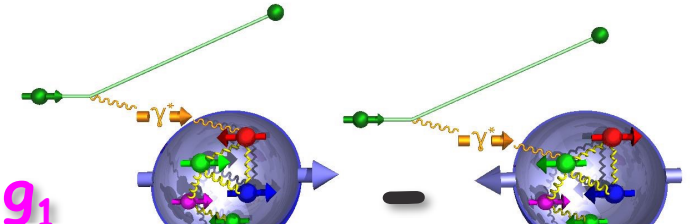
Gluon momentum fraction related to:

$$x_V = x_B (1 + M_{J/\Psi}^2 / Q^2)$$

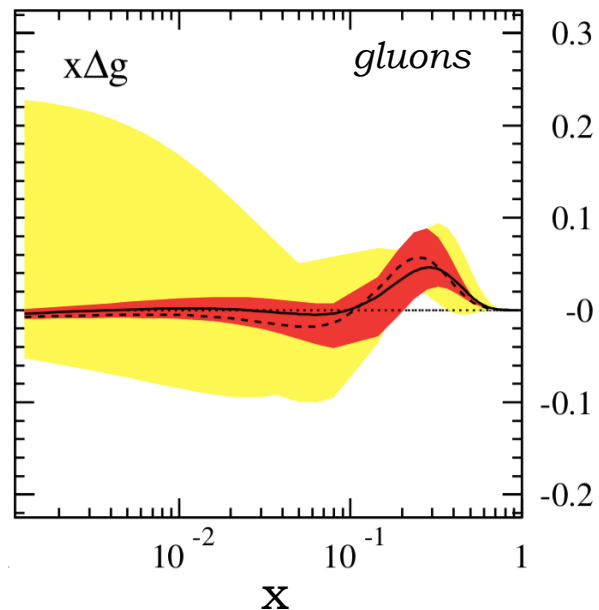
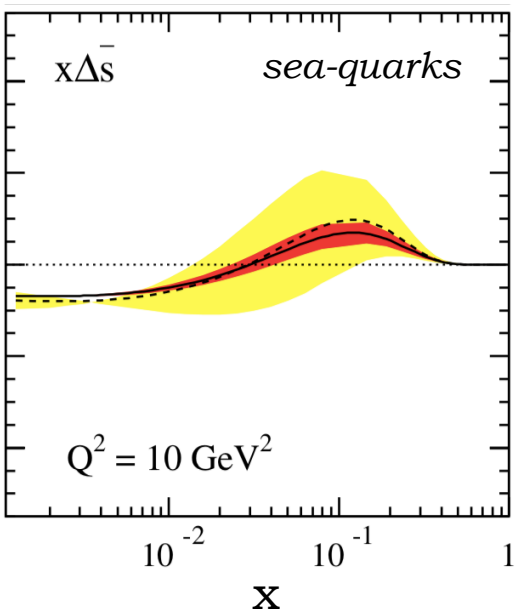
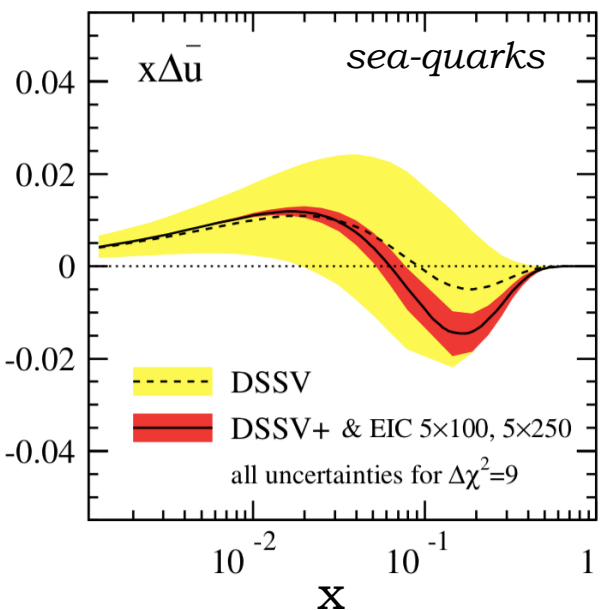
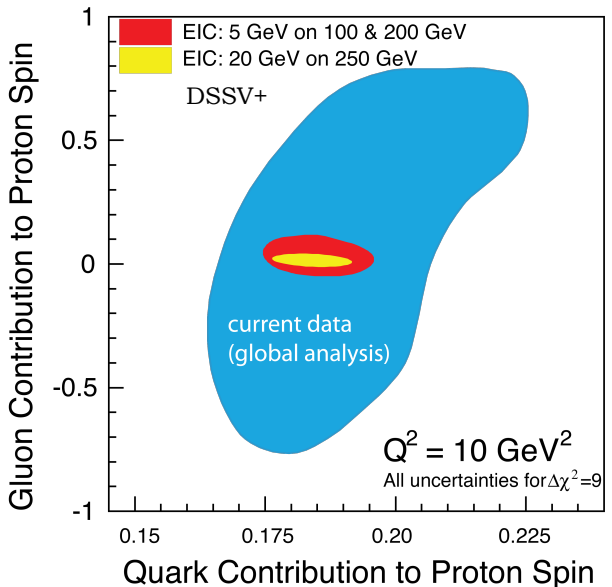
- * 3D images of sea quark and gluon distributions from exclusive reactions: DVCS and DVMP.

Gluon spin

- * DIS and SIDIS will contribute extremely precise measurements of the helicity distributions of sea-quarks and gluons.



$$\Delta\Sigma(Q^2) = \int_0^1 g_1(x, Q^2) dx = \int_0^1 \Delta q_f(x, Q^2) dx$$



E. Aschenauer *et al.*,
Phys. Rev. D 86, 054020 (2012)

DSSV: D. de Florian, R. Sassot, M. Stratmann, W. Vogelsang,
Phys. Rev. D **80**, 034030 (2009).

DSSV+: arXiv:1112.0904 [hep-ph]